

Thesis for the Master's  
degree in chemistry

**Neha Amit Parekh**

**Assessment of  
phosphorus fractions in  
streams draining  
different land use and  
development of new  
monitoring method.**

**60 study points**

**DEPARTMENT OF CHEMISTRY**

Faculty of mathematics and natural  
sciences

**UNIVERSITY OF OSLO 04/2012**





## **Preface**

The present work was carried out at the Environmental Department of Chemistry, University of Oslo (UiO) during the period from February 2010 to April 2012.

First of all, I would like to thank my supervisor Rolf D. Vogt for great guidance and support. I truly appreciated that your door was always open when I needed help. Thanks to my co-supervisor Oddvar Røyset, at NIVA, for believing in my ability as a scientist and for helpful advices. Thanks to Alexander Engebretsen and Christian Mohr for sharing valuable knowledge and experience with me.

Thanks to Cathrine Brecke Gundersen and Moisha Balingene for sharing many enjoyable moments and good laughs. A warm thanks to Yemane Gebreslasse, Ykalo Hadush Desta, Sahle Smur Weldehawaria for good conversations.

At last, I would like to thank my family and my dearest  $\text{ଅମିତ}$ , thanks for your constant support and encouragement during these years.

## Abstract

This study was an integrated part of the interdisciplinary research project EUTROPIA, funded by Research Council of Norway (190028/S30). The goal of the nature science part of the EUTROPIA project is to improve the understanding of hydro-biogeochemical processes governing the P-mobility to the MORSA catchment, with the Western Vansjø Lake as a main study area. This study has examined different phosphorus fractions from the nine tributaries to the lake draining the different contingency of agriculture and forested land. In addition, this work has also examined the novel monitoring method Diffusive Gradients in Thin Films (DGT) for simultaneous time averaged sampling of bioavailable free-PO<sub>4</sub> (orthophosphate) and organic P compounds.

The levels of three to four different phosphorus (P) fractions were determined in the stream water samples collected from nine inlet streams to the Western Vansjø Lake over a period of several months. DGT samplers deployed at three of the nine monitoring streams to study the performance of this new sampling method and DGT samples were analysed for total-P and free orthophosphate. Temporal and spatial variations in the stream water chemistry, with emphasis of P fractions, were assessed in order to distinguish the effect of environmental pressures, such as climate change, that may counteract the mitigations measures.

The nine studied streams draining from the Western Vansjø catchment were selected in order to capture gradient in land use from agriculture to increasing proportion of forested area. The concentration and composition of P fractions were greatly influenced by land use distribution and runoff. The organic bound P constituted from 30 to 60% of the total P transport (~ 6-12 µg P/L) in the runoff from the forested area, due to high transport of DOC. In the agricultural areas the concentration of total-P were mainly constituted by particle bound P. Results from the four hydrological years (2006-2010) showed that autumn rainstorms, winter mild-spells and spring snowmelt were important periods of P transfer from land to water. Inter-annual variation in winter temperature is found to be important factor that may govern the variation in inter-annual flux of P. A higher flux of total-P in the streams was found during the years 2006/07 and 2007/08 mainly due to higher winter temperatures than normal causing snowmelt, accompanied with higher precipitation, generating several runoff episodes during the winter season. During the hydrological years 2008/09 and 2009/10, the main peak of total-P release occurred during the normal spring snowmelt period.

Elevated concentrations of free-PO<sub>4</sub> and dissolved organic bound P (DOM-P) were found during the episodes of flood and snow smelt. Increased runoff and milder winter temperature may lead to increased leaching of free-PO<sub>4</sub> bound to the soils through Fe (III) from water logged soils due to reduction to Fe (II) and trapping as FeS. This may be a governing factor for the strong negative effect of the flood in the year 2000, still 11 years after flood. Furthermore, the drainage pipes in agriculture soils in the Western Vansjø catchments are installed in apatite containing clay, which are eroded by flow to and through tiles. This is found to be an important governing factor for the total-P loading and a significant flow-path of total-P flux to the streams.

The DGT samplers with two adsorbents were studied, the new Metsorb (Titanium dioxide) adsorbent and the more established Ferrihydrite (Iron hydroxide) adsorbent. Laboratory studies of the two DGT samplers showed time linear uptake of the low molecular weight organic P compounds e.g. AMP and IP<sub>6</sub> (Adenosine Monophosphate, Inositol 6-Phosphate). DGTs based diffusion-coefficients for AMP was ranged between 3 to 3.5 E-06 cm<sup>2</sup>s<sup>-1</sup> which is close to the theoretical value (3.9E-06) while the value of 1.5E-06 for IP<sub>6</sub> was lower than the theoretical value. The elution efficiencies for ferrihydrite DGT and Metsorb DGT were found to be 100% and 85%, respectively. Metsorb DGT method performs similarly to ferrihydrite DGT method for orthophosphate ions, but collects organic P compound at ~ 25% higher efficiency than ferrihydrite DGT method. The concentrations of free-PO<sub>4</sub> in the stream water sample are found to be lower when obtained by the DGT samplers than when determined in grab samples. This is probably due to that the conventional field sampling method for free-PO<sub>4</sub> includes P in small colloids and surface adsorbed P, while DGT samplers exclude these fractions. Moreover, low molecular weight organic fractions collected by the DGT samplers showed large variation from agriculture to forested site. DGTs thus offers a completely new sampling method for this fraction of P in water which often have been missing in transport budgets, and thus add considerable new value to such studies.

## Table of content

Preface.....	i
Abstract .....	i
List of figures .....	vii
List of tables .....	xi
Symbols and Abbreviations.....	xii
1 Introduction .....	1
1.1 World water resources with emphasis on water pollutants .....	1
1.2 Water Framework Directive (WFD) .....	1
1.3 Background information about the Morsa catchment .....	2
1.4 Mitigation actions and current status of Western Vansjø.....	4
1.5 Development of new sampling technique DGT (Diffusive gradient in thin film) .....	7
1.6 EUTROPIA project .....	8
1.7 The aim of the study.....	8
2 Theory .....	9
2.1 Eutrophication and phosphorous chemistry .....	9
2.1.1 Eutrophication .....	9
2.1.2 Classification of trophic condition .....	10
2.1.3 The deterioration of lake .....	11
2.1.4 Phosphorous in the earth .....	12
2.1.5 Global Phosphorous cycle and Phosphorus in water.....	14
2.1.6 The effect of red-ox on phosphorous.....	18
2.1.7 The transport of P from land to water .....	20
2.1.8 Role of increased DNOM leaching and reduce aluminium leaching .....	22
2.1.9 Climate changes and phosphorus mobility.....	24
2.2 Analytical theory of Diffusive Gradient in Thin Films (DGT) .....	26
2.2.1 Diffusive Gradient in Thin Films (DGT) .....	26
2.2.2 Structure of DGT-device .....	27
2.2.3 Diffusion.....	29
2.2.4 Principles of the DGT theory in water.....	30

2.2.5	Estimation of diffusion coefficients .....	33
3	Site description, sampling and analytical methods.....	34
3.1	Field site description .....	34
3.1.1	Vansjø-Hobøl (Morsa) Catchment .....	34
3.1.2	Geology of Vansjø-Hobøl catchment.....	36
3.1.3	Site description .....	37
3.1.4	Soil types and erosion risk in the monitoring catchments .....	40
3.1.5	Meteorology and runoff.....	42
3.2	Sampling.....	45
3.2.1	Stream water sampling and sample preparation.....	45
3.2.2	DGT sampling and sample preparation.....	47
3.3	Laboratory location and facilities.....	50
3.4	Water samples analysis .....	50
3.4.1	Filtration of water samples and determination of suspended solids (SS).....	51
3.4.2	Electrical conductivity and pH .....	52
3.4.3	Alkalinity.....	52
3.4.4	Absorbency at UV (254 nm) and VIS (400 nm) .....	52
3.4.5	Major anions.....	52
3.4.6	Major cations.....	53
3.4.7	Analysis of Aluminium fractionation.....	53
3.4.8	Phosphorous fractionation in EUTROPIA project water sample.....	53
3.4.9	The carbon, nitrogen and phosphorus autoanalyser .....	55
3.4.10	Analysis of Phosphorous.....	55
3.4.11	Analysis of TON, NO <sub>3</sub> -N, NH <sub>4</sub> -N and DOC .....	56
3.4.12	Analysis of P and SS in Morsa monitoring program.....	56
3.4.13	Compilation of P- data.....	57
3.5	Elution and analysis of DGTs samples.....	58
3.5.1	Elution of Metsorb and ferrihydrite gels .....	58
3.5.2	Analysis of DGT samples.....	58
3.6	Calculation of flow-weighted mean concentration and flux of P.....	59

3.7	Statistical analysis .....	59
3.7.1	Hierarchical cluster analysis.....	59
3.7.2	Principal component analysis.....	60
4	Results and discussion.....	60
4.1	Results from water sample .....	60
4.1.1	Stream water pH and alkalinity .....	60
4.1.2	Major cations and anions distribution .....	62
4.1.3	Concentration of Dissolved natural organic carbon .....	66
4.1.4	Distribution of total N .....	67
4.1.5	Distribution of total phosphorus and its fractions (EUTROPIA data set).....	68
4.1.6	Seasonal and yearly variation in the total-P concentrations (Bioforsk data set) .....	78
4.1.7	Flow-weighted mean concentration of SS.....	79
4.1.8	Flux of total-P to the lake .....	81
4.1.9	Total-P fractions (EUTROPIA data set) during the snow free period in the Støa1 and Dalen streams .....	89
4.1.10	Statistical analysis on water samples (EUTOPIA data set).....	91
4.2	Results from DGT samplers -laboratory and field evaluation.....	94
4.2.1	Uptake of the organic P compounds AMP and IP <sub>6</sub> in a laboratory test.....	94
4.2.2	Diffusion coefficients calculated from the laboratory test .....	96
4.2.3	Elution efficiency .....	99
4.2.4	Sampling precision of P by DGT samplers at the sampling location Støa1 .....	100
4.2.5	Fraction of total-P determined from DGT samplers and in the stream water.....	101
4.2.6	Organic P fraction determined from DGT samplers .....	103
4.2.7	Fraction of free-PO <sub>4</sub> determined from DGT samplers and in the stream water.....	106
	Conclusion.....	107
	List of Appendix.....	119



## List of figures

Figure 1: The Morsa Catchment (Norwegian Forest and Landscape Institute, 2011).....	2
Figure 2: Concentration of Total-P in Storefjorden and Western Vansjø from 1976-2010(Skarbøvik et al., 2011).....	6
Figure 3: Systematic representation of global P cycle (Roncal, 2009).....	15
Figure 4: Conceptual idea of P processes in the lake. P-DNOM = Dissolved natural organic material bound phosphorous, P-particales= Particulate bound phosphorus, PO <sub>4</sub> = free orthophosphate (Vogt, 2011 (Pers.comm)). .....	16
Figure 5: The speciation of the orthophosphate species as the function of the pH in (A) Støa1 stream and (B) Huggenes stream, with window showing the range in which pH were measured in these streams. The mean water chemistry and concentration of total-P found in the Støa 1 and Huggenes streams were used in this calculation. ....	17
Figure 6: The solubility of phosphate minerals as the function of the pH (Stumm & Morgan 1996, modified by Roncal, 2009). Window shows the pH range that is found in the different stream samples from Western Vansjø catchment. ....	18
Figure 7: Transport and site management factors influencing the potential for P loss from agricultural land to surface waters (Sharply, 2001). ....	21
Figure 8: Yearly amount of precipitation for Eastern Norway 1900-2011 relative to the norm (Met.no 2012).....	25
Figure 9: Temperature deviations from the norm during winter in Eastern Norway from 1900-2011 (Met.no 2012).....	25
Figure 10: The structure of DGT device (Zhang, 2005).....	27
Figure 11: Schematic representation of the steady state concentration gradients in a DGT device in contact with aqueous solutions (Zhang, 2005). ....	30
Figure 12:Temperature dependence curve of D is described in a separate function from 0 <sup>0</sup> C to 30 <sup>0</sup> C (Røyset 2011, (Pers.comm)).....	32
Figure 13: The Vansjø-Hobøl Catchment with monitoring sites of the studied streams indicated by red points (Norwegian Forest and Landscape Institute, 2011), revised by Alexander Engebretsen).....	35
Figure14:Map showing the marine limit of the Vansjø-Hobøl Catchment (with height above sea level) (Skarbøvik et al., 2007). ....	36
Figure 15: Land use distribution map of Western Vansjø catchment with boundaries of the sub-catchment of the studied streams (Norwegian Forest and Landscape Institute, 2011) revised by Alexander Engebretsen). ....	38
Figure 16: Percentage of land-use distribution in the catchments of the studied streams sorted in terms of increasing percentage of forest (data from Skarbøvik et al., 2011). ....	39
Figure 17: Erosion risk distribution in Western Vansjø catchment with boundaries of the sub-catchment of the studied streams (Norwegian Forest and Landscape Institute, 2011, revised by Alexander Engebretsen). ....	42

Figure 18: Temperature from Rygge (Senorge.no, 2011) and runoff from Skuterud stream (Bioforsk-data) during the hydrological years (A) 2006/2007 and (B) 2007/2008. The blue line is the hydrograph showing runoff data. Red line is the reference line for 0 <sup>0</sup> C temperatures. ....	43
Figure 19: Temperature from Rygge (Senorge.no, 2011) and runoff from Skuterud stream (Bioforsk-data) during the hydrological years (A) 2008/2009 and (B) 2009/2010. The blue line is the hydrograph showing runoff data. Red line is the reference line for 0 <sup>0</sup> C temperatures. ....	44
Figure 20: Auto sampler installed at sampling site of the Dalen (Photo taken by Rolf D. Vogt 29.08.11).....	46
Figure 21: Picture of Staø1 stream (Photo taken by Rolf D. Vogt 29.08.11).....	46
Figure 22: (A) Illustration of how the DGTs were deployed to the water surface (Mohr, 2010). (B) Photo of the Støal stream where DGTs were deployed (Photo taken by Rolf D. Vogt 29.08.11). ....	48
Figure 23: (A) Molecular structure of IP <sub>6</sub> (B) Molecular structure of AMP (Figures are from Wikipedia, 2011). ....	49
Figure 24: (A) 50 L tank which was used as exposure chamber with motorized lid, (B) Lid for tank with 15 volt electrical motor on top and circular rotor plates mounted below the lid on which Metsorb and ferrihydrite DGTs were fitted interlock clips. ....	49
Figure 25: The phosphorus fractionation scheme for water samples (Modified from Vogt, 2011(Pers.comm)).....	54
Figure 26: Instrument setup of CNP autoanalyser (Røyset, 2011(Pers.comm)). ....	55
Figure 27: pH in the nine investigated streams. Bars show median values. The red and black lines represent 25 <sup>th</sup> and 75 <sup>th</sup> percentiles of data series value. Numbers of data are shown at the bottom of graph.....	61
Figure 28: Mean concentration of major cations and anions in the nine investigated streams. For each stream, the first column represents the concentration of cations and the second column represents the concentration of anions. Numbers of data are shown at the bottom of graph. ....	64
Figure 29: Median concentration of dissolved organic carbon (DOC) in the investigated streams. The black and red lines represent 25 <sup>th</sup> and 75 <sup>th</sup> percentiles of data series value. Numbers of data are shown at the bottom of graph. ....	67
Figure 30: Concentration of nitrate, organic bound N and ammonia in the nine investigated streams. Numbers of samples are shown at the bottom of graph. ....	68
Figure 31: Concentration of total-P in the nine investigated streams (EUTROPIA data set). The black and red lines represent 25 <sup>th</sup> and 75 <sup>th</sup> percentiles of data series value. Numbers of data are shown at the bottom of graph. ....	69
Figure 32: Percent distribution of P fractions(EUTROPIA data set). Numbers of data are shown at the bottom of graph. ....	71
Figure 33: Concentration of total-P and P fractions during different hydrological regimes (EUTROPIA data set). *E indicates the samples collected during the hydrological discharge episodes. The red line shows the environmental goal for Western Vansjø. Numbers of data are given in Appendix (see Table A9, Appendix C.1) .....	73
Figure 34: Percent distribution of total-P fractions during different hydrological regimes (EUTROPIA data set). *E indicates the samples collected during the hydrological discharge episodes. ....	73

Figure 35: Total-P fractions of higher flow regime in the Støa1 stream (EUTROPIA data set).....	76
Figure 36: Total-P fraction of lower flow regime in the Støa1 stream (EUTROPIA data set). ....	76
Figure 37: Total-P fraction during different hydrological regimes in the Huggenes stream (EUTROPIA data set). HF and LF denote the samples collected during the high flow and low flow regimes, respectively.....	77
Figure 38: Flow weighted mean concentration of TP in the nine investigated streams during the four hydrological years (Bioforsk data). The red line shows the environmental goal for Western Vansjø (50µg/L). ....	79
Figure 39: Flow weighted mean concentration of SS in the nine investigated streams during the four hydrological years (Bioforsk data). ....	80
Figure 40: Relation between the SS and total-P in the (A) Vaskeberget and (B) Huggenes streams (Bioforsk data).....	81
Figure 41: Relation between the SS and total-P in the (A) Augerød and (B) Guthus streams (Bioforsk data).....	81
Figure 42: Inter-annual fluctuations in flux of total-P to the lake from the nine investigated streams (Bioforsk data).....	82
Figure 43: Estimated daily total-P release (g/daa/day) in the Støa1 stream for 06/07. ....	83
Figure 44: Estimated daily total-P release (g/daa/day) in the Augerød stream for 06/07. ....	83
Figure 45: Estimated daily total-P release (g/daa/day) in the Støa1 stream for 07/08. ....	84
Figure 46: Estimated daily total-P release (g/daa/day) in the Augerød stream for 07/08. ....	85
Figure 47: Estimated daily total-P release (g/daa/day) in the Dalen stream for 07/08.....	85
Figure 48: Estimated daily total-P release (g/daa/day) in the Støa1 stream for 08/09. ....	86
Figure 49: Estimated daily total-P release (g/daa/day) in the Augerød stream for 08/09. ....	87
Figure 50: Estimated daily total-P release (g/daa/day) in the Dalen stream for 08/09.....	87
Figure 51: Estimated daily total-P release (g/daa/day) in the Støa1 stream for 09/10. ....	88
Figure 52: Estimated daily total-P release (g/daa/day) in the Augerød stream for 09/10. ....	88
Figure 53: Estimated daily total-P release (g/daa/day) in the Dalen stream for 09/10.....	89
Figure 54: Concentrations of P fractions during the snow free period 22.3.2011 to 19.9.2011 in the Støa1 stream. The red line shows the environmental goal for Western Vansjø (50µg/L).....	90
Figure 55: Concentrations of P fractions during the snow free period 22.3.2011 to 19.9.2011 in the Dalen stream. The red line shows the environmental goal for Western Vansjø (50µg/L). ....	91
Figure 56: Dendrogram for P-pools with all explanatory variables. ....	92
Figure 57: PCA loading plot .....	93
Figure 58: (A) Mass of AMP accumulated by Metsorb gel as a function of time and (B) The concentration of AMP in the test solutions throughout the experiment. ....	94

Figure 59: (A) Mass of AMP accumulated by ferrihydrite gel as a function of time and (B) The concentration of AMP in the test solutions throughout the experiment. ....	95
Figure 60: (A) Mass of IP <sub>6</sub> accumulated by ferrihydrite gel as a function of time and (B) The concentration of IP <sub>6</sub> in the test solutions throughout the experiment. ....	96
Figure 61: (A) Total-P and (B) PO <sub>4</sub> -P extraction efficiency from the field samples. ....	100
Figure 62: The concentration of bio available fraction of total-P (organic-P + free-PO <sub>4</sub> ) measured in the field using Metsorb and ferrihydrite DGT and determined directly from the stream water. ....	102
Figure 63: Correlations between concentrations of total-P fractions measured directly and by using DGT samplers. ....	102
Figure 64: (A) Concentration of organic P measured by using Metsorb and ferrihydrite DGT samplers and (B) correlation between the two samplers. ....	104
Figure 65: Correlations between concentrations of organic P fraction measured directly and by using DGT samplers. ....	104
Figure 66: Percent Organic P in the fractions of total-P (org P +free-PO <sub>4</sub> ). ....	105
Figure 67: The concentration of free-PO <sub>4</sub> measured in the field using Metsorb and ferrihydrite DGT and determined directly from the stream water. ....	106
Figure 68: Correlation between the stream water free-PO <sub>4</sub> concentrations and concentrations of free-PO <sub>4</sub> measured by using DGT samplers. ....	107

## List of tables

Table 1: Lake status based on chlorophyll a ( $\mu\text{g/l}$ ), total P ( $\mu\text{g}$ ), total N ( $\mu\text{g/l}$ ) and secchi depth (m) and $\text{O}_2$ (mg/l) for natural eutrophic lake such as Vansjø (Direktoratgruppa Vanndirektivet, 2009).....	11
Table 2: Overview of the most common equations used to describe diffusion processes (Garmo et al., 2003).....	31
Table 3: Names, catchment sizes of the nine sampling streams (Skarbøvik et al., 2011).....	39
Table 4: The different quaternary deposit types of the nine sites (Norwegian Forest and Landscapes Institute, 2011).....	40
Table 5: Texture groups and erosion risks of the plow soil layers in catchments of the studied streams (Norwegian Forest and Landscape Institute, 2011).....	41
Table 6: Overview and terms for different P fractions.....	54
Table 7: Basic principles for analysis methods for TON, $\text{NO}_3\text{-N}$ , $\text{NH}_4\text{-N}$ and DOC.....	56
Table 8: Systematic presentation of elution process.....	58
Table 9: Alkalinity in the nine investigated streams.....	62
Table 10: Concentration of $\text{Fe}_2\text{O}_3$ in the sediment samples (Gebreslasse, 2012).....	65
Table 11: Diffusion coefficients obtained from the lab experiment with AMP test solution.....	97
Table 12: Diffusion coefficients obtained from the lab experiment with $\text{IP}_6$ test solution.....	97
Table 13: Comparison of diffusion coefficients obtained by DGT theory and from Buffle's equation.....	98
Table 14: Elution efficiency accessed.....	100
Table 15: Sampling precision of total P by DGT samplers containing Metsorb and ferrihydrite at Støal stream.....	101

## Symbols and Abbreviations

Ali	Inorganic labile aluminium
Alo	Organic monomeric aluminium
AMP	Adenosine monophosphate
ATP	Adenosine triphosphate
APA	Agarose polyacrylamide hydrogel
Bioforsk	The Norwegian institute for agriculture land and Environmental research
C	Carbon
Ca-P	Calcium bound phosphorus
Co	Time average concentration
CNP-autoanalyser	Carbon, nitrogen and phosphorus auto analyser
D	Diffusive coefficients
DBL	Diffusive boundary layer
$D_{DC\ ferrihydrite}$	Diffusive coefficients for ferrihydrite DGT sampler
$D_{DC\ Metsorb}$	Diffusive coefficients for Metsorb DGT sampler
DGT	Diffusive gradients in thin film
DOC	Dissolved organic carbon
DON	Dissolved organic nitrogen
DOP	Dissolved organic phosphorus
DNOM	Dissolved natural organic matter
DNA	Deoxyribonucleic acid
E	Episodes caused by snowmelt and precipitation
EU	European union
EUTROPIA	Watershed eutrophication management through system oriented process modelling of Pressures, Impacts and Abatement actions)
Fe(II)	Ferrous iron,
Fe(III)	ferric ion
Free-PO <sub>4</sub>	Free orthophosphate determined as phosphorus
IP <sub>6</sub>	Inositol hexaphosphate
LMW	Low molecular weight
N	Nitrogen
NIVA	Norwegian Institute for Water Research
NINA	Norwegian Institute for Nature Research
NIBR	Norwegian institute for urban and regional research
NO <sub>3</sub> -N	NO <sub>3</sub> - determined as N
OECD	The Organization for Economic Co-operation and Development

Organic P	Organic bound phosphorus(dissolved fraction)
P	Phosphorus
PP	Particulate bound phosphorus
RCN	Research council of Norway
RNA	Ribonucleic acid
RPM	Rotations per minutes
RSD	Relative standard deviation
Total-P	Total phosphorus
WHO	World Health Organization
WFD	European Water Frame Work Directive
UIO	University of Oslo
UK	United kingdom
USEPA	United State Environment Protection Agency

# **1 Introduction**

## **1.1 World water resources with emphasis on water pollutants**

Water is an essential for life and it is directly connected to the quality of environment and human life. Throughout history, the world has witnessed increasing demands for reliable, good quality and inexpensive water supplies for domestic consumption, irrigation in agriculture, industry and fisheries. There has also been increasing demands for hydrological regimes that support healthy and diverse ecosystems. This requires that the waters are devoid of interference of pollutants, as water pollution threatens human health and quality of life (UNESCO, 2005; European Commission, 2011). Several different major water pollutants are raising global concerns due to their detrimental environmental impacts. These pollutants are released to the surface waters from point and non-point sources. Diffuse leaching of nutrients from agricultural land due to excess use of fertilizers is the main cause of poor water quality. Influx of nutrients to lakes may cause imbalance in the biogeochemical cycling of nutrients in the lake and thereby deterioration of the water quality (European Commission, 2006). This affects the ecosystem services provided by the lake such as the habitat for aquatic biota and birds, the use of water as a resource for safe drinking water and for recreational purposes.

## **1.2 Water Framework Directive (WFD)**

There has been increased demand by citizens and environmental organization for clean and good water quality. This growing petition spurred the European Commission to call representatives from 25 European countries, including Norway, to take revision on water legislations and to identify water pollution as one of their main environmental issue (European Commission, 2011; European Commission, 2010). In 2000, the EU took an ambitious and comprehensive step towards a more sustainable management of our water resources when it adopted the water legislation known as Water Framework Directive (WFD). This directive established a legal obligation to protect and restore the quality of waters across Europe. The Directive introduced an innovative approach to water management and set a goal for all of EU's surface waters and ground waters to reach good surface water status and that the condition of all water reserves should not have large deviations from their natural condition by the year 2015 (Vannportalen, 2011; European Commission, 2011; European



Commission, 2010). The WFD has the effect that scientists and environmental managers are being required to assess the original and present state of the environment, and to predict future changes based on land-use, climate change and anthropogenic loading scenarios and also to predict effect of different abatement actions (European Commission, 2011; European Commission, 2010). Norway has taken part in the implementation of WFD since 2001. In 2007 the WFD was adopted by the Norwegian government and it incorporated into Norwegian water regulation (WFDN, 2011).

### 1.3 Background information about the Morsa catchment

Vansjø is a large eutropic lake, in the Morsa watercourse, situated near the city of Moss in the Southeast of Norway (Figure 1). The lake is divided into two main basins, the larger Storefjorden (eastern basin), and the smaller and shallower Western Vansjø (Vanemfjorden).

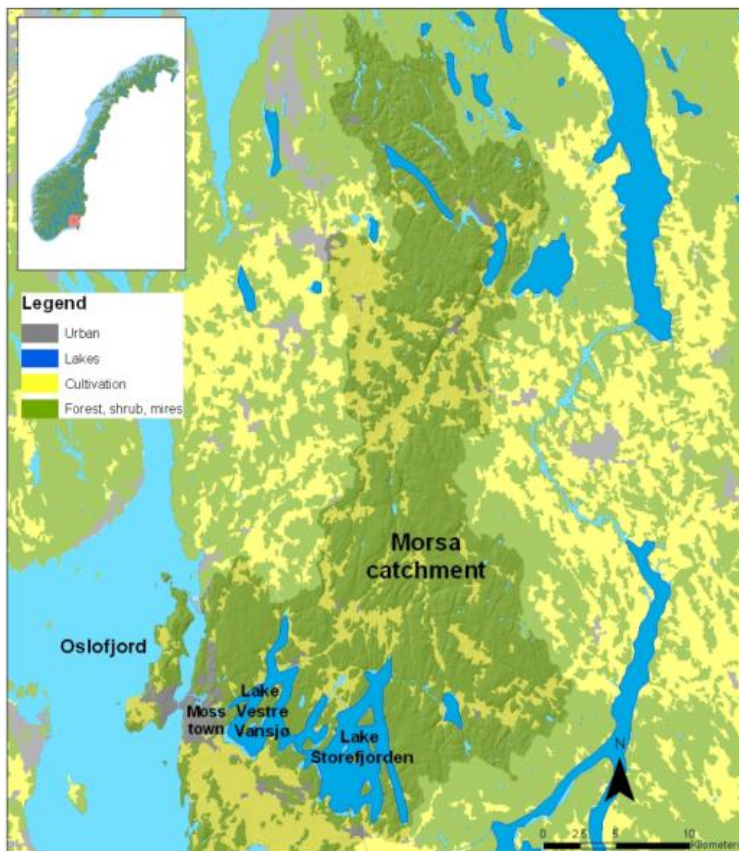


Figure 1: The Morsa Catchment (Norwegian Forest and Landscape Institute, 2011).

Only 10 % of the Morsa catchment is situated above the marine limit at approx. 214 m a.s.l. These areas are mainly found in northern part of the catchment. The rest of the catchment area is located below the marine limit and soils are naturally rich in nutrients (Skarbøvik & Bechmann, 2010). This is due to marine clays with P-containing apatite.

Since year 1950, there have been significant changes in land use distribution in the southeast Norway. Until 1980, the amount of land used for grain producing agricultural purpose increased by 30 to 80 %, with a comparable reduction in grassland over a 30 year period. The change in land use had led to decrease water quality (Lundekvam et al., 2003). About 15 % of the Morsa catchment area is agricultural land. This may not be much in a European context, but the catchment is one of the most cultivated areas in Norway (Skarbøvik et al., 2011). In Norway, only 3 % of the land is used for agriculture purpose. This is due to unfavourable conditions for agriculture in large parts of the country (Lundekvam et al., 2003).

In this master thesis, the Western Vansjø catchment with largest problem of eutrophication is used as a study site. The western part of Lake Vansjø, Western Vansjø, has experienced serious problem of harmful blooming of toxic algae due to high local P loading from their sub-catchments, especially after the flood in year 2000. In 2006, the concentration of microcystis was found to be 7.5µg/L. This value is close to the limit of 10µg/L where the World Health Organization (WHO) discourages people from swimming or bathing. The Norwegian Institute of Water Research (NIVA) recommended the local health authorities to dissuaded public from bathing due to the likely occurrence of layers of blue green algae that may float to the lake surface carrying toxic concentrations of microcystis (Bjørndalen et al., 2007). About 25 % of the land is used for agriculture practice in the Western Vansjø catchment and phosphorous losses from the local catchment of Western Vansjø are higher, especially from sub-catchments where potatoes and vegetable are grown (Aquarius, 2010). The Western Vansjø lake receives nutrient loading from many inlet streams which have total-P concentration that are higher than the environmental goal for Western Vansjø (50 µg P/L), especially in the streams draining watersheds with high contingency of agriculture land. Phosphorus losses from agriculture soils constitute about 90% of the anthropogenic release of total-P to the lake Western Vansjø (Skarbøvik & Bechmann, 2010).

The Morsa catchment is a pilot study area for the implementation of the WFD. The eutrophication condition of the lake Vansjø has been a problem since 1950s, and many efforts

and mitigation actions (e.g. reduced fall tillage and reduced P fertilizer application, vegetated buffer zones and constructed wetlands) are implemented to improve the poor water quality (Skarbøvik & Bechmann, 2010), especially in the Western Vansjø catchment. These abatement actions are further described in section 1.4.

#### **1.4 Mitigation actions and current status of Western Vansjø**

During the last decade, many efforts have been undertaken to improve the water quality of Lake Vansjø (Skarbøvik & Bechmann, 2010). At the end of the 1970s, the Co-ordinating Committee for Vansjø-Hobøl River started a campaign to renovate the sewage systems. During the 1990s, several measures were conducted with the aim to reduce the nutrient runoff from agriculture land, accompanied with actions to remove the remaining point sources from household sewage water (Hovedstyret for Morsa-prosjektet, 2003). In spite of these efforts, no decline in the amount algae was observed in the lake Vansjø. In 1999, seven municipalities, regional authorities and landowner throughout the Morsa catchment joined forces and started the Morsa project. The aim of the project was to apply coordinated mitigation measures that would lead to improvement in the water quality (Hovedstyret for Morsa-prosjektet, 2003).

Based on researchers recommendation in 2004, investigation of lake sediments were conducted in order to gain knowledge regarding the role of internal cycling of nutrients from the sediments of the lake. The concentration of phosphorus was found to be relatively poor in the sediments compared with other nutrient rich lakes. This led to indicate that internal loading of sediments was likely not an important factor governing the high concentrations of phosphorus in the lake water (Andersen & Færøvig, 2007). After this documentation, the investigations and efforts were continued in 2006 and 2007. Results from the other investigations showed that local supply of phosphorus was found to be doubled as high as previously assumed (Vannområdeutvalget, 2011). As a result of the efforts to reduce fertilization, the total supply of P fertilization year 2007 was 8.6 tons less than 2004, corresponding to a reduction of approximately 47 % of total (Øgaard & Bechmann, 2010). Further abatement actions were implemented through an integrated “Mitigation Project for Western Vansjø”. This project was funded by the government and collaborated with public agricultural management, agricultural advisers, farmers and the research institute Bioforsk (Skarbøvik & Bechmann, 2010). In 2008, farmers around the Western Vansjø were

encouraged to sign an environmental concerning contract. Approximately 78% of the farmers had signed contract and thus became the part of this environmental concern program. Through the contract, the farmers received a financial compensation for covering reduced income caused by mitigation options (Skarbøvik & Bechmann, 2010). The abatement actions that were included in the agreement are following:

- Use of less P fertilizer than the national standards for P fertilization. The main aim behind this action was to decrease the access P content in the soils (Øgaard & Bechmann, 2010).
- No soil ploughing in the autumn and no growing of potatoes or vegetables on fields that are frequently flooded. This was done in order to reduce the erosion of particulate bound P by surface water runoff when soils are saturated with water (Skarbøvik & Bechmann, 2010).
- Establishment of permanent grass buffer zones towards open waters and streams. This was done in order to reduce the flux of P through surface runoff and erosion (Øgaard & Bechmann, 2010).
- Establishment of constructed wetlands. These wetlands prevent particles and nutrients from reaching the lake. Constructed wet land holds back 20 to 25% of the total amount of phosphorus reaching the lake (Braskerud & Hauge, 2008).

Because of mitigations measures and as a recovery from the flood in 2000, a somewhat decreasing trend in the total phosphorus concentrations in the Western Vansjø Lake have been achieved. The ecological status for Storefjorden was classified as moderate in 2008 based on total phosphorus and chlorophyll-a concentration and according to WFD classification guidelines (Table 1). Western Vansjø was also classified as moderate based on total phosphorus, total nitrogen and chlorophyll-a concentration. In 2010, the average concentration of total-P was found to be 27 µg P/L. This is close to the value measured in 1989 (Vannområdeutvalget, 2011).

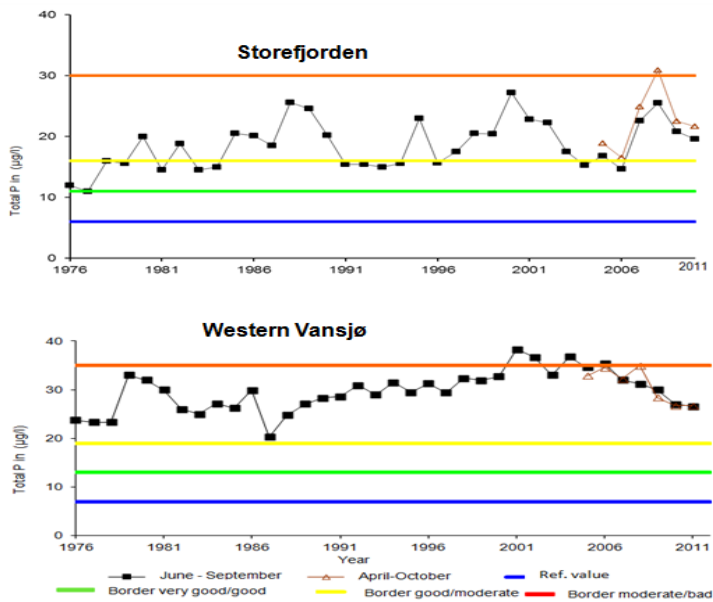


**Figure 2: Concentration of Total-P in Storefjorden and Western Vansjø from 1976-2010 (Skarbøvik et al., 2011).**

The effects of the abatement actions are positive but water conditions are still not satisfactory. As shown in Figure 2 there is no apparent improvement in the concentration of total P in Storefjorden, while in Western Vansjø there are improvements but, effects of abatement actions are limited. The processes that govern the P-fluxes to the lake can be affected by several different factors. Fluxes of phosphorus from the terrestrial to the aquatic environment are known to be strongly governed by climate change. Mitigation measures may thus be greatly offset by changes in environmental pressures. Over the past 20 years there has been an increased amount of precipitation and average winter temperature have usually been 2<sup>0</sup>C above the norm in eastern Norway. Milder winters and more rainfalls with high intensity are expected to continue due to climate changes. Studies from Western Vansjø show that discharge episode events may lead to higher flux of nutrients to the lake. Climate change may also lead to a larger risk for flooding due to increased precipitation. It is postulated that the flood in 2000 led to deteriorated water quality of the Western Vansjø Lake. This is believed to be one of the major factors that have disguised the improvement of the lake condition despite considerable mitigation measures (Vannområdeutvalget, 2011). The precipitation in the summer 2011 was almost twice than the norm and new flood was registered in September 2011 (met.no, 2011). Flooding of agricultural areas causes larger P release from the soil to the water body (Aquarius, 2010) through overland flow and subsurface flow. It is furthermore

hypothesized in this thesis that the reducing conditions during flooding of soils lead to reduction of Fe (III) with subsequent loss of the soils capacity to hold phosphate. Therefore, more attention is given to episode studies in EUTROPIA project. Reduction in acid rain is another important factor that governs the flux of phosphorous to the lake. Reduced deposition of acid rain has led to a reduction in the leaching of labile inorganic aluminium ( $Al_i$ ). This aluminium is known to be a strong flocculate and sedimentation agent for phosphate. Furthermore, the reduced acid rain is believed to be the main cause for the increased colour and levels of dissolved natural organic matter (DNOM) that is seen in acid sensitive regions previously suffering acid rain in the Norway and the UK. In natural systems the main transport mechanism for phosphorous is by DNOM. The decreased acid rain has thus caused an increased in natural background flux of P.

### **1.5 Development of new sampling technique DGT (Diffusive gradient in thin film)**

In natural waters, phosphorus exists as both inorganic and organic species distributed between the dissolved, colloidal and particulate phases (Maher & Woo, 1998). In the term of eutrophication, organic P and free orthophosphate are most important total-P fractions for algae growth. Free orthophosphate can be measured by several different methods and techniques in water sample. It required several different procedures in order to use these methods and techniques e.g. sample collection, filtration and preservation, transported and storage prior to analysis. Some of these requirements are time consuming and it is difficult to maintain the original sample composition. In some cases, processes such as precipitation, adsorption, hydrolysis, and microbial uptake and release during storage can affect the original concentration of free orthophosphates and sample may not be representative of that concentration at time of sampling (Maher & Woo, 1998; Monbet & McKelvie, 2007; Panther et al., 2010). The diffusive gradient in thin film (DGT) is a well-established in situ sampling technique that is believed to selectively collect the free orthophosphate ions in water. Little is known of the uptake of organic P by DGT samplers. Development of the new sampling techniques is a part of this master thesis. DGT samplers containing Metsorb and ferrihydrite adsorbents were used to assess time-averaged levels of total-P fractions in the stream water. The ability of both DGTs to capture fractions of total-P is evaluated through laboratory experiments and compared.

## **1.6 EUTROPIA project**

This master thesis is a part of the EUTROPIA (Watershed eutrophication management through system oriented process modelling of Pressures, Impacts and Abatement actions) project<sup>1</sup>. The EUTROPIA project is an interdisciplinary research collaboration, which links the University of Oslo with the research institutes NIVA, NINA, Bioforsk, UMB-IØR, and NIBR. The project is established to address the challenges related to poor water quality and generate more process understanding needed in order to meet the aim of EU Water Framework Directive. The main aim of this project is to understand the processes and mechanisms that govern the higher P flux in the Lake Vansjø and thereby increase our ability to predict effects of abatement measures and changes in the environment. The main strategy of the project is to assess temporal and spatial variation in different P fractions, and to identify thresholds and barriers in society towards abatement actions. The project has five different work packages. This master study is related to the first two work packages, which are: (1) Development of sampling and laboratory methods for P fractionation and (2) Catchment processes - the influence of climate and land-use on nutrient fluxes into aquatic systems

## **1.7 The aim of the study**

The main aim of this study is to get a better understanding of the biogeochemical and physio-hydrological processes in the catchment that governs the fate and transport of the total-P fluxes into the lake. Main focus of the study is related to the water chemistry part and the development of the new sampling method. Water samples were collected from nine different streams in the Western Vansjø catchment and analysed for different P fractions. The sub-catchment of these streams differs in land use distribution, slope, soil type and catchment sizes. Most of these sub-catchments represent “hot spots” for total P loading to the lake Western Vansjø. This study has been conducted in order to get better understanding of the effect of land use on the leaching of P fractions and to identify high-risk stream sites in terms of their contribution of different P-fractions. The total-P fractions under different hydrological regimes were studied to look at the effect of differences in runoff intensity on total-P concentrations in the streams. The data from four hydrological years (2006-2010) are used to

---

<sup>1</sup> <http://www.mn.uio.no/kjemi/english/research/projects/eutropia/index.html>

access how the effect of climate change affect the mobility and transport of total-P fractions and thus may disguise the effect of abatement actions.

In term of eutrophication, only a minor fraction of P is considered to be bioavailable for algae growth. DGT samplers containing Metsorb and ferrihydrite adsorbents were used in this study to collect this bioavailable fraction (org-P and free-PO<sub>4</sub>) of total-P. DGT containing ferrihydrite adsorbents is a well-established method, whereas DGT containing Metsorb adsorbents is new and only three to four studies have been conducted using this material. The main focus of this part of the study was to improving the knowledge on performance of Metsorb and ferrihydrite adsorbents for simultaneous sampling of organic P and determine diffusion coefficients for organic P if the performance was satisfactory. This is the first time that uptake efficiency of Metsorb DGT for organic P is evaluated. Comparison between the concentration of P fractions in water samples and results obtained by DGT samplers will be used to get better understanding of the bioavailable fraction (org-P and free-PO<sub>4</sub>) of the total phosphorus.

## **2 Theory**

### **2.1 Eutrophication and phosphorous chemistry**

#### **2.1.1 Eutrophication**

The word Eutrophication comes from Greek eutrophos meaning well-fed, implying that the term describes an ecosystem that receives excess amount of nutrients. Eutrophication occurs naturally as a very slow process which is also known as the natural aging process of a water body. A distinction is therefore made between “natural” and “cultural” eutrophication (Rast & Thornton, 1996). Natural eutrophication is highly dependent on natural characteristics and geology of the catchments. The term cultural eutrophication refers to an increased anthropogenic influx of nutrients causing large-scale algae blooms. Cultural eutrophication is thus defined as a human interference that causes imbalance in the biogeochemical cycling of nutrients (Rast & Thornton, 1996; Henderson & Markland, 1986). According to United State Environment Protection Agency (USEPA), the process of eutrophication is identified by several different criteria (Henderson & Markland, 1986) e.g. excess amount of nutrients,



especially P and N, increased amount of suspended solids, low concentrations of hypolimnetic dissolved oxygen, decreasing light penetration and higher P concentration in sediments.

There are several different factors that cause imbalance in the biogeochemical cycling of nutrients e.g.:

- Diffuse access leaching of nutrients from agricultural land due to overuse use of inorganic fertilizers and manure
- Point sources, such as leakage of sewage from inadequate and/or faulty sewage systems
- Climate change that affects the hydrological and biogeochemical cycles of water bodies

Under the advanced classification system by Water Framework Directive (WFD), there are new definitions that described ecological states of lakes (Direktoratgruppa Vanndirektivet, 2009). This is further discussed in section 2.1.2.

### **2.1.2 Classification of trophic condition**

Nutrients richness and the primary production of lakes are primary parameters that are indicative of the trophic state of lake. A lake with poorly nourished primary production is denoted oligotrophic. Oligotrophic lakes are typically seen as clear water lakes (Dodson, 2005). A lake with highly nourished primary production is denoted eutrophic and apparent by their less transparent water. A medium nourished mesotrophic lake falls between these two groups.

Total-P concentration, chlorophyll a concentration, and water transparency are thus key parameters that are used to determine the trophic state of a lake. It is generally assumed that waters with total-P concentrations exceeding 50µg/L are considered as polluted (Leinweber et al., 2002). The Organization for Economic Co-operation and Development (OECD) regards a lake with total-P concentration between 35-100 µg/L as a eutrophic lake. The problem is that the same amount of total-P can give different ecological response from one lake to another. This causes problem in simply using total-P concentration as a sole criterion for identify

tropic condition. Many lakes have natural high influx of nutrients and are naturally eutropic. OECD classification system does not address whether the tropic condition is problem or not. Addressing this shortcoming, the Directorate group for implementation of the Water Framework Directive published guidelines in 2009 for trophic classification of lakes (Direktoratgruppa Vanndirektivet, 2009). Lake depth, size, region, humus content, alkalinity etc. are used to classify the natural type of a lake. Once the type of lake is established, the total P concentration, chlorophyll a concentration, and water transparency are used subsequently to determine the trophic state of the lake (Table 1).

**Table 1: Lake status based on chlorophyll a ( $\mu\text{g/l}$ ), total P ( $\mu\text{g}$ ), total N ( $\mu\text{g/l}$ ) and secchi depth (m) and  $\text{O}_2$  (mg/l) for natural eutrophic lake such as Vansjø (Direktoratgruppa Vanndirektivet, 2009).**

Status	High	Good	Moderate	Poor	Bad
Chlorophyll a ( $\mu\text{g L}^{-1}$ )	3,5	7	10,5	20	40
Total P ( $\mu\text{g L}^{-1}$ )	7	13	19	35	65
Total N( $\mu\text{g L}^{-1}$ )	300	300	450	550	900
Secchi depth(m)	5	3	2	1	0,5
$\text{O}_2$ ( $\text{mg L}^{-1}$ )	12	9	5	2	1

### 2.1.3 The deterioration of lake

Growth of aquatic biota relies on the availability of several different nutrients, especially carbon (C), nitrogen (N) and phosphorus (P). Since the abundance of C, N and P is regulated by reciprocal interactions between aquatic organisms the molecular ratio of carbon, nitrogen and phosphorus in plankton are generally close to the Redfield ratio ( $\text{C}_{106}\text{N}_{16}\text{P}_1$ ) (Goldman, 1975; Redfield, 1934). This ratio is not constant but changes in response to increasing or decreasing amount of nitrogen and phosphorus (Paytan & McLaughlin, 2007). Phosphorus is found to be the limiting element for primary production in most aquatic system. Control on the fluxes of this nutrient to surface waters is therefore of prime importance in reducing the accelerated eutrophication of fresh water (Sharply & Rekolainen, 1997).

There are several effects of eutrophication on the aquatic environment. The direct effect of eutrophication is an increase in the lake productivity that is initially beneficial to many species such as fish. The high biological productivity provides nourishment for fish and

generate high amount of oxygen in the water (Rast & Thornton, 1996; vanLoon & Duffy, 2007). Gradually, undesirable growth of aquatic biomass becomes so excessive that it reduces water quality. The green colour of the water due to algae blooming, often accompanied by an unpleasant odour, is an early apparent negative effect of the eutrophication (vanLoon & Duffy, 2007). Advanced eutrophication with increased blooming of algae and dissolved oxygen depletion caused by their decomposition leads to problem with the use of the water resources for fisheries, recreation, industries and as raw water source for tap water (Henderson & Markland, 1986; Sharply & Rekolainen, 1997). Algae blooms contribute to reduced light penetration into eutrophic and turbid water body that causes reduced euphotic zone<sup>2</sup> and thereby bears consequences for photoautotroph. When the euphotic zone is reduced, the phototrophic organisms either die or migrate toward surface. The migration toward surface causes increase concentrations of biomass on the surface. This further reduces light penetration into the surface layer (Dodson, 2005; Mohr, 2010).

Wide varieties of methods are available for rehabilitation of eutropic lakes. Eutrophic regime can be recovered to oligotrophic regime by reducing inputs of phosphorus (Carpenter, 2005). However, restoration may be a long time process, especially in the agricultural region, due to leaching of large pools of P in the soils and internal recycling of phosphorus from the lake sediments.

#### **2.1.4 Phosphorous in the earth**

Phosphorus is an essential element for life and the 11<sup>th</sup> most abundant element on the earth. It has no direct toxic effects on animal, plants or humans. Phosphorous practically never exist in pure form in the environment as it is always bound to other elements. Most of the phosphorous found on the earth exists in the form of 180 different minerals (Henderson & Markland, 1986). Phosphorous makes up 0.1% w/w (Stewart, 2005) of the Earth's crust and exists mainly in the form of mineral apatite (Henderson & Markland, 1986). In living cells, phosphate is a central building block of deoxyribonucleic acid (DNA) and ribonucleic acid (RNA). Phosphate also plays a vital role in the storage of energy within low molecular weight nucleotides (e.g. ATP, adenosine triphosphate) (Newesely, 1989) and in the formation of

---

<sup>2</sup> Euphotic zone is the layer of water in which 1% of the surface radiation remains (Klaff, 2002).

phospholipids. Low molecular weight compound, such as AMP (adenosine monophosphate) play an important role as energy sensor and regulator of metabolisms. In vertebrates, phosphate minerals are essential in forming and strengthening of teeth and bones. Phosphate esters of Inositol [ $C_6H_6(OH)_6$ ] (Brady & Weil, 2004) as well as nucleotide fragments (e.g. AMP) are the most abundant dissolved organic phosphorus compounds in the water.

The use of inorganic fertilizers and manure in agriculture is an important anthropogenic source of phosphorous to surface waters. The term phosphate ( $PO_4^{3-}$ ) and phosphorus (P) are generally used interchangeably in the world of fertilizer (Sims & Sharply, 2005). The term phosphate is commonly referred to as orthophosphate and various poly-phosphate forms of phosphorous (Sims & Sharply, 2005). About 80% of the phosphate produced worldwide is used in the production of fertilizer. The rest is used for detergents, animal feed and special applications (Steen, 1998). About 80% of the currently world phosphate productions come from sedimentary deposits, especially from marine deposits. Igneous deposits and their weathering derivatives provide about 17% of the world production. The other 3% comes from residual sedimentary and guano-type deposits (Sims & Sharply, 2005; FAO, 2004). The main raw material of phosphate fertilizer is phosphate containing sedimentary rocks, mainly apatite (Holtan et al., 1988). Approximately 90 % of the mined apatite minerals are used for the production of fertilizers (Djordjic, 2001). The general formula of this P containing mineral is  $Ca_{10}(X)(PO_4)_6$ , where  $X = F^-, Cl^-, OH^-$  or  $CO_3^{2-}$  (Pierzynski et al., 2005). According to their abundances, the three major apatite minerals groups are fluorapatite, hydroxylapatite and chloroapatite. Approximately 95% of phosphorus is found as fluorapatite (Holtan et al., 1988).

From an agricultural perspective it is important that soil P levels are maintained at an optimum level for crop production and plant growth. Even though phosphate is rapidly assimilated by plants and readily bounded to soil particle, the content of total and available phosphorus in many agricultural soils has become so high that a small part of this P can be lost with runoff. This may have large consequences on the recipient aquatic ecosystem (Pierzynski et al., 2005; Brady & Weil, 2004).

## 2.1.5 Global Phosphorous cycle and Phosphorus in water

### 2.1.5.1 Global P cycle

Figure 3 show a schematic representation of the global P cycle. The global cycle of P is unique in having no significant gaseous phase so that the atmospheric content is insignificant. A minor flux of P through the atmosphere is nevertheless found in association with soil dust particles and sea-spray (vanLoon & Duffy, 2007). There is also a possible significant transport by animals preying on marine organism and spreading their guano containing P on land. The redox potential of most soils is way above what is needed for production of phosphine gas ( $\text{PH}_3$ ) which is only produced under extreme anoxic conditions (Barlett, 1986). P is mainly found bound to oxygen as orthophosphate. The valance state of P in phosphate ions is almost always +5.

The global phosphorous cycle has several important pathways. These pathways include exposure of phosphorous bearing rocks to the force of weathering, phosphorus movement from the rocks by physical erosion, the flux of P carried by river to lakes and eventually to the ocean, and the last process involve the marine sedimentation of phosphorus (Ruttenberg, 2003).

Most of the phosphorous in terrestrial environment is derived from the weathering of calcium phosphate minerals, especially apatite (Schlesinger, 1997). It enters the biosphere by the weathering of sedimentary and igneous rocks and erosion of marine clay. The main flux of P in the global P cycle is carried by river (Meybeck,1982) and only 10% of this flux is potentially available to marine biota, the rest is strongly bound to soil particles that are rapidly sedimented on the continental shelf (Schlesinger, 1997). The world average phosphorous concentration in soil is 0.08%w/w while in marine sediments is 0.12%w/w (Nriagu & Moore, 1984). This indicates that P in marine sediments is richer than in the soil. The P resources are non-renewable due to a slow return in the cycle via tectonic uplift of sediments (Henderson & Markland, 1986).

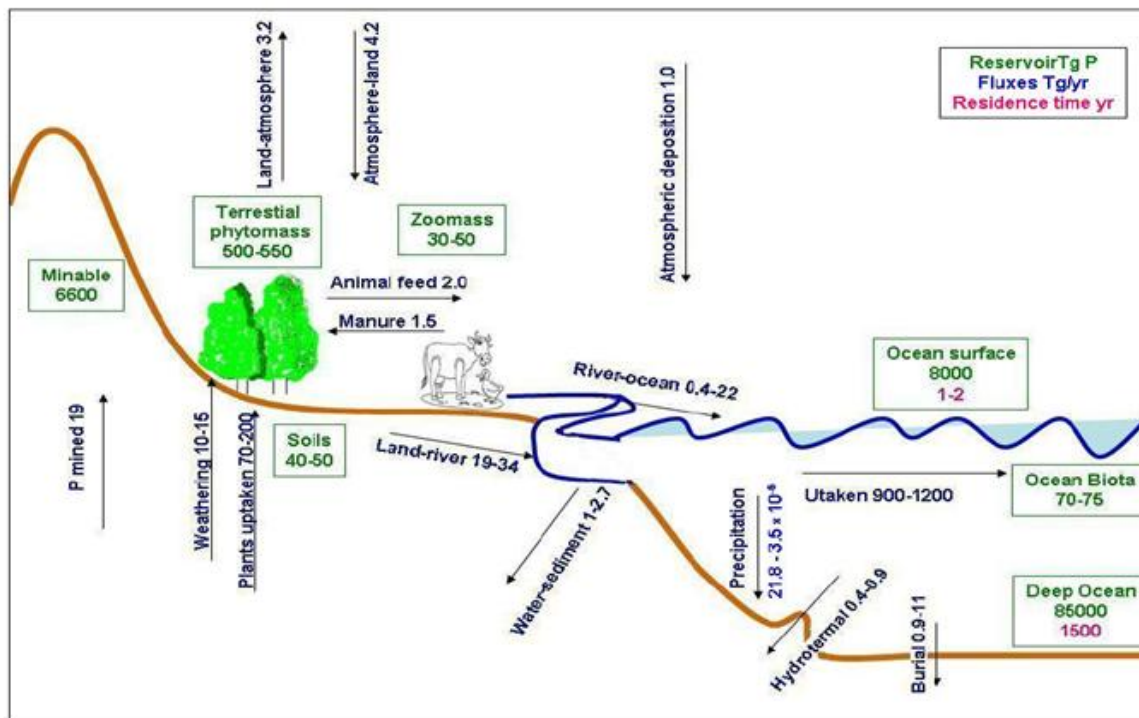


Figure 3: Systematic representation of global P cycle (Roncal, 2009).

### 2.1.5.2 Phosphorus in water

Figure 4 shows conceptual idea of the different phosphorus fraction in the internal P cycles of lakes, together with the major processes that govern fluxes between the fractions of phosphorus. The different P fractions shown in the Figure 4 are further explained in the section 3.4.8. The input of the phosphorus to the lake is very small under most natural condition (Schlesinger, 1997). Transport of particle bound phosphorus is a main transport path of phosphorus entering the lakes (Sonzogni et al., 1982).

The proportion of phosphorus that is found in an available form for assimilation by algae and macrophytes is very small because most of the bio-available P is readily assimilated and bound up in the living biomass. The rest of the P is mainly absorbed to clay particles or bound in dissolved natural organic matter (DNOM). The most important forms of bioavailable phosphorus are the orthophosphates. Orthophosphate is the sum of  $H_3PO_4$ ,  $H_2PO_4^-$ ,  $HPO_4^{2-}$ , and  $PO_4^{3-}$ . Orthophosphates are highly reactive and easily sorbed onto particulate surfaces such as soil and sediments, i.e. the equilibrium between phosphorus found in soils and soluble phosphorus tends strongly towards the phosphorus bound in the soil (Krogstad & Løvstad,

1987). The concentrations of orthophosphate therefore remain typically below detection limit or constitute much less than 1% of the total P in the solution (Ryding & Rast, 1989). An exception is for water draining from phosphate rich sandy soils due to the high infiltration capacity and because sands absorb orthophosphate poorly (Henderson & Markland, 1986). A major point here is that particle size distribution of the soils affects the phosphorus adsorption capacity for soils. Phosphorus adsorption capacity for soils with a large amount of clay and silt content is larger than sandy soils due to larger surface areas (Brady & Weil, 2004).

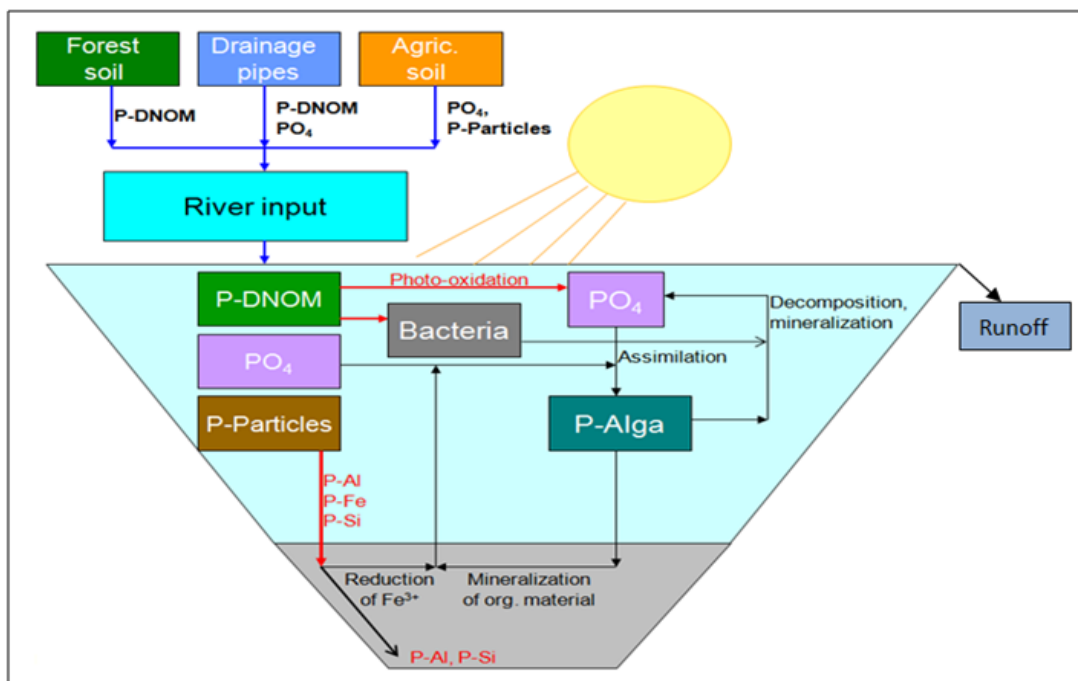
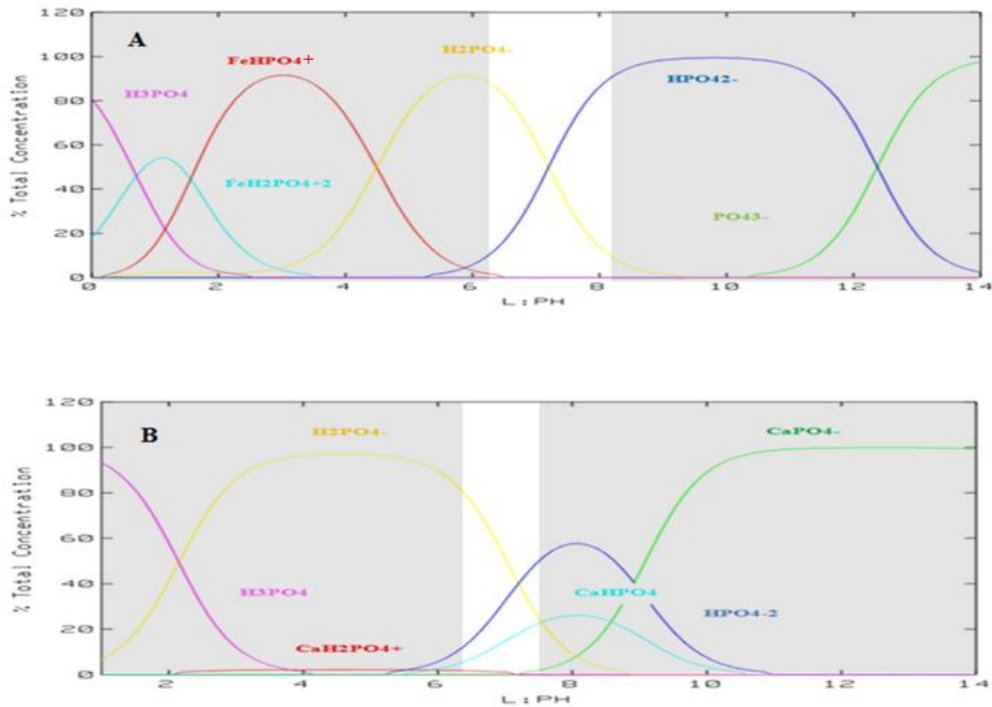


Figure 4: Conceptual idea of P processes in the lake. P-DNOM = Dissolved natural organic material bound phosphorous, P-particales= Particulate bound phosphorus, PO<sub>4</sub>= free orthophosphate (Vogt, 2011 (Pers.comm)).

The speciation and thus the bioavailability of phosphorus in form of orthophosphate are highly affected by oxides and hydroxides of positively charged metals, especially iron, aluminium and calcium. Phosphorus is most mobile at pH from around 6.5 to about 9 due to low solubility of aluminium, iron and calcium bound phosphates both at acidic and alkaline pH (vanLoon & Duffy, 2005). In acid rain exposed environments high concentrations of inorganic Al may be found at pH below 5.5 due to low solubility of Al (OH)<sub>3</sub> at higher pH, whereas elevated concentration of calcium is found at pH above 7 due to the calcium

carbonate weathering. P speciation based on average water chemistry of Støa1 and Huggenes using the MINEQL software program is shown Figure 5.



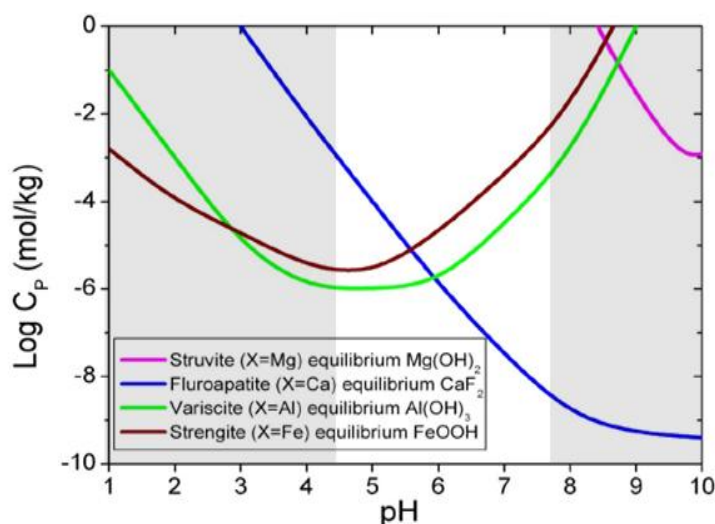
**Figure 5: The speciation of the orthophosphate species as the function of the pH in (A) Støa1 stream and (B) Huggenes stream, with window showing the range in which pH were measured in these streams. The mean water chemistry and concentration of total-P found in the Støa 1 and Huggenes streams were used in this calculation.**

Figure 5 shows the percent distribution of important  $PO_4$  species at different pH in Støa1 and Huggenes stream water (inlet streams from Western Vansjø catchment), with window showing the ranges in which pH were measured in these streams. At pH  $\sim 6.5$ ,  $H_2PO_4^-$  dominates at both Støa1 and Huggenes stream. There is also dominance of  $HPO_4^{2-}$  at Støa1 stream whereas  $CaHPO_4$  and  $HPO_4^{2-}$  species are significant at Huggenes stream. It also illustrates that pH does not affect the solubility of orthophosphate directly, but pH has an effect on the solubility of the metal compounds.

The most common calcium containing phosphate mineral is apatite  $Ca_{10}(PO_4)_6(F, Cl, OH)$  and most common aluminium and iron containing phosphate minerals are variscite  $AlPO_4 \cdot 2H_2O$  and strengite  $FePO_4 \cdot 2H_2O$ , respectively (Lindsay et al., 1989; Stumm &



Morgan, 1996). In natural water, aqueous phosphorus concentration at high pH is limited by the presence of apatite, which is the least soluble species at pH above 6. In contrast, at pH below 6 variscite and strengite may limit phosphate availability (Lindsay et al., 1989; Stumm & Morgan, 1996). The solubility of these phosphate minerals as a function of the pH is shown in the Figure 6. Where the pH is neutral to alkaline orthophosphate precipitates out in the form of apatite compounds with lowest solubility e.g.  $\text{Ca}_3(\text{PO}_4)_2$  or  $\text{Ca}_{10}(\text{PO}_4)_6\text{OH}$  (Brady & Weil, 2004). Below pH 6 the orthophosphate is precipitated out as Variscite and Strengite by equilibrium with  $\text{Al}(\text{OH})_3$  and  $\text{FeOOH}$ , respectively.



**Figure 6: The solubility of phosphate minerals as the function of the pH (Stumm & Morgan 1996, modified by Roncal, 2009). Window shows the pH range that is found in the different stream samples from Western Vansjø catchment.**

### 2.1.6 The effect of red-ox on phosphorous

Release of P due to changing redox condition influences strongly the partitioning of P between the solid and solution phases. Substantial release has been reported to occur when soils are flooded with water due to the heavy rainfall or snowmelt (Ponnamperuma, 1965; Scalenghe et al., 2002). Under anoxic condition, the phosphorous release rates from soils and sediments have been found to increase by an order of magnitude and so greatly accelerate the process of eutrophication (Henderson & Markland, 1986). E.g. a study done by Moore et al. (1993) on the sediment samples from the mud zone of Lake Okeechobee Florida showed that

under aerobic conditions, soluble reactive P concentrations were low ( $\sim 0.1$  mg P/L), whereas under anaerobic conditions soluble reactive P increased to over  $1$  mg P L<sup>-1</sup>. Soluble reactive P was extremely high ( $18$  mg P/L) under reducing ( $E_h < 0$  mV) conditions (Moore et al., 1993).

Depending on the redox potential ( $E_h$ ) in the environment, the redox sensitive element iron may exist as either Fe (II) or Fe (III). Phosphorus forms insoluble compounds, FePO<sub>4</sub> ( $K_{sp} = 4 \cdot 10^{-27}$ ; Aylward & Findley, 2008), with ferric ion (Fe (III)). Furthermore, orthophosphate is often adsorbed to Fe (III) hydroxides and to iron bridging between an organic coating. This phosphate sorption decreases likewise with decreasing redox potential due to the reduction of Fe<sup>3+</sup> to Fe<sup>2+</sup> (Holtan et al., 1988).

A progressive decrease in redox potential accompanied with sequence of reactions along the redox ladder occurs when soils are flooded (Ponnamperuma, 1972). Electrons are released from the biological oxidation of organic matter. After O<sub>2</sub> is depleted other elements serve as electron acceptors. Nitrate is reduced first, followed by reduction of Mn (III), Fe (III) and S(VI) successively (Patrick & Jugsujinda, 1992).

Phosphorus can also form quite insoluble compounds with ferrous iron, Fe (II), e.g. vivianite (Fe<sub>3</sub>(PO<sub>4</sub>)<sub>2</sub>) ( $K_{sp} = 1 \cdot 10^{-36}$ ; Aylward & Findley, 2008). The reason this does not occur to any significant extent is due to that the Fe (II) is trapped by precipitation with sulphide (S<sup>2-</sup>). Under anoxic conditions the next step on the redox ladder is the reduction of sulphate to sulphide. The sulphide formed will compete efficiently with phosphates to bind with Fe<sup>2+</sup> in anaerobic condition since S<sup>2-</sup> reacts with Fe<sup>+2</sup> to form insoluble FeS ( $K_{sp} = 3 \cdot 10^{-19}$ ; Aylward & Findley, 2008) which is less soluble than the iron (II) phosphate minerals. This is the main explanation for why Fe (III) binds phosphate better than Fe (II). Thus, phosphate concentrations in the water logged soils as well as in sediment pore water are indirectly linked to rates of sulphide (S<sup>2-</sup>) production or reoxidation (Roden & Edmonds, 1997). The interaction between phosphorus, iron and sulphur are some of the most important mechanisms that govern the temporal variation in the amount of soluble phosphorus leached from soil to surface waters.

Large amounts of Fe (II) are leached out of anaerobic soils. When this iron is exposed to oxic condition in the stream the Fe<sup>+2</sup> is oxidized to form Fe<sup>+3</sup> which precipitates out as amorphous oxy-hydroxides, co-precipitating orthophosphate. The floc produced generally fall to the sediments (Henderson & Markland, 1986).

### **2.1.7 The transport of P from land to water**

Several non point P sources contribute significantly to the flux of P from land to aquatic water bodies. The most important diffuse P source being agricultural land (Lander et al., 1998; Sharpley, 2000). The physiochemical properties of agricultural soil determine P sorption capacity, erosion risk and water flow paths and these are therefore key explanatory factors for the temporal variation in the transport of P to aquatic water bodies. Figure 7 illustrates the different hydrological pathways that are involved in the phosphorous transfer from soil to surface water. These pathways includes, (i) overland flow, (ii) subsurface flow including matrix flow and rapid flow through macropores at the soil profile and artificial tile drainage and (iii) ground water flow, generally being less important (Bechmann, 2005). Erosion is the most important mechanism governing the flux of total P. Erosion removes preferentially the finer- sized soil particles, which have higher capacity to adsorb P. As results, a higher P content and reactivity is typically found in eroded material than source soil (Haygarth & Sharpley, 2000).

The transport of dissolved P in runoff is initiated by the release of P from soil, plant material, and suspended sediments. This process occurs when the water flowing over the surface of agricultural land interact with the upper soil (1 to 5 cm) rich in P entrained from the inorganic fertilizers and manure and decomposed plant material (Sharpley, 1985). It also occurs in the recharge zone, close to the stream, where the water table reaches the soil surface. The proportion of rainfall and depth of soil involved are highly dynamic due to variations in rainfall intensity, soil tilth, and vegetative cover, making them difficult to quantify in the field (Sharpley, 1985). This is also important in natural forests due to a large internal cycling causing large labile P pools in the forest floor. Mohr (2010) found very higher value of organic P content in the forest floor of the Western Vansjø catchment due to internal nutrient cycle. A study by Sharpley et al. (2001) showed a positive correlation between dissolved P in runoff and soil P concentration of surface soil (1 to 5 cm) (on soil samples with known manurial histories). The relation between dissolved P in runoff and soil P levels vary also according to agricultural practice, soil types and hydrological regimes as well as spatial and temporal variation in erosion within a runoff regime (Sibbesen & Sharpley, 1997).

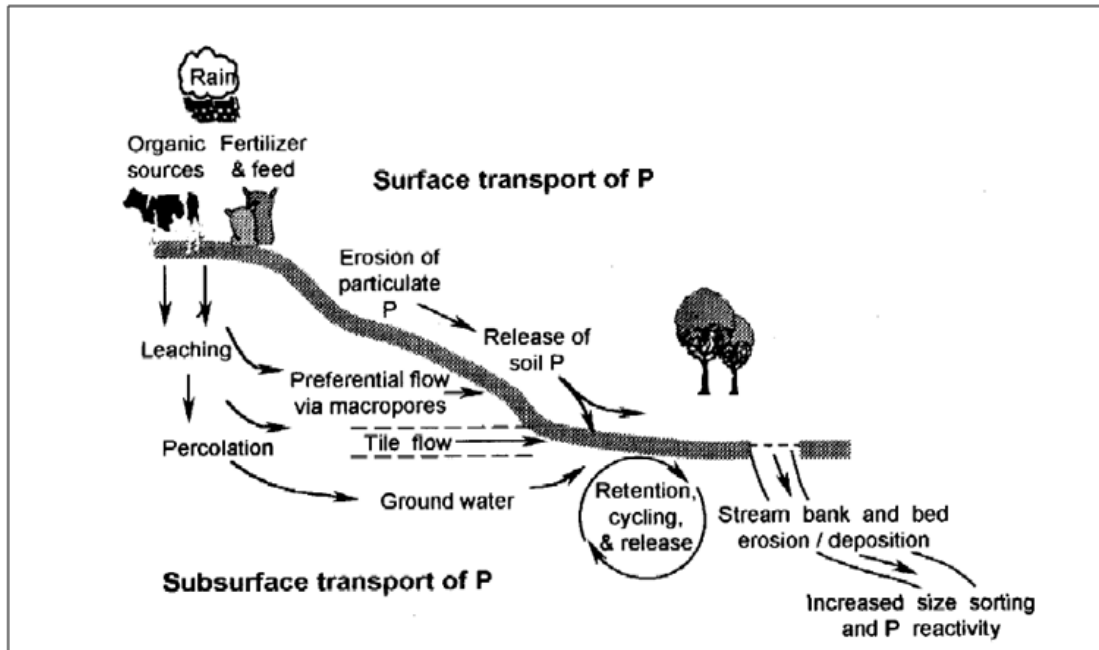


**Figure 7: Transport and site management factors influencing the potential for P loss from agricultural land to surface waters (Sharply, 2001).**

Dissolved P in infiltrate water, move inside the soil profile through subsurface flow. This type of transport is known as leaching. Transport of P via subsurface runoff is usually conceived to be of less importance than overland transport (Heathwaite et al., 2000). The leachate is mainly dominated by unreactive P due to that the reactive P is readily sorbed to the soil the water is passing through and thereby efficiently prevented from leaching (Turner & Haygarth, 2000).

P losses in subsurface flow are greatly influenced by artificial drainage pipes. Most of the water flow occurs through natural macropores in the soils. Macropores serve as vents and allows the reactive P to pass through the Ap and B horizon down to the drainage pipes with minimal contact with soil matrix (Simard et al., 1989; Turner & Haygarth, 2000). Such pores may be created due to extensive soil cracking in expanding clays (e.g. Illite) or biogenic by earthworms or roots. The P movement through macropore flow is important on structured clay soils in southeastern Norway (Bechmann, 2005). A study by Øyegarden et al. (1997) showed cracks of up to 10mm to a depth 50 cm in southeastern Norway. Opland (2011) also showed the presence of macropores in the soil samples taken from the soil down to 84 cm depth in the catchment of Western Vansjø. The existence of such large pores also allows

larger particles to be transported from the soil surface down into the soils (Øyegarden et al., 1997).

P transported from agricultural land by overland and subsurface flow through drainage pipes is mainly dominated by particulate P. Erosion of particulate bound P is the dominant mode of P transfer from soils to surface waters for most areas in world (Leinweber et al., 2002). Also in Norway, it is found that the transfer of P is dominated by the particulate bound P fraction. The transfer of suspended sediments is therefore an explanatory variable explaining much of the transfer of P in areas of arable cropping and high erodibility (Lundekvam, 1998; Bechmann & Stålnacke, 2005). The proportion of the particulate P fraction in overland flow varies as a function of erosion. Greater erosion lead to increased amount of particulate P fraction indicating link between soil erosion and amount of total P transferred from soils to surface water. The amount of erosion greatly depends on factors like slope, soil texture, soil management and runoff intensity etc. Thus, P movement in cultivated land is also affected by these factors (Lundekvam & Skøien, 1998).

In general, forested areas keep the soil intact due to the protection by canopy cover and that the soils in forested areas are bound up by the root of perennials plant. This forest floor vegetation thereby prevents the risk of erosion by runoff, thus P export is minimally affected by erosion. Surface runoff from forest areas and erosion resistant soils carries small amount of eroded particles and thus the total P loading is mainly dominated by dissolved form of phosphorus in the streams draining the forested catchments (Gebreslasse, 2012).

## **2.1.8 Role of increased DNOM leaching and reduce aluminium leaching**

### **2.1.8.1 Increased leaching of DNOM**

There are several natural eutrophic lakes due to natural high background nutrient flux (Mack, 2010). Many lakes in areas with marine deposits have a natural high influx of nutrients. Western Vansjø Lake is an example of such a natural eutrophic lake. E.g. Solheim et al. (2001) found that 20 to 25 % of the total-P loading to Lake Vansjø was due to background flux. Little is known of the natural background flux of P, though estimates have shown that the natural background flux may contribute a substantial fraction of the total-P loading to

surface waters. More knowledge about this natural loading is clearly needed. Free orthophosphate is not readily transported in a natural environment as it is efficiently assimilated or adsorbed to the soil. Instead, the main natural P transport is by being an inherent part of Dissolved Natural Organic Matter (DNOM). The natural background P fluxes from the forested catchments are therefore mainly related to the transported amount and characteristic of DNOM.

Climatic factors, such as the intensity of precipitation and temperature, govern the fluxes of DNOM (Honve et al., 2004). In runoff from forests with acid soils in southern Norway, there has been almost doubling in the concentration of DNOM since late 1980s and is expected to increase in the future due to the climate change (Honve et al., 2004; Haaland et al., 2009). Anthropogenic sulphur deposition in the southeast part of Norway, which peaked in the 1970s and 1980s, led to higher concentration of inorganic labile aluminium ( $Al_i$ ) in the runoff from acid sensitive forested catchments. During this period, reduction in DNOM concentration was reported in region affected by acid rain (Haaland et al., 2009). This was likely due to the increased ionic strength (Nygaard & Wit, 2000) and  $Al_i$  concentrations caused by the acid rain. The excellent properties of  $Al_i$  as a flocculent and coagulant may be clearly envisioned at water treatment works. Flocculation of DNOM by using aluminium sulfate ( $Al_2(SO_4)_3$ ) is a commonly used procedure at water treatment work with high levels of DNOM in their raw water (Haaland et al., 2009; Fettig et al., 1998). Since the 1980s, mean lake concentration of non-marine sulfate have decreased by 70% in the southern eastern part of Norway while  $Al_i$  concentration have been reduced from  $> 100 \mu\text{g/L}$  to  $45 < \mu\text{g/L}$  (55% decrease) in the same period (Skjelkvåle & Wollan, 2009). Reduction in the mean concentrations of sulphate and inorganic labile aluminium are two important factors that likely govern the increased amount of DNOM (Haaland et al., 2009). DNOM readily complexes with metals such as aluminium and iron (Currie et al., 1996; Nasholm et al., 1998). It also binds orthophosphate via Al and Fe ions complexed (E.g. P-Fe-OM or P-Al-OM) by organic matter. Therefore, higher content of organic matter can be responsible for the higher amount soluble phosphorus in the streams draining the forested catchments (Gerke, 1993). It is therefore postulated that this increased leaching of DNOM has led to increased P fluxes originating from natural background leaching from forested catchments.

### **2.1.8.2 Reduced aluminium leaching**

In Norway, most agriculture areas have forest within its catchments. These forested area are generally located upstream of the agriculture area. Where the forested runoff, containing aluminium, downstream passes through agricultural land it mixes with alkaline and P rich seepage water. The alkaline runoff from agricultural catchment influences the aluminium speciation and shifts the equilibrium concentration of aqueous aluminium forms toward less charged species. Consequently, the ionic aluminium species in the acidic forest water form aluminium oxohydroxides and precipitates upon passing through agricultural land (Kopáček et al., 2001). The aluminium that precipitates out as amorphous oxohydroxides has large surface area and may co-precipitate orthophosphates (Broberg, 1984; Kopáček et al., 2001). This is also used in sewage treatment plants to remove P as well as a remediation action in eutrophic lakes (Cooke et al., 1993). It is therefore postulated that reduced leaching of aluminium from upstream forests due to the reduction in acid rain has led to a loss of a very important phosphate removal process during the acid rain epoch.

### **2.1.9 Climate changes and phosphorus mobility**

Climate change and its effect on environmental conditions have had great affect on the nutrients mobility and water quality (Førland et al., 2007). It is postulated here that changes in climate over the past 20 to 30 years and their effect of nutrient fluxes may have disguised the effect of mitigation measures. In term of climate change, an increased amount of precipitation and increased average winter temperature are two important climatic pressures that may have had an effect on nutrient fluxes. Figure 8 shows that the amount of precipitation has increased and remained above norm in eastern Norway over the last 30 years. This increased precipitation causes more frequent high runoff episodes and floods. During the first decade after the flood in the year 2000, the Western Vansjø experienced harmful blooming of toxic algae due to increased input phosphorus (Skarbøvik et al., 2011; Vannområdeutvalget, 2011). Increased surface runoff due to the more frequent intensive rain and floods causes increased erosion and thereby increases concentration of total phosphorous (Skarbøvik et al., 2011). Moreover, increased loading of especially bioavailable P is also partly due to the water logged iron rich soils. As described in section 2.1.6,  $Fe^{+3}$  is reduced to  $Fe^{+2}$  in water-saturated soils. This decreases the soils ability to hold phosphate which is thereby washed out.

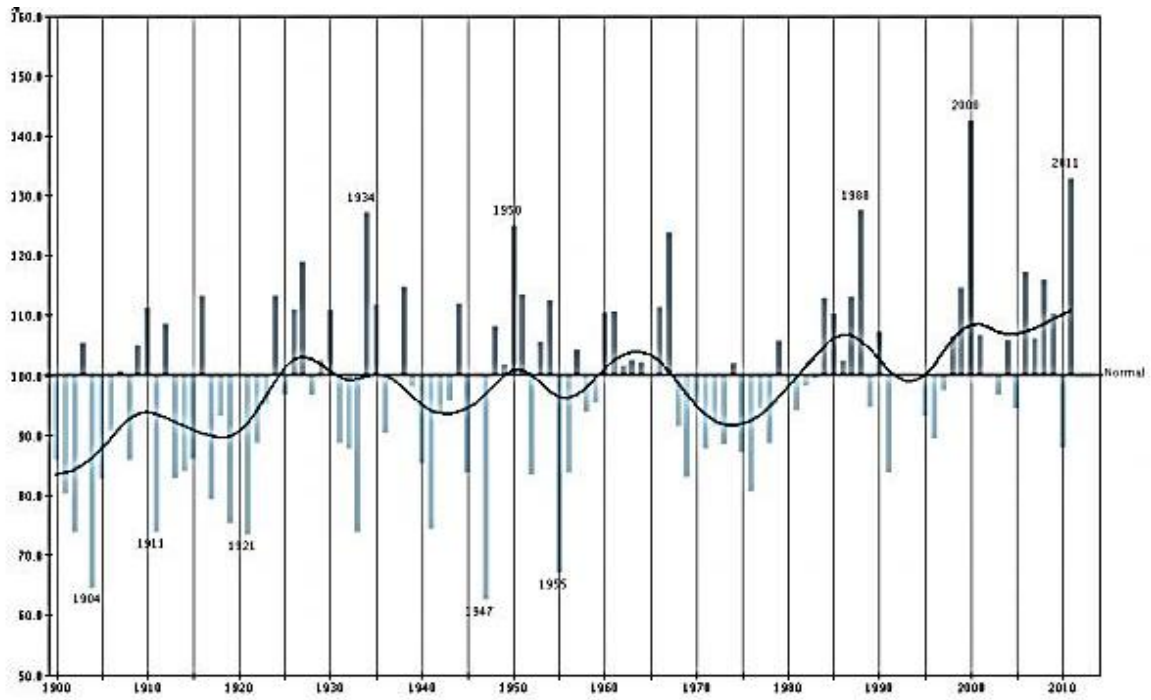


Figure 8: Yearly amount of precipitation for Eastern Norway 1900-2011 relative to the norm (Met.no 2012).

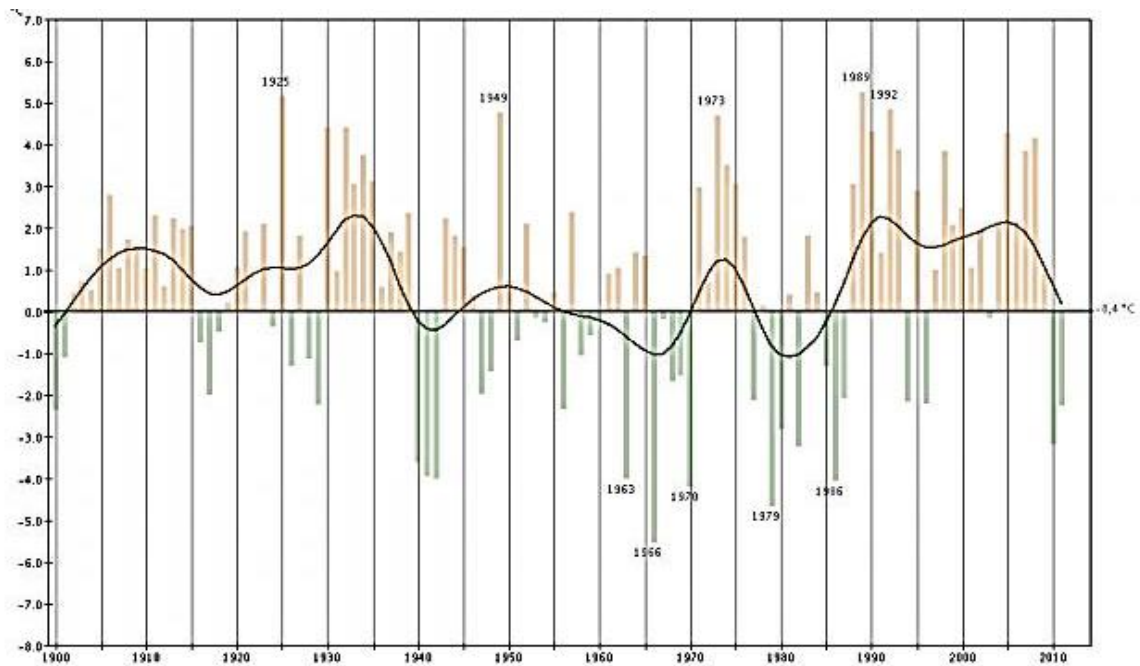


Figure 9: Temperature deviations from the norm during winter in Eastern Norway from 1900-2011 (Met.no 2012).



The average winter temperature has been remained about 2<sup>0</sup> C higher than norm in Eastern Norway during the years 1989 - 2009 (Figure 9). Extreme events in form of floods and heavy rainfall may occur, especially during autumn and winter, due to the more frequent/intense precipitation during these times of the year. Winter mild-spell and spring snowmelt are the main periods of transport of P on tilled soils (Øyegarden, 2000). During autumn, soils become saturated with water and overland flow is common due to the intense precipitation. These seasons are thereby important periods of P transfer from land to water (Bechmann, 2005).

Warmer winter temperatures causes the temperature to frequently exceed 0°C leading to freeze-thaw episodes which causes higher soil erosion that may further lead to greater influx of nutrients absorbed on soil particles. The erodibility of the soil is documented to be highest for partly frozen soils (Kirby & Mehuys, 1987). Extreme events in form of floods may occur where deeper soils are frozen and have low hydrological conductivity while surface soils layer may be thawed. This causes higher erodibility by forcing the water to run over soil surface and thus higher transfer of particle bound P in runoff (Øyegarden, 2000). Furthermore, freezing causes lysis of plant cell releasing P, which is not assimilated due to the dormant vegetation. This causes higher transport of dissolved phosphate in runoff (Bechmann et al., 2005)

## **2.2 Analytical theory of Diffusive Gradient in Thin Films (DGT)**

### **2.2.1 Diffusive Gradient in Thin Films (DGT)**

DGT is a passive sampling technique for *in situ* sampling and speciation of free ions and labile species in water. DGT technology was developed in the early 1990s, and first described in nature in 1994 by Zhang & Davison (Davison & Zhang, 1994). DGT theory is based on the diffusional characteristic of metals or ions through a hydrated gel membrane (diffusive membrane layer). Diffused ions are collected and concentrated on an adsorbent layer often called the resin gel layer (Davison & Zhang, 1994). The pre-concentration obtained over the sampling period make it possible to detect very low concentrations (e.g. 4 picomolar, pM) and reduce effects of contaminations (Davison & Zhang, 1994). This simple method is also suitable for sampling in soils and sediments.

## 2.2.2 Structure of DGT-device

A DGT device consists of a plastic base (called the piston) with a socket of 25 mm diameter (Figure 10). On top of the socket placed the resin gel (the adsorbent at the bottom towards the socket), overlaid the diffusive gel and then a membrane filter at the top. A plastic top (cap) fits over it and holds the device in place, and prevent the inner content from exposure to the environment. The outer plastic top has a window of 20 mm in diameter (Zhang, 2005), through which the diffusive sampling takes place.

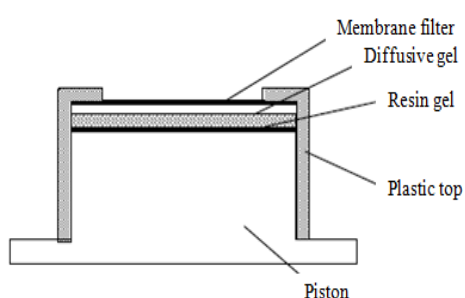


**Figure 10: The structure of DGT device (Zhang, 2005).**

### 2.2.2.1 Membrane filter

The soft diffusive gel layer is protected by a membrane filter (Figure 10). The membrane filter has normally a thickness of 100 to 150  $\mu\text{m}$  and a pore size of normally 0.45  $\mu\text{m}$ . It acts as protector for the fragile diffusive layer by preventing the accumulation of larger particulate compounds that can be stuck on the gel surface (Zhang & Davison, 1995).

### 2.2.2.2 Diffusion membrane layer

The diffusion membrane layer in the DGT devices is made from an agarose polyacrylamide hydrogel, APA gel (Zhang, 2005). Pore size of normal APA gel is between 5 and 10 nm. This membrane excludes particles and colloids that are larger than the pore size. It collect

dissolved ions and small molecules that can pass through pore structure of the membrane. It also acts as a reaction layer as the thickness of the diffusive gel layer and pore structure influence the uptake of ions. E.g. a study by Davison & Zhang (1994) showed that for a typical APA gel layer of 1mm thickness, the reaction time is about 5 min for passage through the membrane. DGTs can be expected to accumulate ions (e.g. organically complexed metal ions) that are dissociates into free ions within the reaction time (Davison & Zhang, 1994). About 90% of the normal APA gel is water. Because of the porosity of the APA polymer matrix, transport of metal ions and small molecules through the gel occurs by molecular diffusion (Davison & Zhang, 1994; Zhang & Davison, 1999).

### **2.2.2.3 Adsorbent layer (resin gel layer)**

The type of adsorbent must be constructed so that it collects and accumulate the ions or molecules of interest. Normally the adsorbent material is imbedded in a gel layer of the same type as the diffusive membrane therefore the adsorbent layer is sometimes a bit confusingly known as resin gel layer. Several different types of adsorbent layers have been developed to concentrate or collect various compounds e.g. metal ions, sulphides, radionuclide ion (Cs) (Zhang, 2005) .The Chelex ion exchange resin is the most common type of resin layer for metals. Adsorbent resin gels with AgI (silver iodide) have been developed for sulphides (Zhang, 2005). At NIVA several adsorbents has been studied, such as Chelex resins and paper filter immobilized phosphonic acid (for metal ions), immobilized MnO<sub>2</sub> (for Ra), Ferrihydrite (for PO<sub>4</sub>, SeO<sub>4</sub>, AsO<sub>3</sub>) (Røyset, 2011 (Pers.comm)).

### **2.2.2.4 Adsorbents for phosphate ions**

DGTs with ferrihydrite gels (iron (III) hydroxide) are commonly used for orthophosphate, as phosphate forms stable precipitates with iron (III) or are adsorbed at iron (III) hydroxide colloid surfaces (Zhang, 2005; Zhang et al., 1998). Recently, DGTs with titanium dioxide based adsorbents have been introduced to collect the orthophosphates in water (Panther et al., 2010) in the same ways by use of Ferrihydrite. In this thesis, both adsorbent are evaluated to collect the bioavailable fractions (Org P + free-PO<sub>4</sub>) of total-P and compared. Both adsorbents have positive surface charge and can adsorb a number of oxyanions e.g. PO<sub>4</sub>, ASO<sub>3</sub>, SeO<sub>4</sub>.

Metsorb is a patented metal adsorbent. It is made from titanium dioxide (TiO<sub>2</sub>), and delivered as a fine particulate material (< 50). The Metsorb was imbedded in an APA gel. Ferrihydrite adsorbent produced by precipitation of Fe(III) by hydroxide to Fe(OH)<sub>3</sub>, which is also imbedded into a APA gel.

### 2.2.3 Diffusion

The DGT theory is based on diffusion that can be defined as spreading of molecules from one region to another because of random molecular motion (Crank, 1975; Li & Gregory, 1974).

Hydration of free ions or molecules affects the diffusion velocity or diffusion rate in water. A general theory is that a high ion potential (charge to mass ratio) provides a thick hydration layer of water molecules around the ions that slows diffusion (Li & Gregory 1974; Cussler, 1997).

Diffusion coefficients for specific ions/molecules are normally measured experimentally in diffusion cells. In water, it is also possible to calculate diffusion coefficients from conductivity data. When the resistance is inversely proportional to the conductance through the cell and conductance is again proportional to the ion fluxes, diffusion coefficients can be estimated by using Equation 1 (Cussler, 1997).

$$D_i = \left[ \frac{K_B \cdot T}{|Z_i|} \right] \cdot \lambda_i \quad (1)$$

$K_B$  is Boltzmann's constant

$D_i$  is diffusion coefficient of ion

T is absolute temperature

$\lambda_i$  is equivalent ionic conductance at infinite dilution

$|Z_i|$  is absolute value of the charge of ion

Cussler (1997) describes the theory of diffusion in more detail. The diffusion coefficients estimated by DGT theory are effective diffusion coefficients and represents a combination of the diffusion rate of ions through the diffusive gel membrane and the binding ability of the

receiving adsorbent. As the APA diffusive membrane has some resistance to molecular movement, the diffusion coefficient values obtained from DGTs, are normally somewhat lower than those achieved from water (Røyset et al., 2004).

## 2.2.4 Principles of the DGT theory in water

Figure 11 shows the concentration gradients in a DGT device in contact with an aqueous solution. The ion exchange resin gel, which is separated from the external solution by the diffusive boundary layer (DBL) and the filter membrane, accumulates ions/molecules (Alfaro-De la Torre et al., 2000). The thickness of the diffusion boundary layer depends on the rate of water movement (Alfaro-De la Torre et al., 2000). The transport through the diffusive gel layer, membrane filter and diffusion boundary layer is solely by molecular diffusion. A steady state linear concentration gradient, established between the solution and the resin gel, make it possible to measure the concentration of ions/molecules by using Fick's first law of diffusion (Zhang, 2005). Mathematic of DGT theory is based on several different equations. Overview of the most common equations used to describe diffusion processes is shown in Table 2 below. The equations are explained in the text.

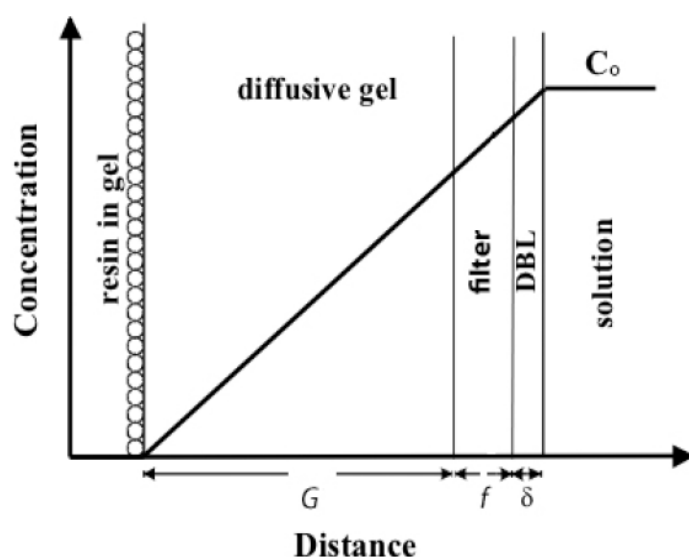


Figure 11: Schematic representation of the steady state concentration gradients in a DGT device in contact with aqueous solutions (Zhang, 2005).

**Table 2: Overview of the most common equations used to describe diffusion processes (Garmo et al., 2003).**

Equation 2	Flux	$Flux = \frac{dm}{dt} = -D \cdot \frac{dC}{dz}$
Equation 3	Time integrated uptake	$m(t) = C_o \cdot t \cdot D \cdot \frac{A}{L}$
Equation 4	Time averaged concentration	$C_o = \frac{m}{t} \cdot \frac{L}{DA}$
Equation 5	Time averaged concentration	$C_o = \frac{m}{t} \cdot \frac{(G + f + \delta)}{DA}$
Equation 6	Temperature correction of D (Stokes-Einstein)	$\frac{D_t \eta_t}{T_t} = \frac{D_o \eta_o}{T_o}$
Equation 7	Temperature correction of viscosity	$\log \frac{\eta_o}{\eta_t} = \frac{1,37023(t-25) + 0,000836(t-25)^2}{109 + t}$
Equation 8	Diffusive boundary layer (DBL) thickness	$\delta = 3.3 \cdot \sqrt[3]{\frac{D}{v}} \cdot \sqrt{\frac{vx}{U}}$

- Equation 2 is the general diffusion formula derived from the Fick's first law of diffusion. Fick's first law describes the relationship between the flux of ions/molecules ( $dm/dt$ ) over a concentration gradient ( $dC/dz$ ) multiplied by diffusive coefficient of the ions in the gel (Garmo et al., 2003).
- The time integrated mass uptake of ions/molecules can be determined by integrating equation 2 over the concentration gradient, forming equation 3 (Garmo et al., 2003). Here L, A and D are constant and represents, the length (L), cross section area (A) and diffusion coefficient (D), respectively. This is based on the assumption that the sampler absorbent is an efficient sink for molecules or ions, meaning that the

concentration of ions/molecules that are collected at adsorbent surface is close to zero, no back diffusion occurs from the adsorbent. For most practical purposes, this assumption is valid as long it remains well below the saturation point of the adsorbent.

- Equation 4 and Equation 5 are obtained by solving equation 3 for the concentration term ( $C_0$ ) i.e. the time-averaged concentration of ions /molecules outside the sampler. Equation 5 are obtained by expanding the term  $L$  which consists of three components (see Figure 10): the thickness of diffusive gel membrane ( $G$ , mm), the filter membrane ( $f$ , mm) and the diffusive boundary layer ( $\delta$ , mm) (Garmo et al., 2003).
- A few important parameters have to be considered for the uptake rate of analyte by the DGT sampler. The most important parameter is the temperature since the rate of diffusion varies significantly with temperature. The temperature dependence of diffusion coefficients are described by the “Stokes Einstein equation” (Equation 6), showing that  $D$  is linked with absolute temperature  $T$  and viscosity  $\eta$  of water (Garmo, 2006; Li & Gregory, 1974). The viscosity of water is temperature dependent, and Equation 6 describes the temperature dependence. The exact temperature corrected diffusion coefficients at different temperature must therefore be determined by combining Equation 6 and Equation 7. Figure 12 shows temperature dependence curve of  $D$  that is described in a separate function from  $0^{\circ}\text{C}$  to  $30^{\circ}\text{C}$  (Røyset, 2011(Pers.comm)). This factor is used to correct  $D$  values to average temperature during exposure in the field (Garmo et al., 2003).

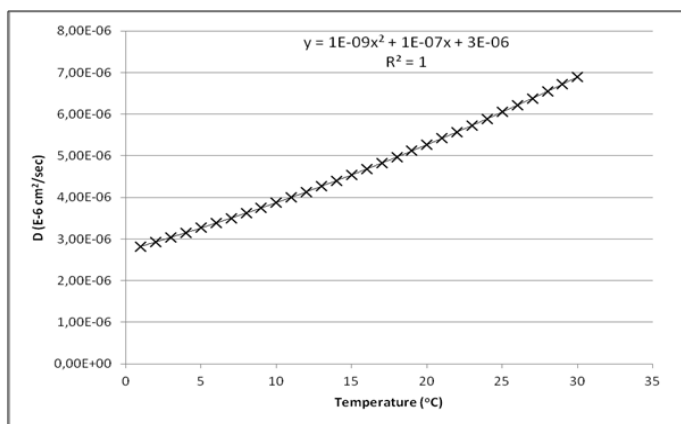


**Figure 12: Temperature dependence curve of  $D$  is described in a separate function from  $0^{\circ}\text{C}$  to  $30^{\circ}\text{C}$  (Røyset 2011, (Pers.comm)).**

- The second important parameter, which affects the uptake in the DGT device, is the mass transport controlled by molecular diffusion across the diffusive boundary layer, DBL (Zhang & Davison, 1995; Garmo et al., 2003). As described in the simplified view of the DGT sampler, the DBL is a layer of “not-moving” water at the surface of the filter in the exposure window of the sampler (placed between the filter membrane and bulk solution and act as an additional diffusion layer). The thickness of the DBL layer depends on the flow velocity of the water over the surface of the DGT window. The DBL layer adds to the diffusion length, as shown in equation 5. Equation 8 gives an approximate estimation of the DBL layer thickness related to water velocity. A practical assumption often used for the DBL thickness is 0.1 mm, as this relates to a water velocity of 10 cm/sec.

The pH of the solution and ionic strength can also influence the efficiency of the DGT to accumulate the analyte. A case study done by Zhang & Davison (1995) showed that the collection efficiency of Chelex-100 gel is influenced by lower or higher pH due to the swelling of the gel at pH > 11 and competition from hydrogen ions at pH < 3. However, the collection efficiency of about 25 elements normally used for Chelex based DGT is reasonably quantitative in the pH range 5-9, which is the normal pH range of natural water (Garmo et al., 2003). A case study done by Sangi et al. (2002) showed that when ionic strength increase, the competition between different cations binding to the diffusion gel layer also increases. This effect is considered to be small, and generally, the D values are not strongly influenced by ionic strength up to fully seawater.

### 2.2.5 Estimation of diffusion coefficients

A study done by Buffle et al. (2007) showed that compounds which have similar molar masses ( $M_m$ ) have comparable diffusion coefficients (D) values. In particular, molecules in ranges of 200 – 10<sup>5</sup> Dalton show a semi-empirical relationship between diffusion coefficients and molar masses at 25 °C.

$$D = 2.84 * 10^{-09} / M_m^{1/3} \quad (9)$$



Equation 9 can be used to estimate expected values of diffusion coefficients based on molecular weights. The results derived from equation 9, can be used to compare the value of diffusion coefficients obtained from field experiments based on the Equation 2- 8 above.

### **3 Site description, sampling and analytical methods**

#### **3.1 Field site description**

##### **3.1.1 Vansjø-Hobøl (Morsa) Catchment**

Vansjø is a large eutrophic lake located near the city of Moss in the southeastern part of Norway (Figure 13). The lake is a part of the Morsa catchment that has an area of about 690 km<sup>2</sup>. In total only 15% of the catchment area is covered by agricultural land and 7% accounts for water bodies, bogs and open areas. The remaining 78% is dominated by forest. The proportion of the agricultural land may not be high in a European context, but the catchment is one of the most cultivated areas in Norway since in Norway, as a whole, only 3% of the land is used for agriculture (Skarbøvik & Bechmann, 2010). The Hobøl River (Hobølelva) is the largest river in the catchment area and contributes about 40% of the total discharge into the lake Vansjø (Skarbøvik & Bechmann, 2010). The lake Vansjø comprises a surface area of 36 km<sup>2</sup> and consists of several sub-basins that are separated by narrow and shallow passages. The lake is divided into two main basins, the larger Storefjorden (eastern basin) with an area of 24 km<sup>2</sup>, and, the smaller and shallower part Western Vansjø (Vanemfjorden) with an area of 12 km<sup>2</sup>. The outlet river is the Moss River (Mosseelva). The lake water flows from Storefjorden to Western Vansjø and from Western Vansjø water drains out into the Oslo Fjord via the Moss River (Bjørndalen et al., 2007).

Vansjø has a large number of users and stakeholders with multiple and conflicting interests. Water from Vansjø is a raw water source of drinking water for approximately 60,000 people. It is a widely used place for recreational activities such as bathing, boating and fishing etc. The lake is also an important habitat for birds. In addition, Vansjø Lake receives nutrients rich runoff from farming. There are therefore significant conflicts of interest among the different users that depend on safe adequate water quality and those who use Vansjø as recipient of waste water and diffuse seepage from farming (Bjørndalen et al., 2007).

The Vansjø Lake has received considerable attention due to eutrophication problem causing frequent bloom of harmful algae. The Vansjø Lake is a natural eutrophic lake and eutrophication has been problem since 1950s. Today diffuse leaching of P from agricultural land due to excess use of fertilizers is the main cause of eutrophication. The Toxic algal blooms are mainly due to excess inputs of total-P flux despite considerable mitigation measures to reduce input of P loading (Bechmann et al., 2005).

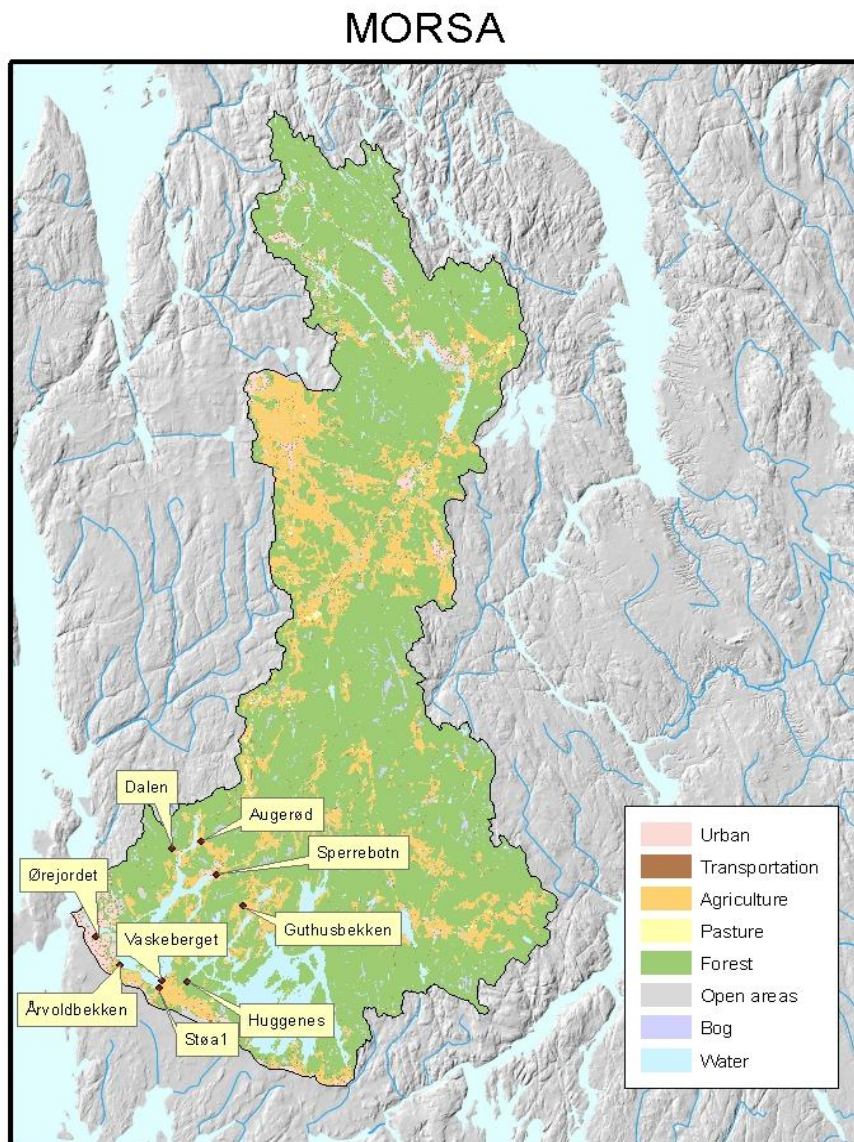


**Figure 13: The Vansjø-Hobøl Catchment with monitoring sites of the studied streams indicated by red points (Norwegian Forest and Landscape Institute, 2011), revised by Alexander Engebretsen).**

### 3.1.2 Geology of Vansjø-Hobøl catchment

The highest altitude in the catchment area is 346 m a.s.l. (Figure14). The bedrock mainly consists of poorly weatherable gneiss and granite. Only 10 % of the Morsa catchment is situated above the marine limit at approx. 214 m a.s.l. These areas are mainly found in northern part of the catchment and are dominated by forest. The areas below the marine limit were submerged below the sea during the end of Pleistocene at about 10 000 years ago (Skarbøvik & Bechmann, 2010).

Since the last ice age the land has risen from the sea. As the sea level passed through the landscape wave actions washed the ridges clear of deposits leaving rock outcrops. Sandy beaches on the slopes are today found as acid sandy soil. In the valley bottoms and flat lowing lying reaches the fine sediments where left intact or accumulated further leaving thick marine deposits of clay. In these areas, the marine clay deposits with P-containing apatite became the more fertile agricultural soils (Skarbøvik & Bachmann, 2010). In the southwestern part of the Vansjø-Hobøl catchment, a large glacio-marine end moraine, known as “Ra” is damming the lake from the south. This makes the catchment drain to the west.

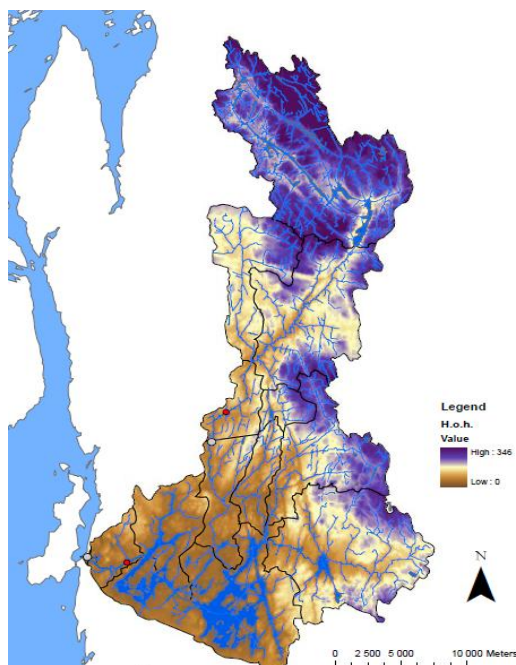


Figure14:Map showing the marine limit of the Vansjø-Hobøl Catchment (with height above sea level) (Skarbøvik et al., 2007).

### 3.1.3 Site description

The Western Vansjø area, having the largest problem of eutrophication, is the study site of this master thesis. The catchment area of Western Vansjø is 54 km<sup>2</sup> and 20% of the catchment area is used for agriculture practice. Lake water eutrophication has been a problem for decades and many abatement actions are implemented (section 1.4) to amend this problem, but still the total P concentrations in the streams that drains high contingency of agriculture land are greatly higher than the environmental goal for Western Vansjø (50 µg P/L) (Skarbøvik et al., 2011). The flood in year 2000 led to increased input of nutrients and worsened the water quality of Western Vansjø. During the first decade after the flood, the Lake Vansjø experienced annual harmful blooming of toxic algae. The Western Vansjø Lake receives runoff from many tributary streams. Nine streams draining the different proportion of the agriculture and forested land were selected in order to capture gradient in land use from agriculture to increasing proportion of forested area. Sub-catchments of these streams represent “hot spots” for total P loading to the lake Western Vansjø.

Human activities in the lower part of the catchment started 4000 years ago (Martinsen, 2007) and the number of habitants increased during the years 1000-1400. Since year 1400, the number of habitants grew further which led to changed in land distribution of the catchment. Since then, land-use changed from forest to agriculture as inhabitants started living on farming (Skarbøvik & Bechmann, 2010). Agricultural practices have recently also changed to more intense agriculture and fewer husbandries (Skarbøvik & Bechmann, 2010). Figure 15 shows the larger scale land use distribution map of the Western Vansjø catchment with boundaries for the sub-catchment of the studied streams. The red points indicate the streams where the water samples were collected. The sub-catchment sizes and land distribution of the investigated streams are listed Table 3.

# MORSA

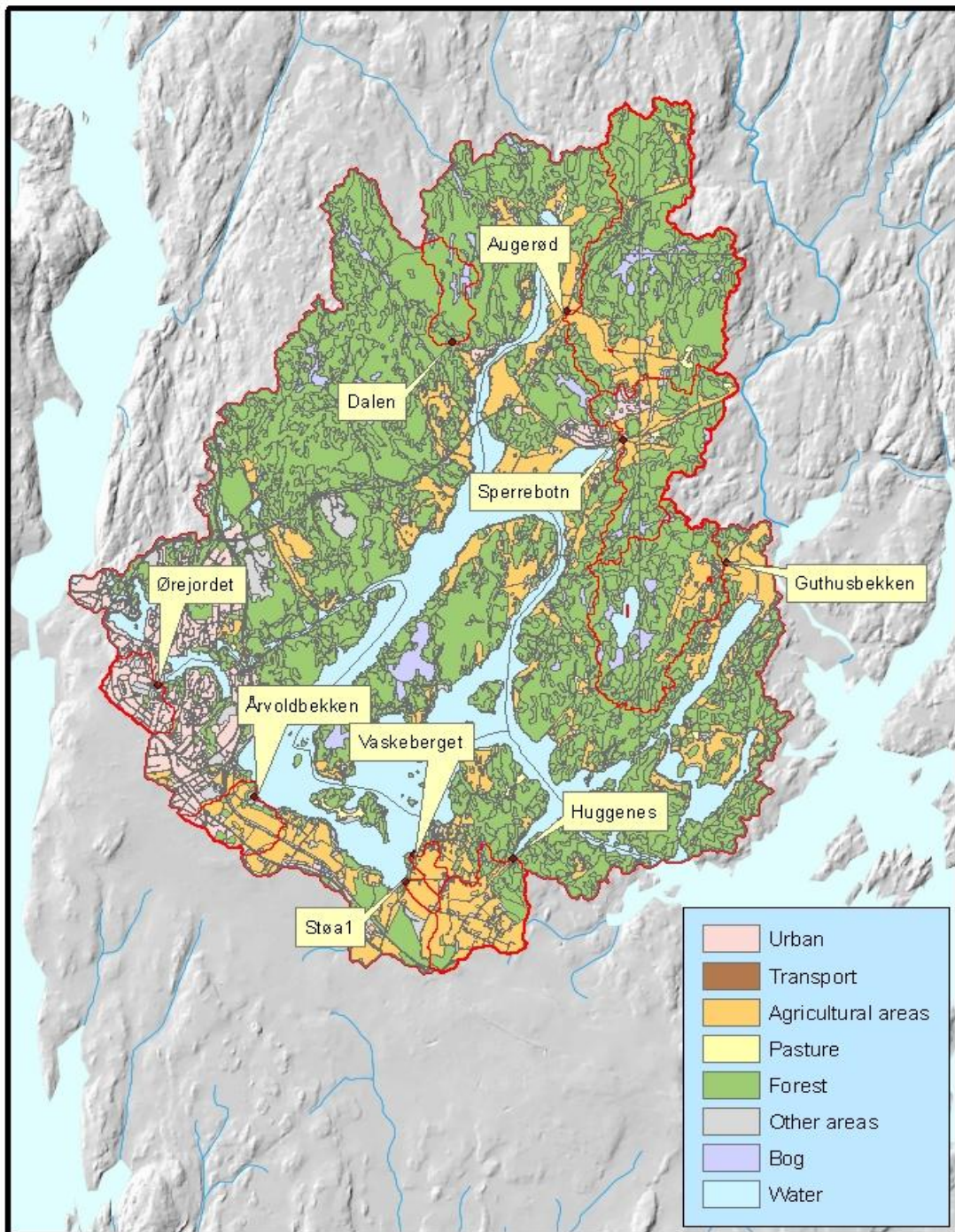
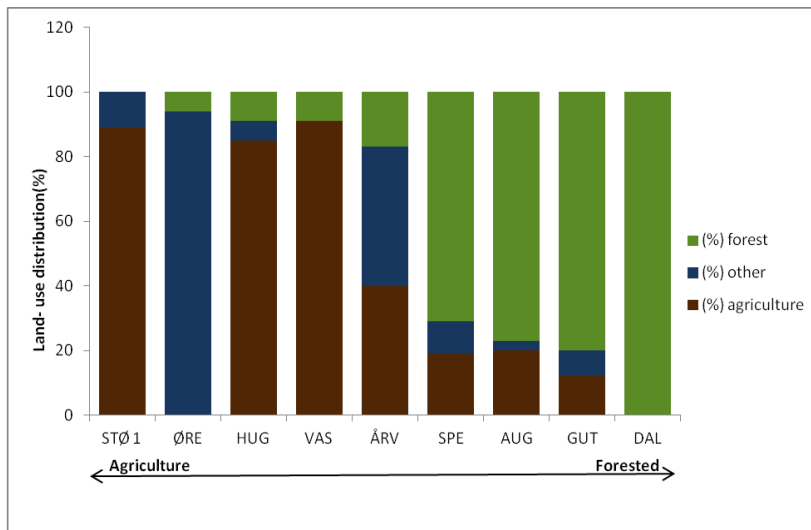


Figure 15: Land use distribution map of Western Vansjø catchment with boundaries for the sub-catchment of the studied streams (Norwegian Forest and Landscape Institute, 2011) revised by Alexander Engebretsen).

**Table 3: Names, catchment sizes of the nine sampling streams (Skarbøvik et al., 2011).**

Sampling Stream	Abbreviation	land area (daa)
Støa1	STØ 1	157
Ørejordet	ØRE	692
Huggenes	HUG	810
Vaskeberget	VAS	130
Årvold	ÅRV	486
Sperrebotn	SPE	2481
Augerød	AUG	4778
Guthus	GUT	3150
Dalen	DAL	882

The land-use distribution in the catchments of the investigated streams sorted in term of increasing forested proportion is shown in Figure 16. The streams are sorted in this order in figures presenting the data throughout this thesis in order to assess the effect of land-use, as land-use is believed to be the main factor explaining the spatial variation in P amount and P fractions in the streams.



**Figure 16: Percentage of land-use distribution in the catchments of the studied streams sorted in terms of increasing percentage of forest (data from Skarbøvik et al., 2011).**

The streams that have watersheds with highest proportion of agriculture land-use (Table 2) are all located on Raet (the main glacio-marine end moraine from the last ice age), thus the soils are naturally nutrients rich (Skarbøvik & Bechmann,2010). These sites include Støa 1,

Huggenes, and Vaskeberget. More than 80% of the watershed areas of these streams are used for agriculture purpose. These streams constitute a large proportion of the total P flux to the lake Western Vansjø (Skarbøvik & Bechmann, 2010). The Årvold site is also located between Vansjø and Raet though represents only 40% agricultural area. Guthus, Sperrebotn and Augerød are located on northeast side of Vansjø Lake and have more mixed composition of land-use. These streams drain 10 - 20% agriculture land while the rest is covered by forest. Ørejordet is a stream draining residential area in Moss city, and Dalen, which is located on northwest of Western Vansjø, is representative for forested catchments.

### 3.1.4 Soil types and erosion risk in the monitoring catchments

The type of unconsolidated deposits in the catchment area is closely related to the quaternary geological history of the catchment (Skarbøvik et al., 2011). Table 4 shows the different quaternary deposit types of the nine sites. Table 4 shows that forested lands, such as Dalen, Guthus, Augerød and Sperrebotn, are dominated by bare mountain with some humic cover. In contrast, agricultural dominated lands have typically sea fjord and beach deposit types e.g. Huggenes, Vaskeberget, and Støal. Quaternary deposit maps of the studies streams can be found in Appendix I.

**Table 4: The different quaternary deposit types of the nine sites (Norwegian Forest and Landscapes Institute, 2011)**

Sampling sites	Quaternary deposit types (%)				
	BM	THC	SBD	MBDCC	other
Støal	5,5	0,0	80,2	14,3	0,0
Ørejordet	0,0	0,0	13,0	12,0	6,0
Huggenes	13,4	4,2	32,6	49,8	0,0
Vaskeberget	7,1	0,0	92,9	0,0	0,0
Årvold	0,0	0,0	35,2	5,5	4,6
Sperrebotn	54,9	9,8	32,5	0,0	0,0
Augerød	56,9	11,3	25,8	0,0	2,1
Guthus	58,8	4,8	23,8	0,0	2,4
Dalen	50,1	22,4	12,9	0,0	0,0

BM, THC, SBD and MBDCC denote Bare Mountains, Thin Humic Cover, Sea-fjord and Beach Deposits and Marine Beach Deposits Continuous Cover, respectively.

The soils that are predominated by agricultural area have up to 80% clay in the Ap layer (Skarbøvik & Bechmann, 2010). The soils resistance towards erosion is largely determined by the soil texture type. The soil texture type in the plough layer determines the eroding tolerance. Table 5 shows texture groups and erosion risks of the plow soil layers in catchments of the studied streams. Figure 17 shows the erosion risk in the Western Vansjø catchment.

The soil erosion risk of the agricultural land is classified into four classes 1 to 4, representing low, medium, high and very high erosion risks, respectively (Norwegian Forest and Landscape Institute, 2011). As shown in Table 5, the erosion risks of the plough soil layer in the catchments of the studied streams are dominantly low to medium. Only the areas of agriculture land are mapped for erosion risk thus there are no data available for Ørejordet and Dalen stream. Erosion risk maps for studied streams are presented in Appendix J.

**Table 5: Texture groups and erosion risks of the plow soil layers in catchments of the studied streams (Norwegian Forest and Landscape Institute, 2011).**

Sampling sites	Texture code%						Erosion risk%			
	1	2	3	4	5	6	1	2	3	4
Støal	0	88	0	11	0	0	90	9	0	0
Ørejordet	N/A	N/A	N/A	N/A	N/A	N/A	N/A	N/A	N/A	N/A
Huggenes	8	77	0	3	8	2	71	28	0	0
Vaskeberget	0	53	13	33	0	0	50	50	0	0
Årvold	26	36	0	1	22	13	91	9	0	0
Sperrebotn	0	0	7	74	18	0	33	65	0	0
Augerød	0	1	0	40	57	0	35	58	2	0
Guthus	0	3	6	23	52	15	73	26	0	0
Dalen	N/A	N/A	N/A	N/A	N/A	N/A	N/A	N/A	N/A	N/A

Texture code % 1 denote between sand and coarse sand, %2 denote fine sands, %3 denote between silty sand, silty coarse sand, silty fine sand, gravel rich silty medium sand and silty coarse sand,% 4 denote silty fine sand, %5 denote silt and sandy silt and% 6 denote silty light clay. N/A denotes not available data.



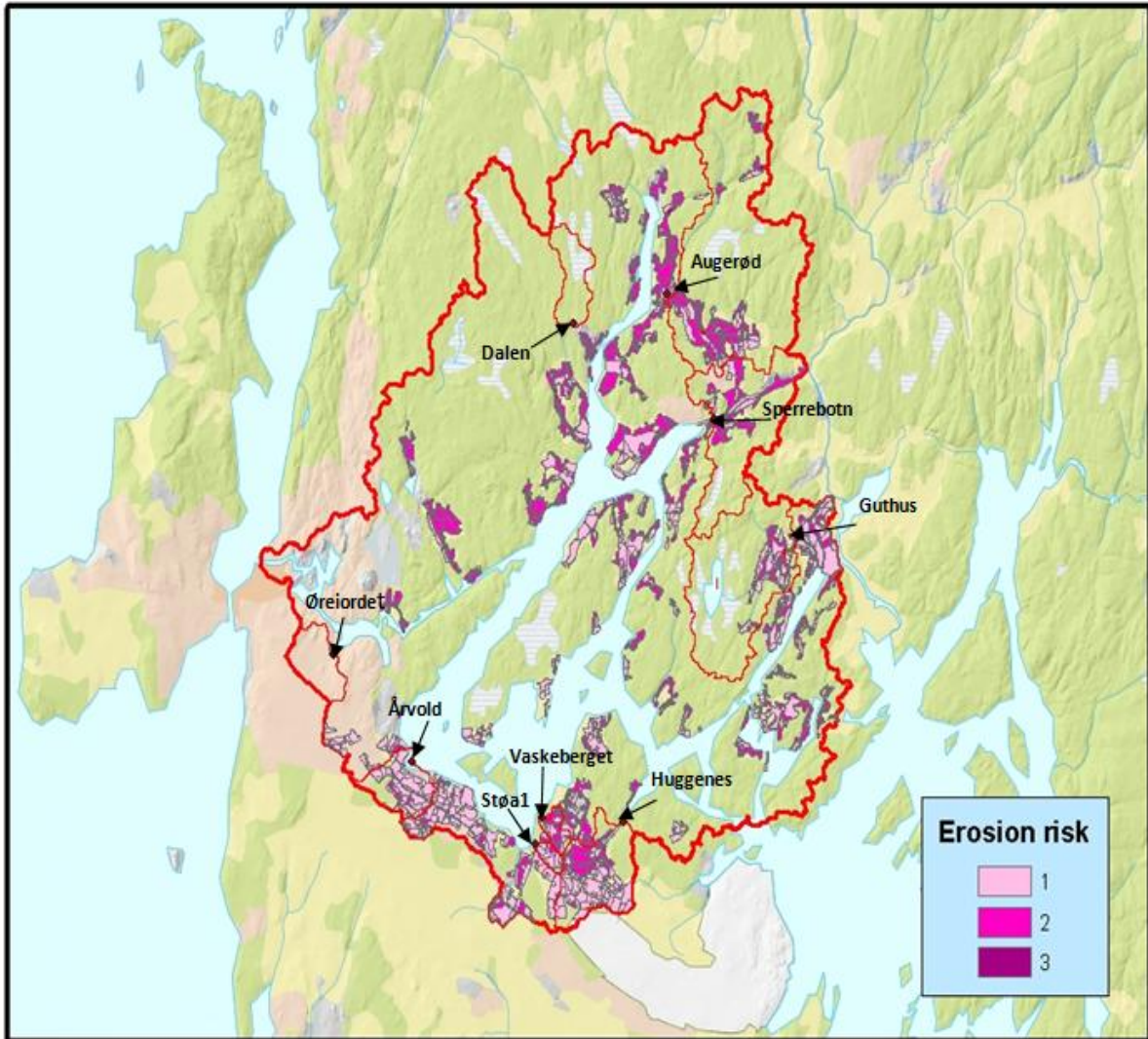


Figure 17: Erosion risk distribution in Western Vansjø catchment with boundaries for the sub-catchment of the studied streams (Norwegian Forest and Landscape Institute, 2011, revised by Alexander Engebretsen).

### 3.1.5 Meteorology and runoff

Meteorology data during the hydrological years 2006-2010 are shown in Figure 18 and Figure 19. The winter of hydrological years 2008/2009 and 2009/2010 were cold, especially the year 2009/2010. Winter temperature remained below freezing point ( $0^{\circ}$  C) for long period. Hydrological years 2006/2007 and 2007/2008 stand out as years with relatively warm winter temperature and temperature fluctuated around the freezing point throughout the winter (indicated by red line).

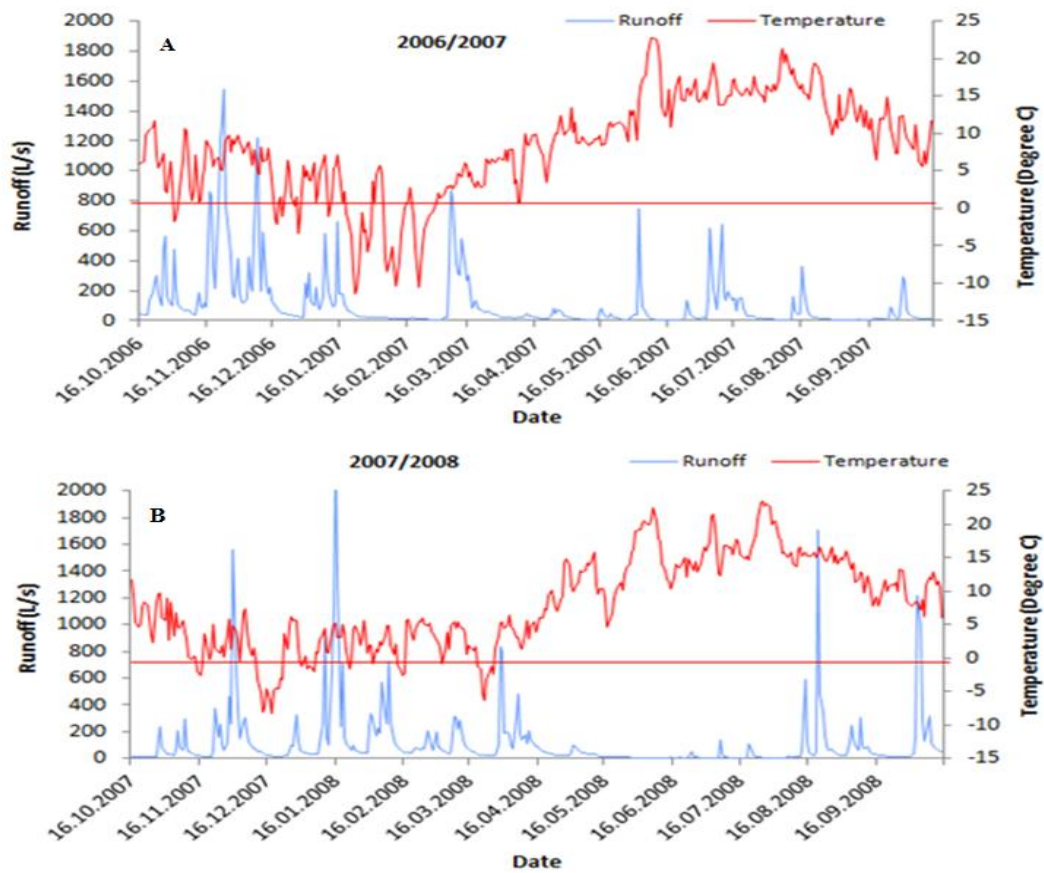
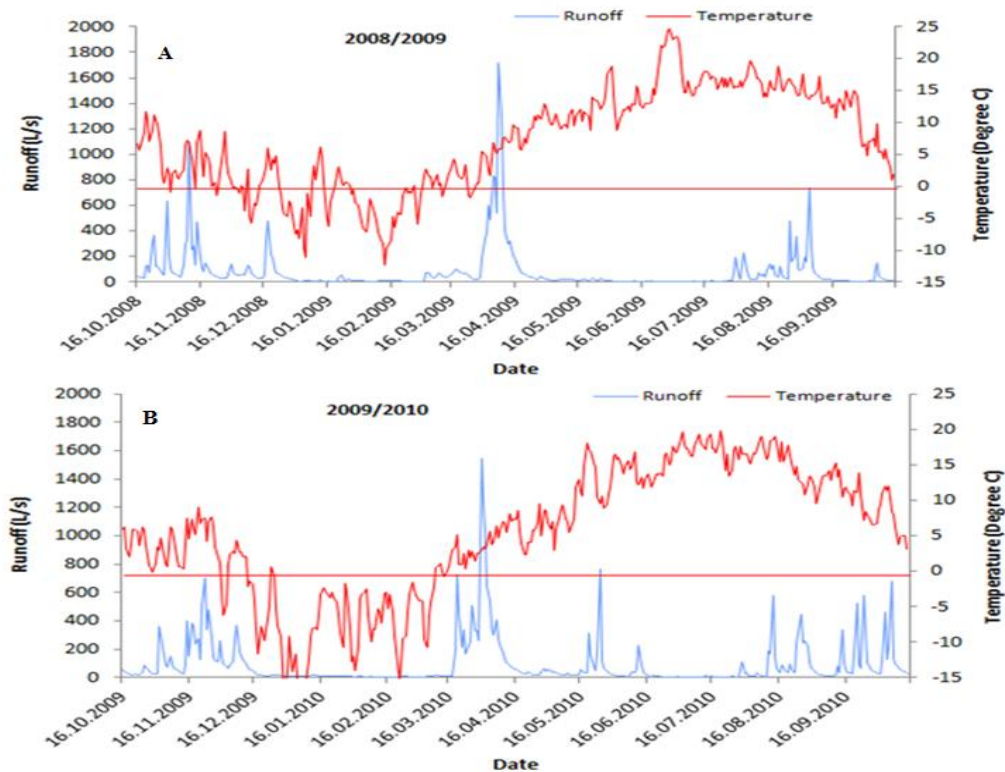


Figure 18: Temperature from Rygge (Senorge.no, 2011) and runoff from Skuterud stream (Bioforsk-data) during the hydrological years (A) 2006/2007 and (B) 2007/2008. The blue line is the hydrograph showing runoff data. Red line is the reference line for 0<sup>0</sup> C temperatures.



**Figure 19: Temperature from Rygge (Senorge.no, 2011) and runoff from Skuterud stream (Bioforsk-data) during the hydrological years (A) 2008/2009 and (B) 2009/2010. The blue line is the hydrograph showing runoff data. Red line is the reference line for 0<sup>o</sup> C temperatures.**

The blue lines in the Figure 18 and Figure 19 are the hydrograph showing runoff data from the Skuterud stream. This stream is located in Ås municipality, which is ~33 km from Western Vansjø catchment. The Skuterud stream represents 61% agriculture land while the rest is covered by forest and housing area (Bechmann et al., 2007). Calculation of transport and flow-weighted mean concentrations of P that are done in this master thesis is based on fluctuations in daily runoff data from Skuterud stream scaled relative to the different sub-catchment sizes. The runoff from the Skuterud stream was selected for this purpose due to its close proximity and thereby similar climate, and since it has approximately similar land-use as the streams on the south side of the lake Vansjø. There are several assumptions made in using the runoff data from Skuterud stream. The proportion of the agriculture land varies widely with both higher and lower share of agriculture area than Skuterud stream (see Table 3). This is an important factor as the proportion of agriculture land compared to forested area has a strong influence on the water storage capacity of the watershed and thereby the runoff intensity (Bechmann et al., 2007). Moreover, it is also differences in the susceptibility for

erosion. These differences are not taken into account within this master thesis. The average runoff from Skuterud stream (1994-2004) of 532 mm is used as a reference for the normal year (Skarbøvik et al., 2011).

The hydrographs show that there were also inter-annual variations in the amount of runoff during the hydrological years 2006 to 2010. Runoff was relatively higher during the hydrological years 2006/2007 and 2007/2008, especially during the winter and autumn season, due to the warm winter temperature accompanied with higher precipitation during these time of the year. During the hydrological years 2008/2009 and 2009/2010, the main discharge episodes were during the end of the March due to snow melting.

## **3.2 Sampling**

### **3.2.1 Stream water sampling and sample preparation**

Stream water chemistry that is studied in this thesis is based on two available dataset. One data set is from EUTROPIA-project and the other is from the Morsa monitoring program.

In the EUTROPIA project the Dalen and Huggenes streams water samples were collected as grab samples and by using an ISCO auto-sampler (Figure 20). The auto-samplers were set to collect water samples every day or every second day, as well as more frequently during targeted hydrological discharge episodes caused by heavy rainfall and/or snowmelt. Samples were stored in pre-washed polyethylene bottles. For other investigated streams, collection of the samples was done manually as grab samples using pre-washed polyethylene bottles. The samples were collected approximately every 14<sup>th</sup> day and more frequently during the hydrological discharge episodes.

Most of the investigated stream water samples for both the EUTROPIA-project and MORSA monitoring program were collected by the same person and at the same time. In the Morsa monitoring programme, the stream water samples were analysed for two operationally defined phosphorus fractions. These are total phosphorus and free reactive phosphate. In EUTROPIA-project water samples were analysed for three to four operationally defined fractions of total-P. These are Particulate bound P, dissolved organic P and free-PO<sub>4</sub> (in raw and filtered water).



**Figure 20: Auto sampler installed at sampling site of the Dalen (Photo taken by Rolf D. Vogt 29.08.11).**



**Figure 21: Picture of Staø1 stream (Photo taken by Rolf D. Vogt 29.08.11).**

All stream water samples in the EUTROPIA project were taken to the Department of Chemistry, UiO, and were stored in a dark cooling room at approximately 4<sup>0</sup> C prior to analysis. In the Morsa monitoring programme samples were stored at Bioforsk and shipped to Eurofins AS for analysis.

### **3.2.2 DGT sampling and sample preparation**

#### **3.2.2.1 Field evaluation**

Diffusive Gradients in Thin films (DGT) are passive samplers that accumulate phosphate and small organic phosphate compounds (Mohr, 2010) in water. They mimic the passive scavenging of phosphate by algae, providing a time averaged measure for fractions of total-P levels avoiding problems with detection limits. DGTs were deployed at three of the 9 investigated streams; Dalen, Støa 1 and Huggenes. These three streams were selected based on different land distribution. The Dalen site is characteristic for forested catchment whereas Støa and Huggenes are mainly dominated by agriculture land (in water chemistry, especially in regards to iron content). The amount of different P fractions in each streams vary significantly due to the different land distribution. The sampling started in end of June to middle of September in 2011. At each sites, DGT samplers using both Metsorb and Ferrihydrite as adsorbents were deployed 30 cm beneath the water surface and were left in the streams for between 7 to 14 days.

As shown in Figure 22 DGT samplers were placed in polypropylene net, ballasted by stone on one end. The other end was tied by a rope to branch or some support. Temperature and pH was measured at the time of collection. Streams samples were also collected along with the DGT in order to compare the different P fractions determined in the water sample and determined by DGTs.

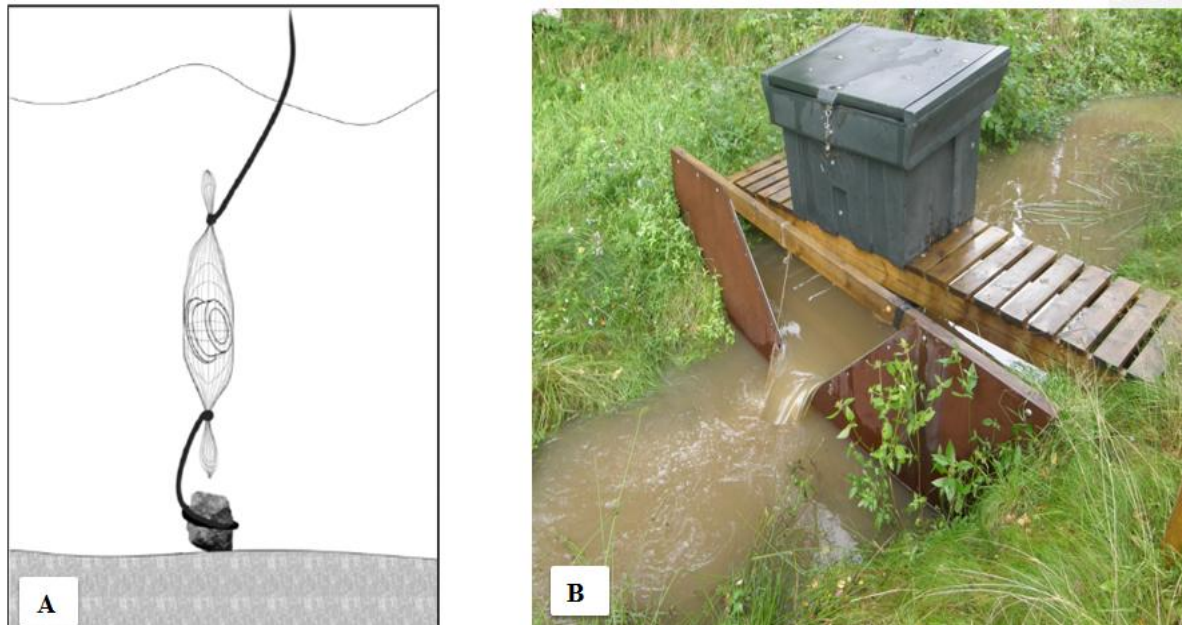


**Figure 22: (A) Illustration of how the DGTs were deployed to the water surface (Mohr, 2010). (B) Photo of the Støal stream where DGTs were deployed (Photo taken by Rolf D. Vogt 29.08.11).**

### **3.2.2.2 Laboratory evaluation for DGTs uptake of organic P compounds**

Most experiments studying the uptake of phosphorous using DGT are done for orthophosphates and little is known of the uptake of organic P by DGT samplers. Laboratory experiments were therefore conducted to measure uptake efficiency of small organic P compounds by DGTs using Metsorb and ferrihydrite as adsorbents. Experiments were performed using adenosine monophosphate (AMP) and inositol hexaphosphate ( $IP_6$ ) (Figure 23).  $IP_6$  and AMP were chosen because of their low molecular weight and that they are common organic phosphate containing compounds in the water. Over 50% of the organic phosphate compounds in the environment are different inositol phosphates as well as nucleotide fragments (AMP like compounds). The small size of these ester bound phosphates makes them easily soluble in water and it is therefore postulated that the outer ester bounded phosphate groups can be absorbed by Metsorb and ferrihydrite adsorbents.

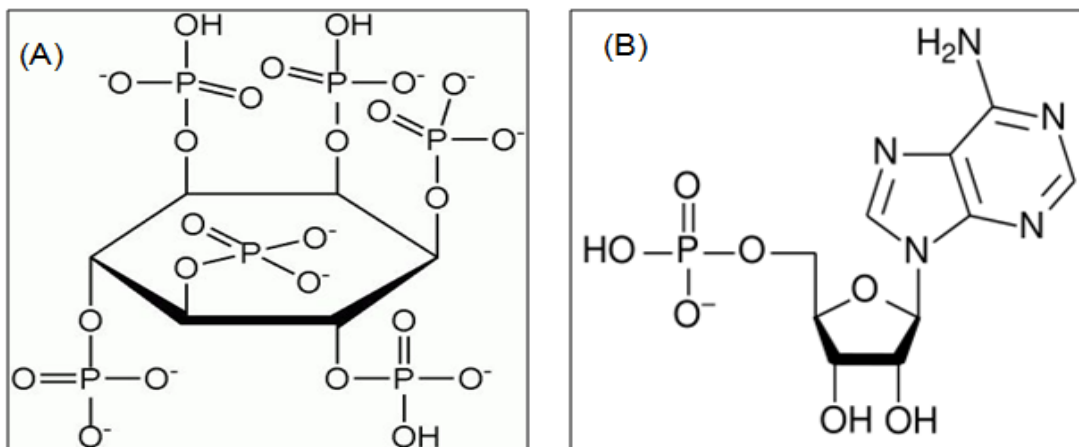


**Figure 23: (A) Molecular structure of IP<sub>6</sub> (B) Molecular structure of AMP (Figures are from Wikipedia, 2011).**

As shown in Figure 24 experiments were performed by using the DGT exposure system. The system was provided by NIVA. 50 L acid washed tank with motorized lid was used as exposure chamber that was filled with test solution. Metsorb and ferrihydrite DGTs were deployed at the rim of rotor plate and the motor speed was adjusted so the rotor plate had same rotating speed to ensure constant fluid velocity during experiments.

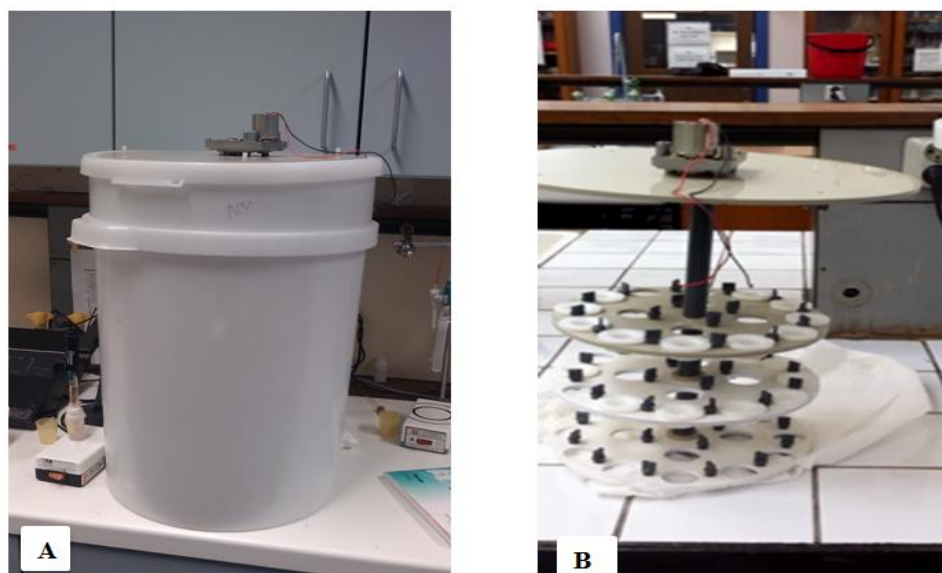


**Figure 24: (A) 50 L tank which was used as exposure chamber with motorized lid, (B) Lid for tank with 15 volt electrical motor on top and circular rotor plates mounted below the lid on which Metsorb and ferrihydrite DGTs were fitted interlock clips.**



First experiment was conducted by deploying DGT samplers using both Metsorb and Ferrihydrite as adsorbents in AMP test solution at pH 5.5 for 1, 3, 5, 8, 11, 13, 15 18 and 20 days at room temperature. The 50 L pre-acid washed exposure tank was filled with ~45L of AMP test solution equivalent to 26 µg/L. Preparation of test solutions is described in Appendix E.1 and Appendix E.2. The selection of desire pH was done on the basis of fresh water pH.

Samples of the test solution in which the DGT where immersed were also taken during the exposure time. This was done in order to control AMP concentration throughout the experiments. Concentration of test solutions might change due to decomposition and wall absorption. DGTs sampler were placed in acid washed plastic bag and stored at ~ 4<sup>0</sup> C, until elution of the phosphate from the adsorbent. Samples of test solution were also stored in dark room at ~ 4<sup>0</sup> C, until analysis.

The experiment using IP<sub>6</sub> was conducted in a similar manner as for AMP described above, though the concentration of P in the test solution was set to 25 µg/L and DGT samplers were immersed in the test solution for only 1 to 8 days.

### **3.3 Laboratory location and facilities**

Quantitative analysis of major solutes in the water samples collected as a part of the EUTROPIA project was performed at the laboratory of Environmental analysis group at the Department of Chemistry, University of Oslo. Analyses of carbon, nitrogen and phosphorus fractions as well as DGT samples were conducted at NIVA's chemical laboratory. The data for Morsa monitoring program were provided by Bioforsk. Analysis was performed by Eurofins AS.

### **3.4 Water samples analysis**

The analysis of pH, conductivity, alkalinity, UV and VIS absorbency, major anions and cations as well as filtration of Suspended Solids (SS) on stream water samples in the EUTROPIA project are performed in a co-operation effort among Master students at UiO who

are assigned to the project. Most of the data and their analytical methods that are described below are compiled from and refer to these other master thesis generated within the EUTROPIA project. The important exception is for the analyses of carbon, nitrogen and phosphorus fractions as the data contributed through this thesis is the concentrations of carbon, nitrogen and phosphorus fractions. The stream water samples from Morsa monitoring program were analysed for suspended solids (SS), total-P fractions at Eurofins AS. Raw data set for EUTROPIA projects is available through DUO<sup>3</sup>. Raw data set for Morsa monitoring program can be found in Bioforsk (2011).

### **3.4.1 Filtration of water samples and determination of suspended solids (SS)**

Filtration of water samples was conducted according to NS-EN 872 (2005). The particles were divided into inorganic suspended solid (SS<sub>i</sub>) and organic suspended solid (SS<sub>o</sub>) according to the method of Krogstad (1992). This was done in order to determine the amount of suspended solids in streams water samples and for further analysis of filtered water samples.

Filtration was done using Whatman GF/F 0.7µm, 47 mm, filter papers. GF/F 0.7 µm was used instead of the standard membrane 0.45 µm filter paper due to that the GF/F is made of glass fibre and therefore can be burned in order to determine the organic content of the suspended particle fraction. These filter papers were pre-washed, pre-burned at 440<sup>0</sup>C, dried, and weighted. After the sample was filtered through filter paper, the filter paper was dried at 105<sup>0</sup>C and re-weighted. Total SS concentration in the sample was determined gravimetrically by weight increased. Organic suspended solid (SS<sub>o</sub>) was found gravimetrically by loss on ignition (LOI) by igniting the dried filter paper at ~ 450<sup>0</sup>C for 4 hours. Inorganic suspended solid (SS<sub>i</sub>) was measured by calculating the weight difference between the clean filter paper and the weight after ignition. More detailed regarding calculation and procedure is given in Appendix A.

---

<sup>3</sup> <http://www.duo.uio.no/sok/search.html/>

### **3.4.2 Electrical conductivity and pH**

pH and conductivity were measured according to ISO10523 (1994) and ISO7888 (1985), respectively. Raw water sample was measured first for conductivity by using a portable conductivity meter, Mettler Toledo AG, FiveGo™. Thereafter pH was measured potentiometrically by using an Orion Research pH-meter with a Ross combination electrode. This was performed by master student Sahle S. Weldehawaria.

### **3.4.3 Alkalinity**

Determination of alkalinity was conducted in raw water sample with a pH > 5.5 according to NS-EN ISO 9963-1 (1995). The analysis was carried out potentiometrically by titration of the sample with 0.02 M HCl until pH of 4.5 was obtained, and determining the volume titrant required. This was done by PhD research fellow Christian W. Mohr and master student Sahle S. Weldehawaria using a  $\Omega$  Metrohm Swissmade 716 DMS Titrino.

### **3.4.4 Absorbency at UV (254 nm) and VIS (400 nm)**

The absorbency of the samples were measured for at UV ( $\lambda$ 254 nm) and VIS ( $\lambda$  400 nm) by using 10 mm quartz glass HELLMA® cuvettes on a Shimadzu UV1201 UV-Vis Spectrophotometer. This was done by PhD research fellow Christian W. Mohr and master student Sahle S. Weldehawaria in order to get a proxy of content and quality of dissolved natural organic matter (DNOM).

### **3.4.5 Major anions**

The concentrations of F<sup>-</sup>, Cl<sup>-</sup>, SO<sub>4</sub><sup>2-</sup>, and NO<sub>3</sub><sup>-</sup> in filtered samples were measured conductometrically after chromatographic separation of the ions using a Dionex ICS-2000 Ion Chromatography System with chemical suppression. The analysis was conducted by PhD research fellow Alexander Engebretsen according to ISO 10304-1 (1992) and in agreement with DIONEX manuals.

Sea-salt corrected sulphate concentrations at Dalen stream was measured by using following Equation (a):  $nssSO_4-S = \text{total } SO_4-S - (0,054 * Cl)$  (Appelo & Postma, 2007).

### **3.4.6 Major cations**

The concentrations of  $Ca^{2+}$ ,  $Mg^{2+}$ ,  $Na^+$  and  $K^+$  in filtered water samples were determined by master student Sahle S. Weldehawaria using an optical emission spectrometry after atomization and excitation in plasma using an inductive coupled plasma optical emission spectrometer (ICP-OES) (Varian Vista AX CCD simultaneous axial view ICP-OES product of Varian Ltd, Australia) in accordance with ISO 22036 (2008).

### **3.4.7 Analysis of Aluminium fractionation**

Determination of the concentration of Aluminium fractionations was conducted by master student Sahle S. Weldehawaria on water samples with  $pH < 5.5$ . The procedure is based on Barnes and Driscoll 8-hydroxyquinoline/MIBK extraction method (Driscoll, 1984; Barnes, 1975). Fractionation of monomeric aluminium ( $Al_a$ ) from polymeric forms was accomplished by complexation with 8-hydroxyquinoline at  $pH 8.3$  with subsequent extraction into MIBK organic phase (Sullivan et al., 1987).

The samples were also run through an Amberlite IR-120 cation-exchange resin column in order to capture  $Al_i$  and thereby separate organic bound monomeric aluminium ( $Al_o$ ) from inorganic labile aluminium ( $Al_i$ ). Aluminium complex with 8-hydroxyquinoline present in the organic extract was determined photometrically at  $\lambda 395$  and  $600nm$ . The concentration of  $Al_i$  lost in the ion exchange column was calculated as the difference between  $Al_a$  and  $Al_o$ .

### **3.4.8 Phosphorous fractionation in EUTROPIA project water sample**

Figure 25 shows the different phosphorus fractions that were determined in the steam water samples collected as a part of the EUTROPIA project. Raw and filtered water samples were analyzed for total-P and  $PO_4-P$  in order to obtain concentration data on bio- and process-

relevant fractions of phosphorus compounds. By this simple fractionation, it is possible to sort out three to four operationally defined fractions of P in water. The amount of particulate bound P (PP) and dissolved organic P (DOP) can be determined by subtracting the Group A from Group B and Group C from Group D, respectively (Figure 25). An overview and terms of different P fractions that are used in this master thesis in regards to these fractions is given in Table 6.

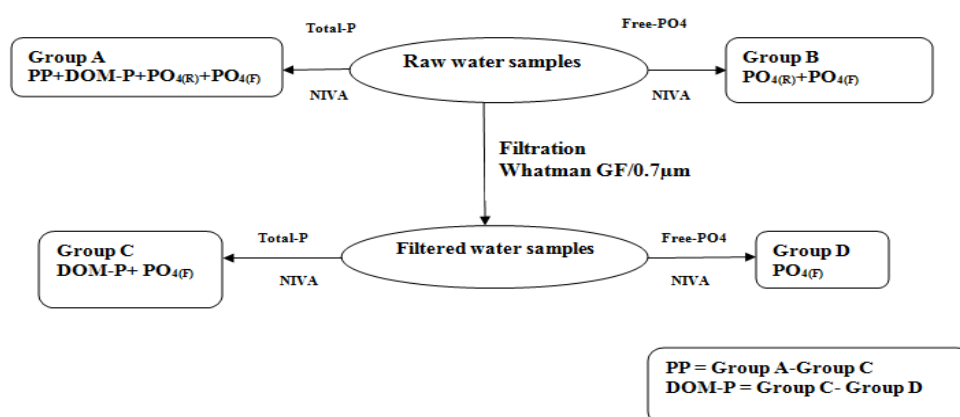


Figure 25: The phosphorus fractionation scheme for water samples (Modified from Vogt, 2011(Per.comm)).

Table 6: Overview and terms for different P fractions.

Fraction	Acronym	Group
Total phosphorus (raw water)	Total-P	A
Reactive phosphorus (raw water)	$PO_{4(R)} + PO_{4(F)}$	B
Total phosphorus (filtered water)	Total-P <sub>(F)</sub>	C
Reactive phosphorus (filtered water)	$PO_{4(F)}$	D
Particulate phosphorus	PP	A-B
Dissolved organic phosphorus	DOP	C-D

### 3.4.9 The carbon, nitrogen and phosphorus autoanalyser

The carbon, nitrogen and phosphorus autoanalyser (CNP autoanalyser) is a NIVA customized Continuous Flow Analyser (SKALAR San<sup>++</sup> Automated Wet Chemistry Analyser). This instrument provides up to seven analytical measurements from a single sample. Major nutrients (PO<sub>4</sub>-P, NO<sub>3</sub>-N, NH<sub>4</sub>-N, and Si), Total P, Total N and DOC were analysed by using this automated analyser. The instrument set up is shown in Figure 26. The instrument generates its own calibration solution by using multi variable stock solution. Details regarding the instrument are not provided in this thesis in accordance with confidentiality agreement with NIVA.

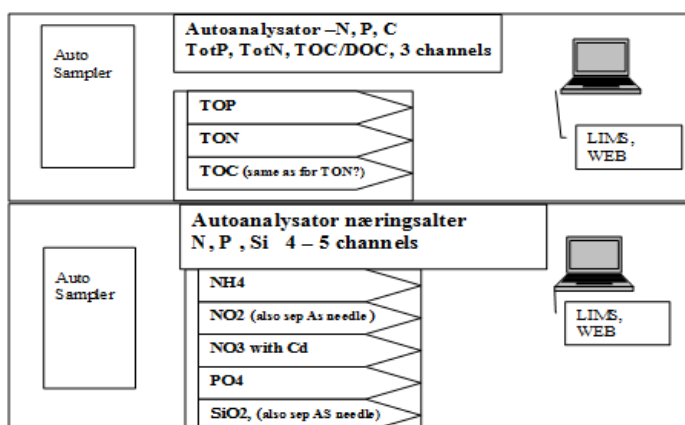


Figure 26: Instrument setup of CNP autoanalyser (Røyset, 2011(Pers.comm)).

### 3.4.10 Analysis of Phosphorous

Determination of total phosphorous and orthophosphate in water samples were performed by using CNP autoanalyser. Analysis of total-P was conducted according to 15681-1 (2004). Method is based on potassium peroxodisulfate (K<sub>2</sub>S<sub>2</sub>O<sub>8</sub>) digestion as described in Norwegian Standard NS 4725 (1984). In order to determine total-P the complex inorganic and organic P compounds in the sample needs to be digested to orthophosphate by decomposition with K<sub>2</sub>S<sub>2</sub>O<sub>8</sub>.

Determinations of phosphate are based on molybdate blue method (MBM) according to ISO 6878 (2004). Ammonium heptamolybdate, catalyzed by potassium antimony (III) oxide tartrate, reacts in an acidic medium with diluted solutions of phosphate to form a yellow

coloured phospho-molybdic acid complex. This complex is reduced to an intensely blue coloured heteropolycomplex by ascorbic acid. The concentration of this complex, and thereby the concentration of orthophosphate in the sample, is measured as absorbency at 880 nm.

Samples and standard were acidified with concentrated H<sub>2</sub>SO<sub>4</sub> to obtain a 0.04M SO<sub>4</sub><sup>2-</sup> concentration. This was done approximately one week before analysis.

### 3.4.11 Analysis of TON, NO<sub>3</sub>-N, NH<sub>4</sub>-N and DOC

The concentration total organic nitrogen (TON), nitrate (NO<sub>3</sub>-N), ammonium (NH<sub>4</sub>-N) and dissolved organic carbon (DOC) were determined by using a CNP autoanalyser. Details of these methods are not described due to a confidentiality agreement with NIVA, but the principals of the methods are provided in Table 7.

**Table 7: Basic principles for analysis methods for TON, NO<sub>3</sub>-N, NH<sub>4</sub>-N and DOC.**

Parameter	Method	analyzed	Detection principle	wavelength
TOC	Persulphate digestion/CO <sub>2</sub> stripping	CO <sub>2</sub>	IR detection	N/A
TON	Persulphate digestion /Cd reduction Griess reagent <sup>4</sup>	NO <sub>2</sub> -N	Photometrically	540
NO <sub>3</sub> /NO <sub>2</sub>	Cd reduction, Griess reagent	NO <sub>2</sub> -N	Photometrically	540
NH <sub>4</sub> -N	OPA method <sup>5</sup>	NH <sub>4</sub> -N	Fluorometrically	450-1200

### 3.4.12 Analysis of P and SS in Morsa monitoring program

Data on total-P fractions and SS in stream water samples from the Morsa monitoring program were provided by Bioforsk (2011). These samples were analysed at Eurofins AS. The analysis of total phosphorus (TP) and free reactive phosphorus (RP) was based on NS EN ISO 15681-1 (2004) and NS EN ISO 15681-2 (2004), respectively. SS concentrations were measured according to NS 4733-2 (1983) and NS-EN872 (2005). It has not been possible to get any

<sup>4</sup> Griess reagent is a solution of sulphanilamide and  $\alpha$ -naphthylamine under acidic conditions.

<sup>5</sup> The sample reacts with orthophtaldialdehyde (OPA) and sulphite. This reaction produces an intense fluorescent product that is measured fluorometrically.

detailed about the analytical procedure conducted at Eurofins As and therefore it was difficult to identify that analysis performed at NIVA and Eurofins As differs in any manner in the way they are actually conducted.

### **3.4.13 Compilation of P- data**

In trying to merge the data set from EUTROPIA project with the phosphorus data from the Morsa monitoring program, it was found that the concentration of total P fractions did not agree well with each other (Table A12 and A13, Appendix D). Even though water samples were taken from the same place and same time, total-P concentrations were found to be higher in the Morsa monitoring program data analysed by Eurofins As, compared with the total P concentrations measured by the EUTROPIA project (Table A12, Appendix D). The concentration of total-P was found to be well correlated ( $r = 0.92$ ) (Figure A7, Appendix D), whereas the concentration of free- $\text{PO}_4$  were poorly correlated ( $r = 0.59$ ; One outlier omitted). The median ratio between the two data sets for total-P and free- $\text{PO}_4$  concentrations were 2.3 and 3.0, respectively.

Determination and fractionation of P are operationally defined. The results are likely to be influenced by sample handling and pre-treatment, and possibly varying analytical procedures conducted by the Environmental Analysis group and Eurofins AS. The reason for this inconsistency has not been possible to identify and is beyond the scope of this study. However, two free- $\text{PO}_4$  and two total-P control samples, as well as three stream water samples were sent to Eurofins laboratory in an attempt to assess the cause for these differing results. These samples were handled in the same manner. These control samples and water sample were also analysed in parallel using the CNP autoanalyser achieving similar results in both parallels (see Table A14, Appendix D). Based on this very limited set of control data we can only simply state that the data from the control sample with low concentration of total-P and free- $\text{PO}_4$  were found to be reported with relatively higher values by the Eurofins laboratory compared with the results obtained by using CNP autoanalyser. The control samples with high concentration of total-P differed by 6 to 30% between the two laboratories. It should be stressed here that this is not sufficient data to draw any general conclusion. The results for stream water samples did not contribute to any clarification as the relative differences between the laboratories differed from previous results. There may be several



different causes that may lead to the differing results e.g. different storage time and different sample handling, and possibly deviating preservative methods and different analytical instrument for analysing sample.

Both datasets from EUTROPIA project and Morsa monitoring program will be used throughout this thesis and it will be specified which data are used in the presentation of results.

### 3.5 Elution and analysis of DGTs samples

#### 3.5.1 Elution of Metsorb and ferrihydrite gels

Metsorb and ferrihydrite adsorbents were eluted in 1M NaOH and 4M H<sub>2</sub>SO<sub>4</sub>, respectively. Systematic elution process is shown in Table 8.

Elution of phosphate from metsorb binding gel was performed twice in order to measure elution efficiency.

**Table 8: Systematic presentation of elution process.**

DGT samplers	
Metsorb	Ferrihydrite
<ul style="list-style-type: none"> <li>Receiving phase was put in 30 ml polypropylene tubes</li> <li>Add 2ml of 1 M NaOH and left over night</li> <li>Add 28 ml TypeII water</li> </ul>	<ul style="list-style-type: none"> <li>Receiving phase was put in 30 ml polypropylene tubes</li> <li>Add 0.3 ml of 4M H<sub>2</sub>SO<sub>4</sub> and 0,7 ml type II water and left over night</li> <li>Add 29 ml of Type II water</li> </ul>

#### 3.5.2 Analysis of DGT samples

After elution, both Metsorb and ferrihydrite samples were analysed for total-P and free-PO<sub>4</sub> by using CNP autoanalyser as described in Chapter 3.4.10. All samples were acidified by using concentrated H<sub>2</sub>SO<sub>4</sub> to achieve a concentration of 0.04 M prior to analysis. Data can be found in Appendix E.

### **3.6 Calculation of flow-weighted mean concentration and flux of P**

In order to estimate runoff for a specific stream the daily runoff from Skuterud stream was multiplied by the ratio of the areas of the sub-catchment of the specific stream and the Skuterud stream (see section 3.1.5).

The flow-weighted mean concentration of total-P for investigated streams is calculated by multiplying the sample concentration with runoff intensity during the time of sampling (which gives transport). Thereafter, flow-weighted mean concentration is obtained by dividing the sum of transport with sum of runoff. Equation is shown in Appendix F.1.

The transport or fluxes of P in the investigated streams were obtained by using linear interpolation based on the correlation between runoff (L/s) and concentration of total-P ( $\mu\text{g/L}$ ) in stream samples that were collected during the monitoring period. The correlation graphs with  $R^2$  values can be found in Appendix F.2. This method was adopted from a Bioforsk report on the monitoring of the Lake Vansjø and its tributaries (Skarbøvik et al., 2011). The equations obtained by linear interpolation were used to estimate the continuous concentrations and P-release pattern throughout the year. There are considerable uncertainties in the calculations since the P concentrations are based on discrete samples of small streams while runoff data are continuous and based only on hydrological response of the Skuterud stream. The transport of P is calculated for four hydrological years 2006-2010.

### **3.7 Statistical analysis**

#### **3.7.1 Hierarchical cluster analysis**

The Hierarchical Cluster Analysis (HCA) is a method of modelling groupings, or clusters of similar parameters or objects. The clusters are visualized with a dendrogram, a two-dimensional chart where the y-axis shows the similarity (where 100 % is very similar and 0 % is very unlike) between the clusters and the horizontal lines denotes the clusters (Esbensen et al., 1994). Analysis was performed by using Minitab 16 Statistical Software (2010).

### **3.7.2 Principal component analysis**

A Principal Component Analysis (PCA) is a way of identifying patterns in large data matrix and expressing the pattern in such a way as to draw attention to revealing “hidden phenomena” in a large data set and to find out similarities and differences between samples and variables (Jolliffe, 2005). Analysis was performed by using Minitab 16 statistical software (2010).

## **4 Results and discussion**

### **4.1 Results from water sample**

#### **4.1.1 Stream water pH and alkalinity**

pH is a key water parameter governing the weathering of soils and mobility of many ions though determining the extent of hydrolysis and thereby their speciation in water. It is also a measure of water acidity. Median value of the pH in the nine investigated streams is shown in Figure 27. Results show clear relation between the pH and land use with streams draining agricultural catchments having higher pH compared to the pH value of streams draining forested catchments. Results show that the pH values of the Støa1, Vaskeberget, Huggenes and Årvold streams, which mainly drain the agricultural catchments, are even found to be slightly alkaline. The higher pH of the streams draining agricultural catchments is due to the agricultural soils which are naturally rich in base saturation and because the soils are artificially limed. The pH of Sperrebotn, Augerød and Guthus streams are significantly higher than what is found in the Dalen stream, even though all these streams mainly drains forested catchments. This indicates that the runoff from agricultural land has great influence on the pH of the stream water, even after passing through a relatively short stretch of agricultural practice. Concentration of  $H^+$  ions in the stream is as such found to be slightly positively correlated ( $r = 0,583$ ) to the amount of forested land within the watershed, while negatively correlated ( $r = -0,401$ ) to the contribution of agriculture land.

Dalen stream drains a completely forested catchment with acid soils that are rich in organic matter (Mohr, 2010). Concentration of dissolved natural organic matter (DNOM) in the Dalen stream is found to be high (median value of 22.8 mg C/L). The natural organic material is a

strong proton donor as it contains weak organic acids (e.g. carboxylic acid) which release  $H^+$ . The low pH of the Dalen stream is mainly explained by this high organic content. It is also explained by that the soils in the Dalen catchment are poorly weatherable sandy mineral soils that give the soils a low base saturation and there by an acidic character.

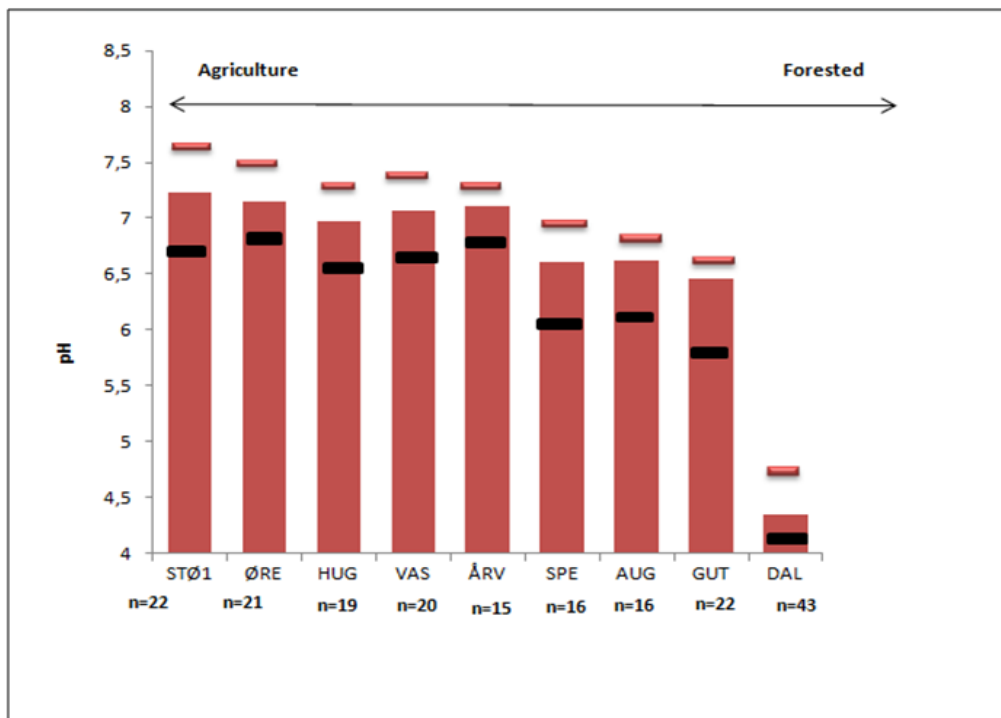


Figure 27: pH in the nine investigated streams. Bars show median values. The red and black lines represent 25<sup>th</sup> and 75<sup>th</sup> percentiles of data series value. Numbers of data are shown at the bottom of graph.

Alkalinity is a measure of the waters ability to neutralize inputs of acid. Without this neutralizing capacity, any acid added to the water bodies would immediately change its pH. Table 9 shows the median value of alkalinity in the nine investigated streams. When the pH value is between 5.5-8.5 inorganic buffering against pH change is provided by  $HCO_3^-$  component and thereby the bicarbonate alkalinity becomes important (Klaff, 2002). All investigated streams, except for the Dalen stream, have pH value above 5.5.

Alkalinity is found to be positively correlated ( $r = 0,535$ ) with the amount of agriculture land use while strong negatively correlated ( $r = -0,895$ ) to extent of forested area. The higher alkalinity of the streams draining agricultural catchments is mainly due to liming and

weathering of carbonate minerals in the agricultural areas since there is likely more carbonate minerals naturally in these soils. These carbonate minerals are more weatherable than the igneous gneiss and granite. The alkalinity is also partly due to that the soils in agriculture land are richer in clay and silt. This allows them to hold more base cations.

The lower alkalinity of the streams draining forested catchments is due to acidification of poorly weatherable soils by natural organic acids. The amount of bicarbonate available to provide buffering is negligible in the Dalen catchment due to acid soils that consists of poorly weatherable soil material with little capacity to hold base cations.

**Table 9: Alkalinity in the nine investigated streams.**

Streams	STØ1	ØRE	HUG	VAS	ÅRV	SPE	AUG	GUT	DAL
Median ( $\mu\text{mol/L}$ )	2132	1419	828	1162	1561	416	302	267	0
25 <sup>th</sup> percentile of data ( $\mu\text{mol/L}$ )	1361	1050	585	958	1274	296	234	193	0
75 <sup>th</sup> percentile of data ( $\mu\text{mol/L}$ )	2511	1646	1162	2156	1756	642	453	433	0
Number of samples	17	15	15	12	11	11	11	11	43

#### 4.1.2 Major cations and anions distribution

In aquatic systems the amount of major anions and cations ions are greatly dependant on the land use distribution. This is an inherent proxy for a number of soil characteristics governing weathering and leaching of the elements from the soil in the catchment area. Mean concentration of major cations and anions in the nine investigated streams are shown in Figure 28. Raw data and correlations curves are given in Appendix B.1.

The correlation coefficients between the sum of anions and cations in the nine investigated streams ranges between  $r = 0.89$  to  $r = 0.98$ . Figure 28 shows that the ionic strength is found to be much higher in the streams draining high contingency of agriculture land compared to the streams draining forested catchments. An exception is Årvold stream that does not follow the pattern. The higher ionic strength in the Årvold stream is likely due to road salting as the stream is flowing along and receives direct drainage from a major highway. The general

higher ionic strength of streams draining catchments with agriculture is due to higher contribution of especially  $\text{Ca}^{+2}$ ,  $\text{Mg}^{2+}$  and  $\text{HCO}_3^-$ . The concentrations of both  $\text{Ca}^{2+}$  and  $\text{HCO}_3^-$  are positively correlated to the amount of agriculture land-use ( $r = 0,596$  and  $r = 0,682$ , respectively) in the watershed. This indicates that both ions mainly come from the weathering of the soil mineral and from the liming of the agriculture soils by using. In contrast, there are only minor contributions of ions from the forest soils due to slow weathering of the acid igneous minerals comprising the soil material in the forested catchments.

$\text{Na}^+$  and  $\text{Cl}^-$  are dominant ions in the stream draining forested catchment. The chemistry of the water passing through the forested watershed is thus mainly influenced by the sea-salt loading and not by soil-soil water interactions. The ratio between the mean concentrations of  $\text{Na}^+$  and  $\text{Cl}^-$  is found to be  $\sim 0.81$  in the runoff from forested area. This is only slightly below that found in the ocean (0.86), indicating a minor loss of sodium relative to the mobile chloride deposited as marine sea-salt aerosols.

Average concentration of  $\text{SO}_4^{2-}$  is  $23\mu\text{eq/L}$  in Dalen stream whereas sea-salt corrected average concentration of  $\text{SO}_4^{2-}$  in Dalen stream is  $18\mu\text{eq/L}$ . This indicates that the anthropogenic input of this anion contributes today less than 22%. The amount of  $\text{SO}_4^{2-}$  in the streams draining agricultural catchments is greatly influenced by the oxidation of sulphides.

Strong correlation ( $r = 0,803$ ) is found between  $\text{Ca}^{2+}$  and  $\text{Mg}^{2+}$  within the streams draining agriculture catchments. The concentration of both cations are positively correlated to the amount of agriculture land-use ( $r = 0,596$  and  $r = 0,911$ , respectively) in the watershed of the stream. This is due to that both cations come from weathering of the same soil minerals, as soils are naturally rich in carbonate minerals and from liming and fertilization of the agricultural fields. The amount of  $\text{Ca}^{2+}$  is as commonly found to be about 3 times higher than  $\text{Mg}^{2+}$ , and the ratio between these two ions keeps constant through the buffering by ion exchange with the soil. In addition, some  $\text{Mg}^{2+}$  and  $\text{Ca}^{+2}$  also come from deposited sea salts. The amount of  $\text{K}^+$  and  $\text{NO}_3^-$ -N is positively correlated to the agriculture land use ( $r = 0,904$  and  $r = 0,576$ , respectively). Correlation between these two ions are also high ( $r = 0,717$ ), indicating the common influence of the fertilizer. Both ions are nutrients that are not mobile unless they exist in surplus of demand.

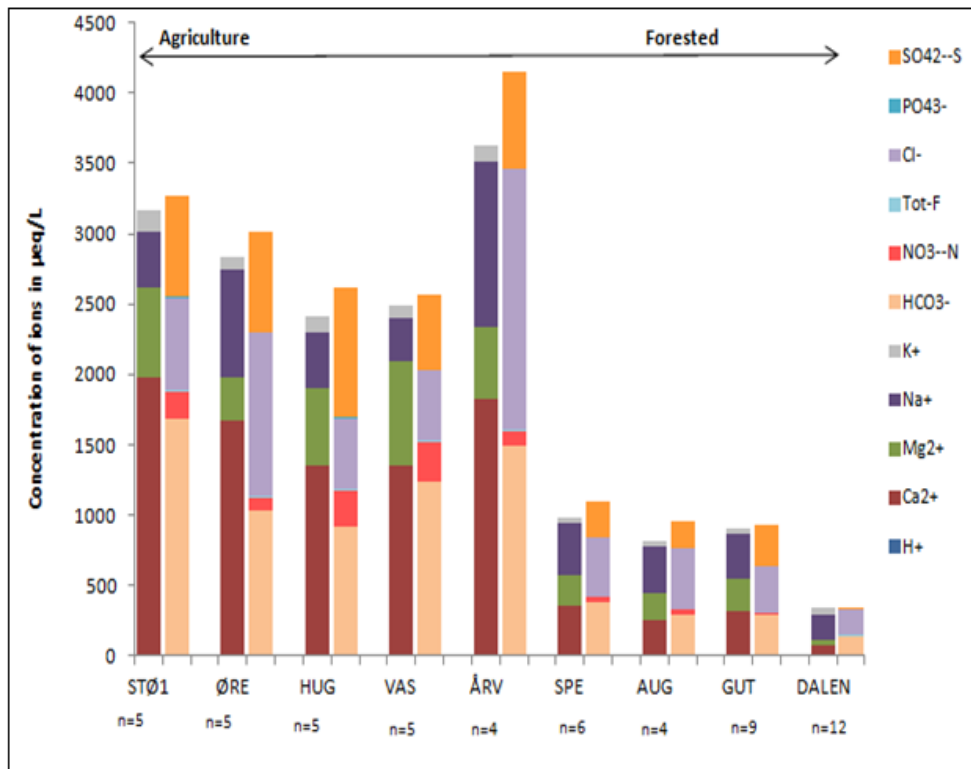


Figure 28: Mean concentration of major cations and anions in the nine investigated streams. For each stream, the first column represents the concentration of cations and the second column represents the concentration of anions. Numbers of data are shown at the bottom of graph.

#### 4.1.2.1 Aluminium fractions in the Dalen stream

It is here postulated that the reduction in acid rain is one of the confounding factors that is counteracting the abatement actions to reduce the flux of phosphate to the surface waters.  $\text{SO}_4^{2-}$  deposition is reduced by 70%. This has led to decreased inorganic labile aluminium ( $\text{Al}_i$ ) concentration due to low solubility of  $\text{Al}(\text{OH})_3$  at higher pH. Labile aluminium is a strong flocculent of orthophosphate. Thus, the decline in acid rain has likely resulted in a decreased loss of P due to reduced co-precipitation of orthophosphate with leached aluminium.

In the 1970ties and 1980ties the southern eastern part of Norway received high loading ( $\sim 122 \mu\text{eq/L}$ ) of anthropogenic  $\text{SO}_4^{2-}$  deposition. This led to elevated concentration of inorganic labile aluminium ( $\text{Al}_i$ ) in the runoff from acid sensitive forested catchments (Skjelkvåle & Wollman, 2009). A significant level of  $\text{Al}_i$  is still found to be  $0.13\text{mg Al/L}$  (average) in the Dalen stream mainly due to the remaining 21% anthropogenic input of sulphate. Activity of

$Al_i$  in water greatly depends on the pH. At  $pH > 5.5$   $Al_i$  concentration are below detection limit at about  $1 \mu\text{mol/L}$  (Appelo & Postma, 2007). Therefore samples with  $pH > 5.5$  are not analysed for aluminium fractions. The reduction in sulphate deposition had also led to increased concentrations of DNOM (see section 2.1.8), thus on average significant level of organically bound monomeric aluminium ( $Al_o$ ) ( $0.49 \text{ mg Al/L}$ ) is also found in the Dalen stream.

#### 4.1.2.2 Iron content

As described in chapter 2.1.6 the iron has a central role in determining the amount of phosphate sorbed to the soil by binding it as amorphous  $FePO_4$  and by functioning as a bridge between an organic coating on the soil particles and the orthophosphate ion. During reducing condition, such as in water logged soils during floods, the Fe (III) is reduced to Fe (II), reducing the irons capacity to hold phosphate. Iron is only soluble in the reducing conditions or when it is bound to DNOM.

XRF<sup>6</sup> analysis was performed by Gebreslasse (2012) on sediments samples in order to determine content of major cations in some of the investigated streams sediments. The content of  $Fe_2O_3$  in the sediments is presented in Table 10. The results from sediments can be useful to assess the iron content in the investigated streams. The amount of iron is found to be higher in the Støa1, Huggenes, Augerød and Guthus streams. Gebreslasse (2012) showed that the iron content in the suspended sediments is found to be much higher in the Støa1 where soils are rich in iron.

**Table 10: Concentration of  $Fe_2O_3$  in the sediment samples (Gebreslasse, 2012).**

Streams	STØ1	ØRE	HUG	VAS	ÅRV	SPE	AUG	GUT	DAL
Content of $Fe_2O_3$ in g/Kg	69.0	N/A	44.6	29.5	N/A	39.6	65.0	48.7	26.5

<sup>6</sup>X-ray fluorescence (XRF) is a quantitative analytical technique used for the rapid simultaneous determination of many major and minor elements in soil, rock and sediment samples in solid forms.



### 4.1.3 Concentration of Dissolved natural organic carbon

Dissolved natural organic matter (DNOM) play a central role in forest ecosystem functioning by governing the water chemistry and in transporting C, P and N in the natural environment. DNOM contain ligands that are capable of complexing metals such as Al (Currie et al., 1996; Nasholm et al., 1998) and Fe. The amount of dissolved organic carbon (DOC) is used as a proxy for DNOM and constitutes approximately 50% w/w of the DNOM. The light absorbency at 254nm may be used as a proxy for DOC.

The median concentration of DOC, measured in the nine investigated streams, ranges from 6.2 mg C/L to 22.9 mg C/L (Figure 29). The amount of DOC is found to be lower in the streams draining agricultural land compared to forested catchments and it is negatively correlated ( $r = -0.549$ ) to the agriculture land use. This is due to that the DNOM is much less mobile in soils with high base saturation. Only a limited amount of DNOM is thus leached from agricultural soils. The amount of DOC is higher in streams draining watersheds with a high proportion of forest. The DNOM that is leached out from the forests, typically located upstream of the agricultural land, is efficiently lost by coating the suspended particles in stream upon passing through the agricultural land by the increased ionic strength and calcium concentration.

DOC concentrations are strongly positively correlated to the extent of forested area in the watershed drained by the stream as well as the concentration of  $H^+$  ion ( $r = 0.841$  and  $0.860$ , respectively). This is due to that the soils in forested land are naturally rich in organic matter and acidic with low content of base cations to precipitate out the DNOM. In organic surface horizons, where the concentration of DNOM is high, most of the Al in solution is organically complexed, whereas in the mineral soil inorganic monomeric Al predominates (Nygaard & Wit, 2000). Organically bound monomeric aluminium ( $Al_o$ ) is a dominant form in the Dalen stream.

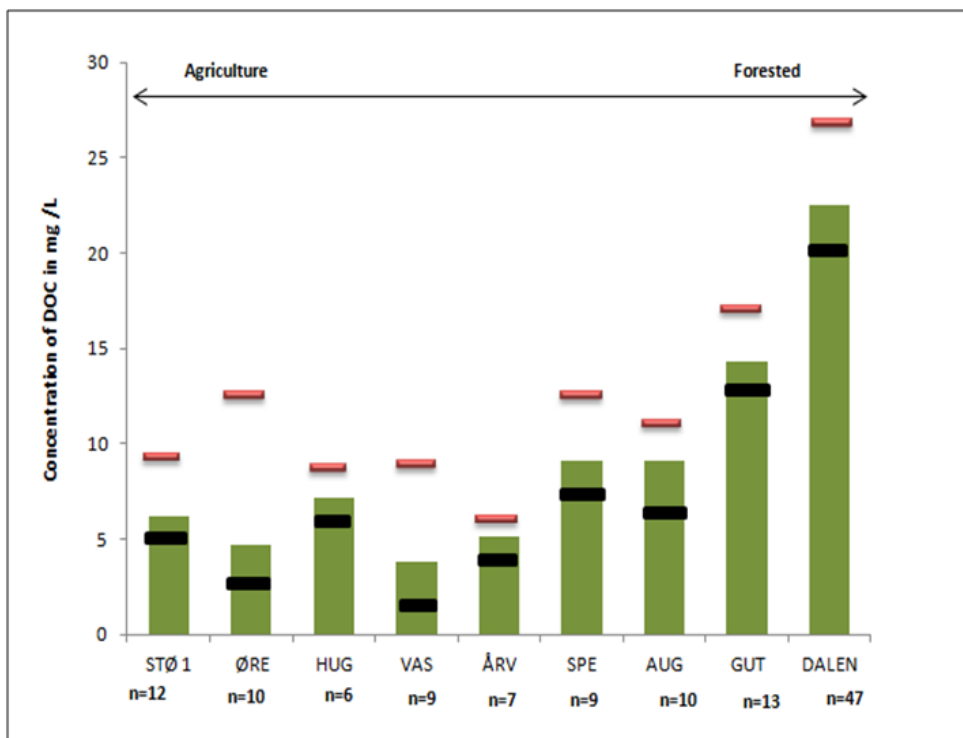


Figure 29: Median concentration of dissolved organic carbon (DOC) in the investigated streams. The black and red lines represent 25<sup>th</sup> and 75<sup>th</sup> percentiles of data series value. Numbers of data are shown at the bottom of graph.

#### 4.1.4 Distribution of total N

Even though phosphorus is found to be the growth-limiting nutrient in most of water bodies, it is also possible to find many aquatic ecosystems where growth-limiting element is nitrogen. Nitrogen imitated system is often found to be a greater problem than P limiting system since the sources of this nutrient are harder to control (Henderson & Markland, 1986).

Median concentrations of nitrate, ammonia and organic bound N in the nine investigated stream are shown in Figure 30. The result shows that the total N concentrations are influenced by land use, likely due to the addition of reactive N with fertilizers in agricultural land. Concentrations of total N are thus generally found to be higher in the streams draining mainly agriculture area and are lower in forested streams. Nitrate constitutes the main fraction of total N in most of the investigated streams, except Dalen stream. Since the forested Dalen catchment is not N saturated than most of the nitrate and ammonia that is deposited is rapidly assimilated and denitrified or accumulated in the soil and biomass. Reactive nitrogen (e.g. nitrate) may be lost in substantial amounts from natural forest systems by being

incorporated into DNOM. The main fraction of the total N in the stream draining the forested Dalen catchment is thus organic bound N. There is an inherent positive correlation ( $r = 0.552$ ) between the amount of organic bound N and DOC in the Dalen stream. The concentrations of ammonium are kept low despite addition to agricultural land through fertilizing due to that it is efficiently nitrified.

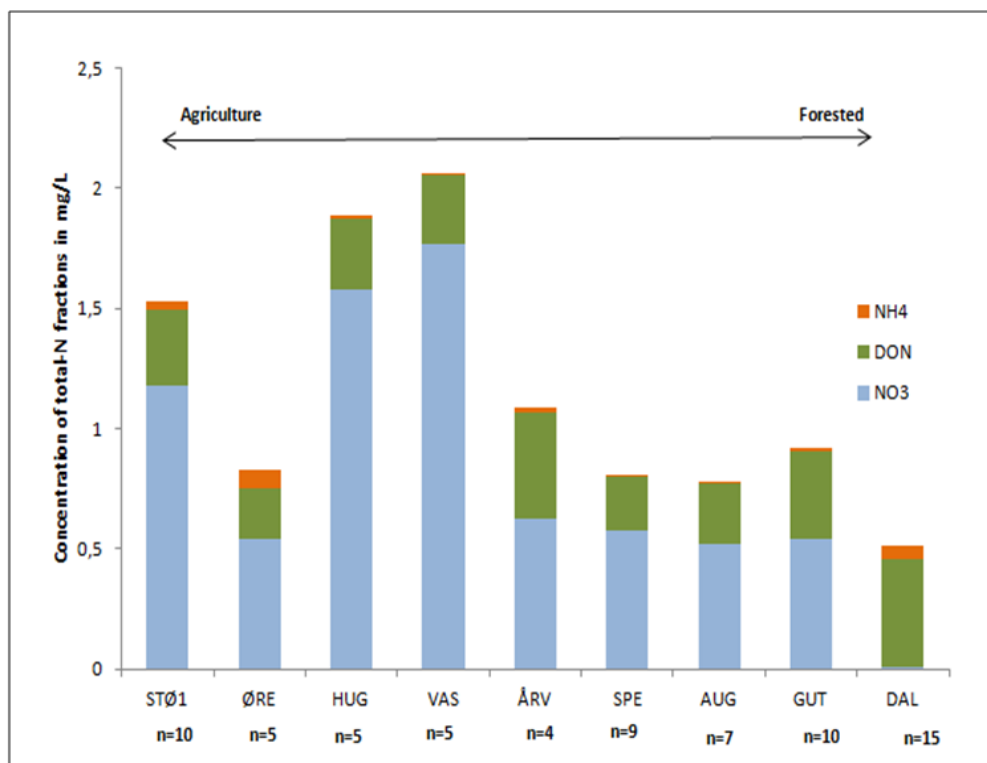


Figure 30: Concentration of nitrate, organic bound N and ammonia in the nine investigated streams. Numbers of samples are shown at the bottom of graph.

#### 4.1.5 Distribution of total phosphorus and its fractions (EUTROPIA data set)

##### 4.1.5.1 Total phosphorus

The total-P was measured in the nine investigated streams in order to look at the variation in the total-P concentration by different land use. As shown in Figure 31, the median concentration of total-P varied from 95.9 to 9.6 $\mu\text{g/L}$ . The total-P concentrations show increasing trend with increasing proportion of agricultural land in the watershed of the streams. The highest amount of total-P is found in the Støa1 stream while the lowest amount

of total-P is found in the Dalen stream giving a positive correlation between the amount of total-P and agriculture land use ( $r = 0.691$ ). This is due to long term excess use of fertilizer making agricultural soils more P rich. It is also expected as anthropogenic input of total phosphorus into Lake Vansjø from the entire catchment is estimated to account for 75 % of the total loading. Agriculture is the largest of the anthropogenic sources, constituting 76 % of the anthropogenic release (Solheim et al., 2001).

The concentration of total P is relatively low in Ørejordet and Årvold streams. The Ørejordet stream represents runoff from residential housing and urban areas and the Årvold stream represents runoff from housing and agricultural practice. The lower amounts of total-P fractions in the Ørejordet and Årvold streams are thus mainly due to the good sewage systems that are upgraded. This is expected as scattered dwellings and manure storage facilities in Western Vansjø are only contributing 4 % of the total-P losses (Aquarius, 2010).

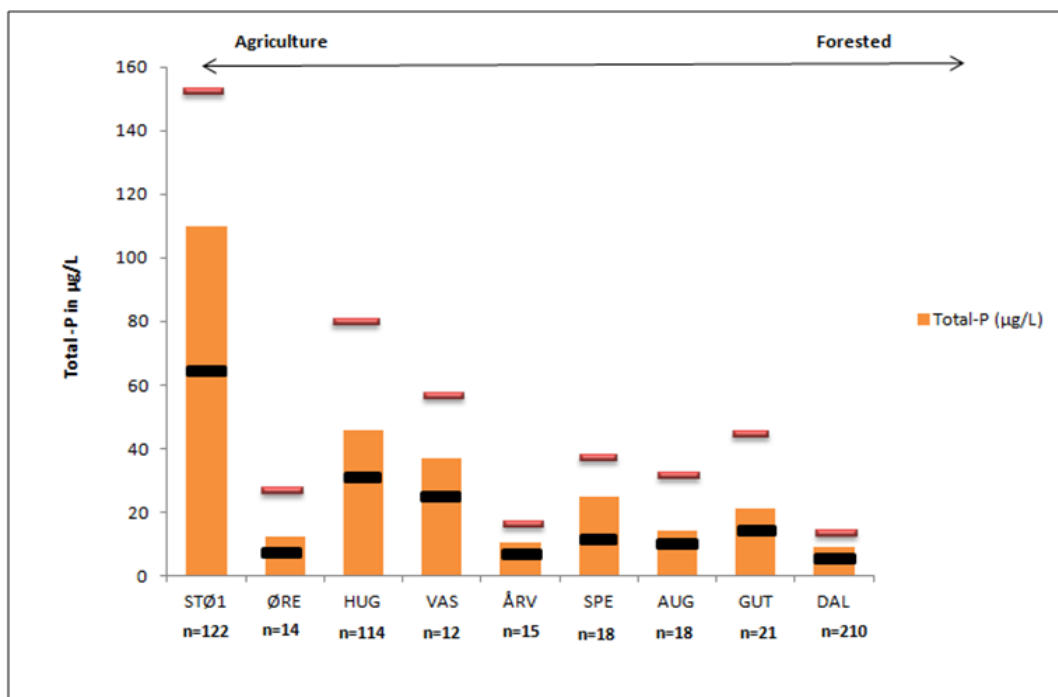


Figure 31: Concentration of total-P in the nine investigated streams (EUTROPIA data set). The black and red lines represent 25<sup>th</sup> and 75<sup>th</sup> percentiles of data series value. Numbers of data are shown at the bottom of graph.

Particle bound P (PP) constitutes the main fraction of the total P (see section 4.1.5.2). The content of P in the soil and erosion of soils are therefore important factors governing the spatial differences in total P concentrations between the studied streams. Physiochemical properties of the soils determine P sorption capacity, erosion risk and water flow paths. These factors together with land-use distribution are thus key explanatory factors for the spatial variation in the total-P concentration. The influence of different land use and agriculture practice can also be seen by the results of the total-P with low values for 100 % forest influenced stream and high values for the 90 % agricultural influenced stream and those in the middle shows combined effect of land use.

#### **4.1.5.2 Distribution of different P fractions**

The distribution of different P fractions found in the investigated streams is presented in Figure 32. The particulate bound P (PP) constitutes a relatively large fraction of the total P found in the stream draining the agricultural catchments, whereas there is an increasing relative amount of the P bound to dissolved organic matter (DOM-P) in the streams draining forested catchments. Results shows that between 50 to 75% of the total P fraction is constituted by PP in the Støa1, Huggenes and Vaskeberget streams. The highest contribution of PP to the total-P is found in the streams draining mixed land use types (e.g. Sperrebotn, Augerød, Guthus).

A strong positive correlation ( $r = 0.96$ ) (see Appendix G) is found between the amount of suspended solids and total-P concentration in the water from the Støa1 stream, which mainly drains 89 % agriculture catchment. This was also found by Skarbøvik et al. (2011) studying the Vaskeberget and Huggenes streams. These streams are also dominated by agriculture catchments. The higher amount of PP in streams draining agricultural land demonstrates large amount of eroded soil material in these streams, as the agricultural catchments are more susceptible for soil erosion. The relationship between the suspended solids and total-P is further discussed in section 4.1.6.2.

It is found a poor but positive correlation ( $r = 0,398$ ) between the absolute amount of DOM-P and DOC in the Dalen stream. The contribution of DOM-P fraction to the total-P ranges between ~ 35 to 47 % in the Sperrebotn, Augerød, Guthus and Dalen streams. These streams

also contain relative high levels of organic matter that inherently lead to elevated amount of DOM-P. Organic matter readily forms strong complexes with metal cations, especially trivalent ions such as aluminium and iron. It can then also bind more orthophosphate via the complexed metals (E.g. P-Fe-OM or P-Al-OM). Higher content of organic matter along with Al and Fe can therefore be responsible for the higher amount of DOM-P in the streams draining forested catchments (Gerke, 1993). Reduction in the acid rain has led to increase the amount of DNOM (see Figure 29). In natural catchments like Dalen, the main transport pathway of P is by DNOM.

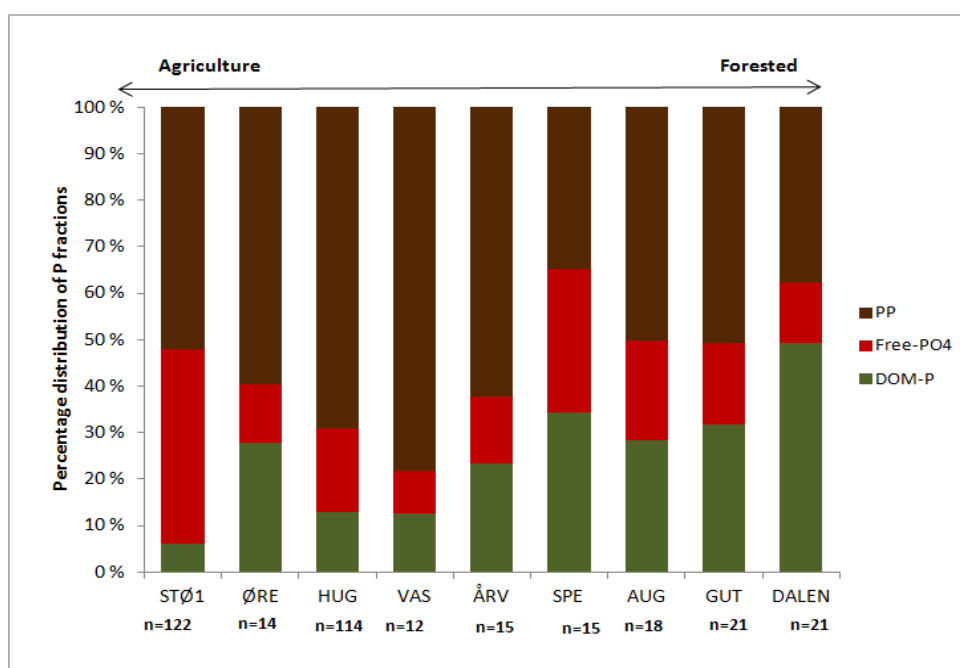


**Figure 32: Percent distribution of P fractions(EUTROPIA data set). Numbers of data are shown at the bottom of graph.**

It is postulated that reduced aluminium leaching in the runoff from forested catchments has led to increase flux of total P to the Western Vansjø Lake.  $Al_i$  concentrations have decreased in the runoff from acid sensitive forested catchments due to reduction in deposition of non-marine sulphate (Skjelkvåle & Wollman, 2009). Labile aluminium ion is widely used as a co-precipitating agent for orthophosphate in sewage treatment plants to remove P (Cooke et al., 1993). This indicate that decreased leaching of Al from upstream forests has led to a decreased co-precipitation of  $PO_4^{3-}$  when these stream passes through agricultural land and

mix with more alkaline agriculture water before entering the lake. This may be a significant contributing factor for the lack of reduced P level in the Western Vansjø Lake, despite considerable mitigation measures to reduced total-P loading to the lake. This is still hypothesis and being studied by other master students in the EUTROPIA project.

The temporal and spatial variation in amount and distribution of different P fractions in stream water can be governed by multiple factors, but land use is a key parameter, and can be used as a proxy for distribution of different P fractions in streams. It is further postulated that the effect of other explanatory variables (e.g. runoff, physiochemical parameters) are also influenced by land use.

#### **4.1.5.3 Total-P and its fractions under different hydrological regime**

Figure 33 shows the average concentration of total-P and its fractions under different hydrological regimes and Figure 34 shows the percent distribution of total-P fractions during different hydrological regimes. High flow samples are marked with an E. The high flow samples were collected during the snowmelt (March and April) and autumn (August to November) season, whereas low flow samples were collected out of these seasons. There is a clear distribution of total-P depending on discharge episodes (E) and land use. Concentration of total-P is found to be significantly higher during the discharge episodes (Figure 33) indicating that total-P concentrations are greatly influenced by runoff intensity. At high flow, the total-P is mainly composed of particulate bound-P in almost all streams except for the Dalen that has higher fractions of DOM-P (Figure 34).

Typical agriculture streams (e.g. Støa1 and Huggenes) with higher erosion risk contain higher amount of Particulate bound P (PP) during episodes of discharge. The amount of erosion greatly depends on the catchment characteristics e.g. land use, slope, soil texture, soil management, size of the catchment. High amount of particulate bound P in these streams is mainly due to that the excess amount of P in the eroded soil particles through runoff from the agriculture fields. Gebreslasse (2012) documented that the amount of total suspended sediments in these streams are highly correlated ( $r = 0.97$ ) with runoff, indicating that higher flow results in more suspended sediment loading, which further lead to more particulate bound P in the stream.

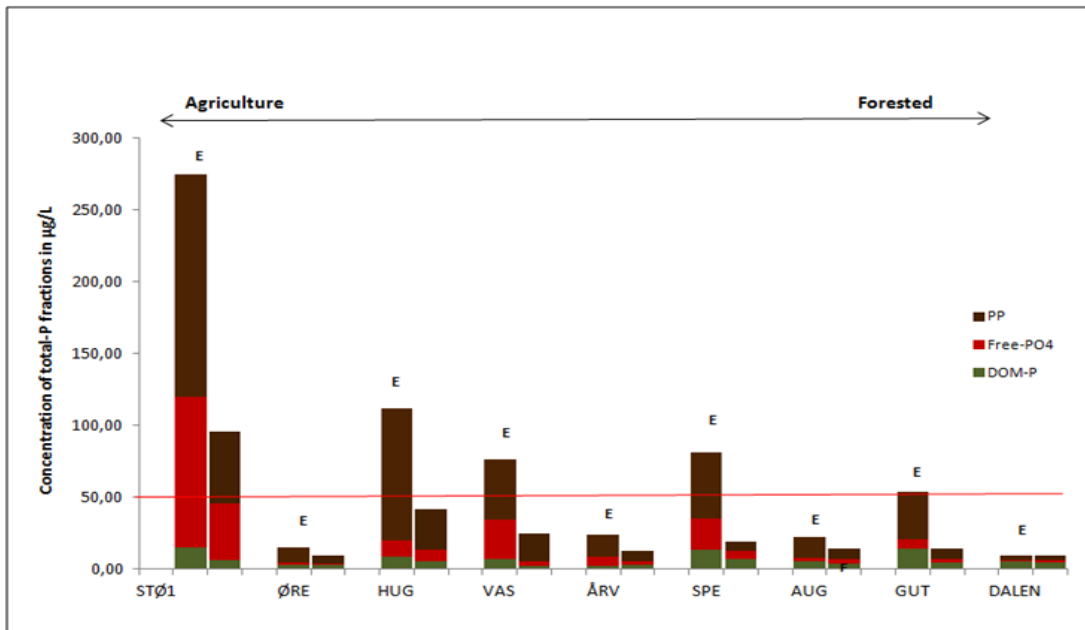


Figure 33: Concentration of total-P and P fractions during different hydrological regimes (EUTROPIA data set). \*E indicates the samples collected during the hydrological discharge episodes. The red line shows the environmental goal for Western Vansjø. Numbers of data are given in Appendix (see Table A9, Appendix C.1)

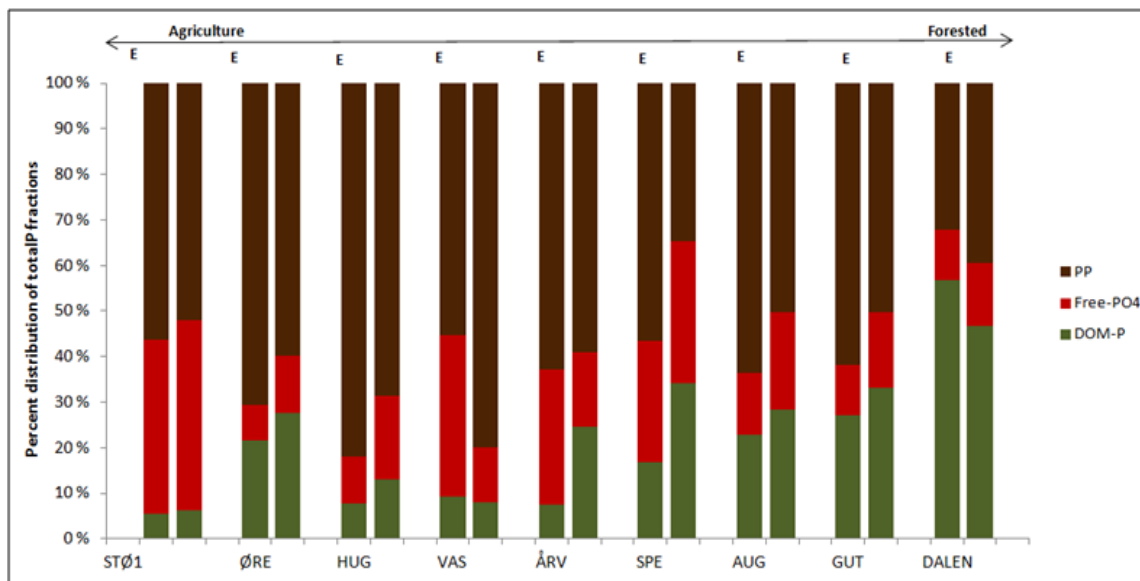


Figure 34: Percent distribution of total-P fractions during different hydrological regimes (EUTROPIA data set). \*E indicates the samples collected during the hydrological discharge episodes.

Marine clay containing apatites are generally found in the valley bottom and flat low land areas below the marine limit in the Morsa watershed (Gebreslasse, 2012). In the agricultural



fields drainage pipes are buried in the marine clay layer. Opland (2011), studying the P-fractions in the runoff from these pipes at Huggenes, found that these drainage pipes causes large losses of total-P due to erosion of the apatite containing marine clay soils in which the drainage pipes are buried. Increased total-P concentration during hydrological discharge episodes is partly due to flushing of these drainage pipes during increased runoff. This is further described in section 4.1.5.4.

During the high flow regime, the second largest fraction of total-P is found to be free- $\text{PO}_4$  and DOM-P in the streams draining the agriculture and forested catchments, respectively. The amount of these fractions can be linked to content of iron and DNOM in the streams. This is further discussed in section 4.1.5.4 below.

A major point to be made here is that most of the abatement actions are conducted in order to reduce particulate bound P. According to Figure 33 more over ~ 50 to 400  $\mu\text{g/L}$  comes with the different tributary streams, but the amount of total-P in the western Vansjø varies only between 20-40  $\mu\text{g/L}$  (Skarbøvik et al., 2010). Most of the water in the Western Vansjø Lake comes from Storefjorden. The amount of total-P in the Storefjorden also varies between ~ 20-40  $\mu\text{g/L}$ . Massive amounts of particulate P comes in from Hobøl River carrying a total P concentration of ~ 96  $\mu\text{g/L}$  (Skarbøvik et al., 2010), but little of this is found in the Storefjorden Lake. The levels of dissolved P in the tributary streams are sufficient to account for the levels of P found in the lake. It may therefore be hypothesized that the PP is rapidly sedimented and lost in the lake and thus contributes little to the total P levels. The abatement actions targeting the PP may thereby be in vain. Furthermore, the one-sided focus on the reduction of erosion may on the contrary lead to more bio-available P due to less scavenging of P by particles that become sedimented and buried, and that the sedimented material becomes less buried in the sediments and thus are more susceptible to contribute to internal loading of P in the lake.

If this is true than the leaching of free- $\text{PO}_4$  and moreover the background P loading from the forested catchments may play an important role in the eutrophication at Western Vansjø.

#### 4.1.5.4 P fractions during different flow regimes in the Støa1 and Huggenes streams

Figure 35 and Figure 36 represents temporal variation in the concentration of total-P fraction from the Støa1 stream under high and low flow regimes, respectively. The high flow samples were collected during the snowmelt (March and April) and autumn (August to November) season while low flow samples were collected out of these seasons. The concentration of total-P during high flow ranged between 101- 428  $\mu\text{g/L}$ . During lower flow regime, concentration of total-P ranged between 22 and 58  $\mu\text{g/L}$ . Furthermore, the concentration of total-P during high and low flow regimes were compared by paired t-test and found to be significantly higher at high flow indicating that runoff is the major factor determining the temporal variation in the concentration of total-P. Results and statistics can be found in Appendix C.2. The Støa1 stream mainly represents runoff from drainage pipes and these high P concentrations indicate that these pipes represent an important pathway for particulate bound P to the rivers. Under the high flow regime, concentration of total-P is highly correlated ( $r= 0.92$ ) with runoff whereas correlation is found to be poor ( $r= 0.38$ ) during the low flow regime.

Both particulate bound P and free- $\text{PO}_4$  are found to be the main fractions of the total-P during the high flow regimes. In contrast, only particulate bound P is the dominant fraction of total-P during low flow regime. This is somewhat surprising as the particle loading during low flow is much smaller. Large contribution of free- $\text{PO}_4$  fraction during high flow can be explained by the higher content of iron in the Støa1 catchment. During hydrological episodes the main process leading to P release is reductive dissolution of the ferric iron, releasing the P bound to Fe(III)hydroxides and Fe-P minerals (Shenker et al., 2005) and by the iron bridging between an organic coating and phosphate (E.g. ferric hydroxide- phosphate complexes). Flooded soils are water saturated and reducing condition may occur in stagnant soil water due to decomposition of organic matter. Under reduction condition, ferric iron ( $\text{Fe}^{3+}$ ) is reduced to form ferrous iron ( $\text{Fe}^{2+}$ ). This will lead to that orthophosphate absorbed to iron is being released as outlined in Chapter 2.1.6.

The absolute fraction of DOM-P is found to be slightly higher during low flow regime compared to high flow regime. This is likely due to the dilution of DOM-P during high flow. Forested catchments which are generally rich in DNOM in the forest floor, and with minor amount of bogs, may experience higher leaching of DOM-P during the high flow. This is due to a predominant sub-lateral water flow-path through the organic horizon directly into the

stream, bypassing the absorptive mineral soil layers (Gebreslasse, 2012). This can be seen in the Dalen stream (Figure 34).

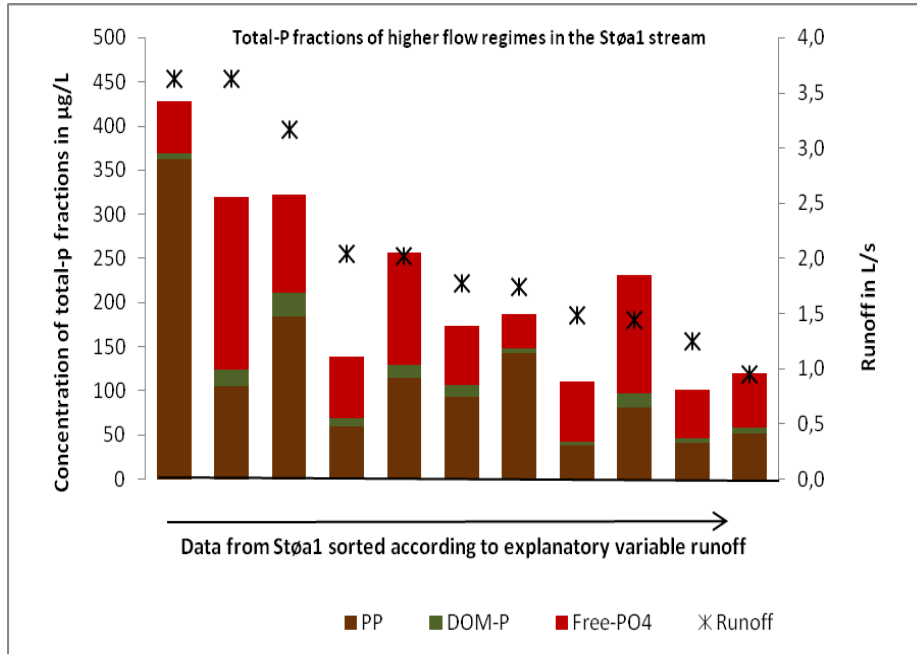


Figure 35: Total-P fractions of higher flow regime in the Støa1 stream (EUTROPIA data set).

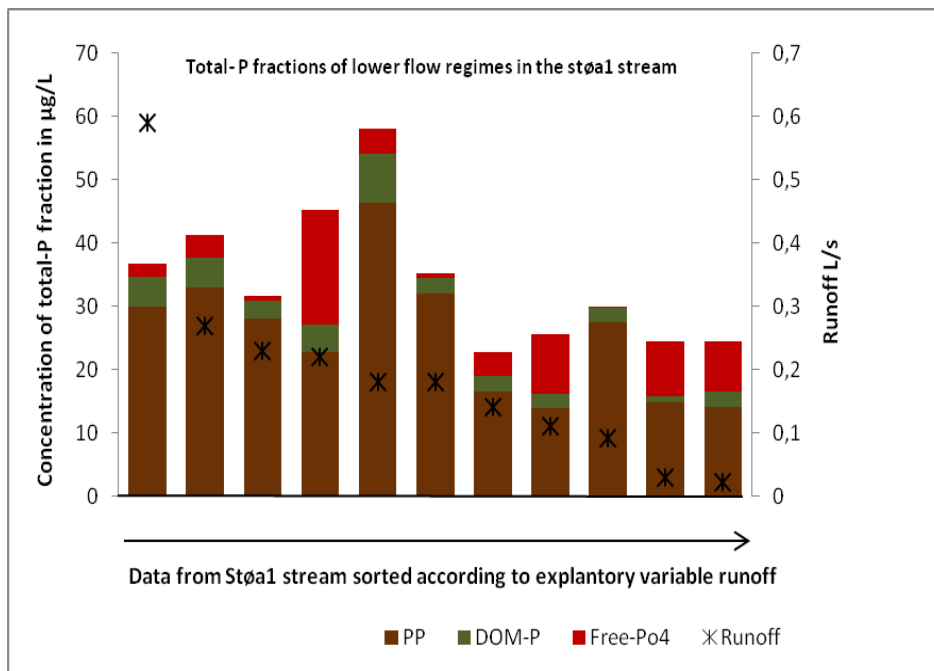
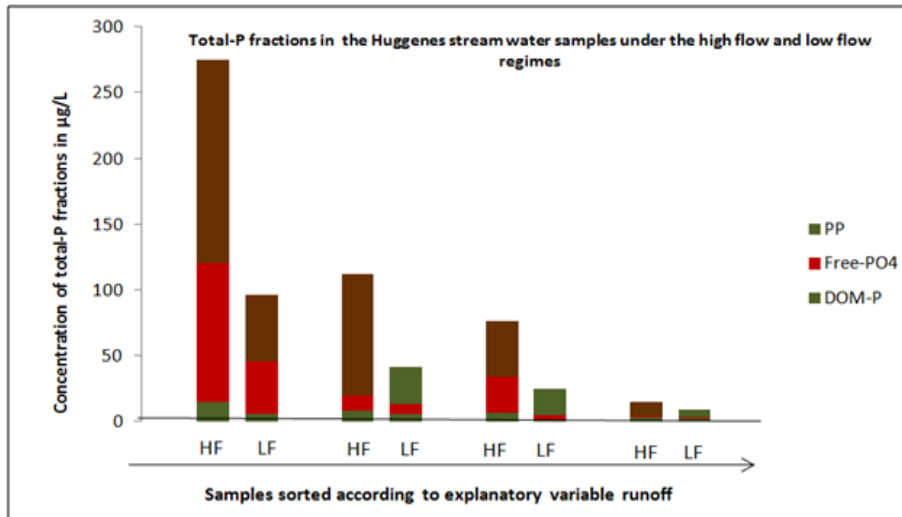


Figure 36: Total-P fraction of lower flow regime in the Støa1 stream (EUTROPIA data set).

The concentration of total-P fractions in the Huggenes stream during high and low flow hydrological regimes is presented in Figure 37. The high flow samples were collected during the fall (19.09.11 and 20.09.11). Low flow samples are from May and July months, with more base flow conditions.



**Figure 37: Total-P fraction during different hydrological regimes in the Huggenes stream (EUTROPIA data set). HF and LF denote the samples collected during the high flow and low flow regimes, respectively.**

Similar as for the Støal stream the concentration of particulate bound P in the Huggenes stream water is much higher during hydrological discharge episodes. P speciation of the water chemistry in the Huggenes stream using MINEQL program shows that  $\text{CaHPO}_4$  is one of the dominant  $\text{PO}_4$  species in the prevailing water chemistry of the Huggenes stream. Gebreslasse (2012) found that most of the inorganic P in the Huggenes stream sediments is bound to calcium. High amount of Ca-P in the Huggenes stream sediments indicates losses of P through drainage pipes that are buried in the apatite rich marine clay layer. During hydrological discharge episodes particles can be eroded from the plough layer and transported both vertically via preferential flow through macropores created by earthworms and dead roots etc and cracks to the drain pipes (Øyegarden et al., 1997). Macropores play therefore an important role in the substantial losses of P through drainage pipes during heavy precipitation following a dry period (Simard et al., 2000). Opland (2011) documented the presence of macropores in the Huggenes catchment soil down to 84 cm depth. Opland (2011) also found that the drainage pipe at Huggenes catchment was an important pathway for P leaching into the Huggenes stream. In addition to the contribution of P from the Ap horizon down to the

drainage pipes through macro-pores there is as discussed above also a substantial release of P by erosion of the apatite rich clay in which the drainage pipe at Huggenes catchment are installed. Opland (2011), studying the soil P pools at Huggenes, found that down to about 1 m depth, where the drainage pipes are located, total phosphorus content increased to quite a high level (70 – 80 mg P/100g) in the soils. Soil eroded from this layer and into the drainage pipes will therefore have a significant P content.

A relative amount of free-PO<sub>4</sub> is also found during the high flow in the Huggenes stream. The soils data at Huggenes by Opland (2011) shows high Fe concentration. High concentration of total-P were found in the streams that are located between the Vansjø and Ra (e.g. Støal, Huggenes), especially in the November and in the summer due to the higher runoff (Skarbøvik et al., 2011). It is therefore postulated that the high content of iron in the catchment of the stream that are located on the Ra (e.g. Støal, Huggenes) may be an important factors governing the negative effect in western Vansjø of the flood in the year 2000, by increasing input of free-PO<sub>4</sub> due to reducing conditions in the soils.

#### **4.1.6 Seasonal and yearly variation in the total-P concentrations (Bioforsk data set)**

##### **4.1.6.1 Flow-weighted mean concentration of total phosphorus**

Flow-weighted mean concentration of total-P (from Bioforsk data) in the nine investigated streams during the hydrological years 2006-2010 is shown in Figure 38. The concentrations are measured by using equation given in Appendix F.1. The results presented here are slightly higher than those previously reported for the same streams and years by Skarbøvik et al. (2011). This is due to that the derived fluctuations in runoff are based on two different streams. Runoff data used in this thesis is based on the Skuterud stream while Skarbøvik et al. (2011) has used runoff data from the Guthus stream. These four hydrological years were selected in order to compare the yearly fluctuation in the total-P concentrations with different climate, temperature and hydrology.

The flood in year 2000 led to an increase in the concentration of total-P in the lake Western Vansjø. As can be seen from Figure 38 the total-P concentrations, now 11 years after the flood, are still higher than the environmental goal for Western Vansjø of 50µg/L. However,

the concentrations shows decreasing trend in almost all streams. This decreasing trend is especially observed in the period 2007-2010 (Skarbøvik et al., 2011). This decreasing trend can be governed by multiple factors. Decline in the total-P concentration is partly due to recovery of the system after the flood. In addition, the year to year variation in the runoff also plays important role in governing the total-P concentration in the streams. This is due to, as described in section 4.1.5.3 and 4.1.5.4, that the total-P concentration is greatly influenced by runoff intensity. It is also partly due to the effect of implemented abatement actions like capture dams, reduced fertilizing, reduced ploughing in the fall, buffer zones etc.

In addition to abatement actions, runoff intensity and the regeneration of system after flood, the inter-annual variations in winter temperature also affect the yearly fluctuation in P concentrations. This is further discussed below.

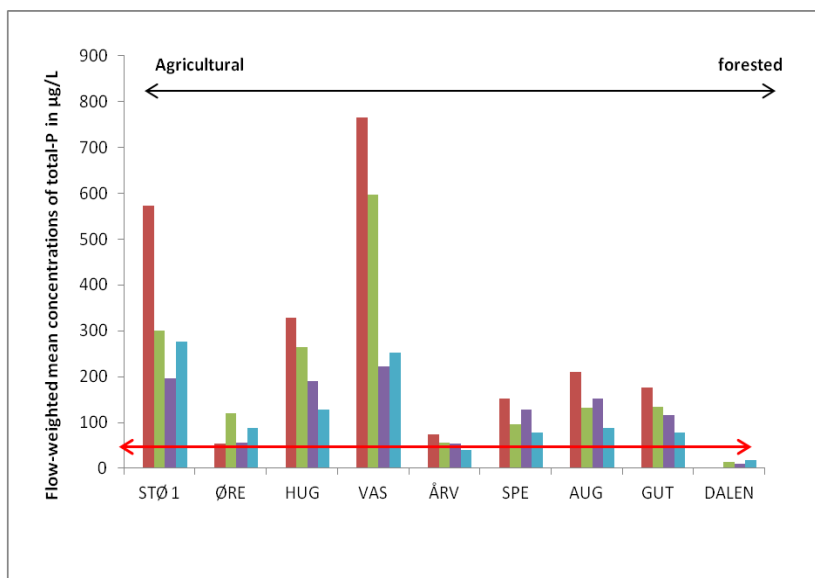


**Figure 38: Flow weighted mean concentration of TP in the nine investigated streams during the four hydrological years (Bioforsk data). The red line shows the environmental goal for Western Vansjø (50µg/L).**

#### 4.1.7 Flow-weighted mean concentration of SS

The flow weighted SS concentration shows the same decreasing trend as total-P during the four hydrological years (Figure 39). This decreasing trend is mainly the effect of implemented abatement actions. Reduced autumn tillage practices and establishment of constructed wetlands

has led to reduced soil erosion and thereby decrease in soil losses from agriculture land. Blankenberg et al. (2008) estimated that during the years 2000 to 2006 the reduced autumn cultivation led to a 20-25% reduction in soil loss from the Western Vansjø catchment.

As described earlier (section 4.1.5.2) a positive correlation between the SS and total-P in the stream draining the agriculture catchments e.g. Vaskeberget and Huggenes streams (Figure 40) are found. The relation between the SS and total-P is found be poor in more mixed land-use catchment streams Guthus and Augerød (Figure 41). This is likely due to that the soils in the forests catchments are more intact and bound up by the roots of perennial plants and therefore prevented from erosion. Gebreslasse (2012) showed that the particle bound P is mainly inorganic in the streams draining agricultural land, while it is mainly organic in the forested streams. The large fraction of total P contributed by particulate bound P and the strong relation between the SS and total P in the streams draining the agricultural land confirms the hypothesis that erosion and transport of particles from agricultural field plays important role in the inputs of total P (Skarbøvik et al., 2011).

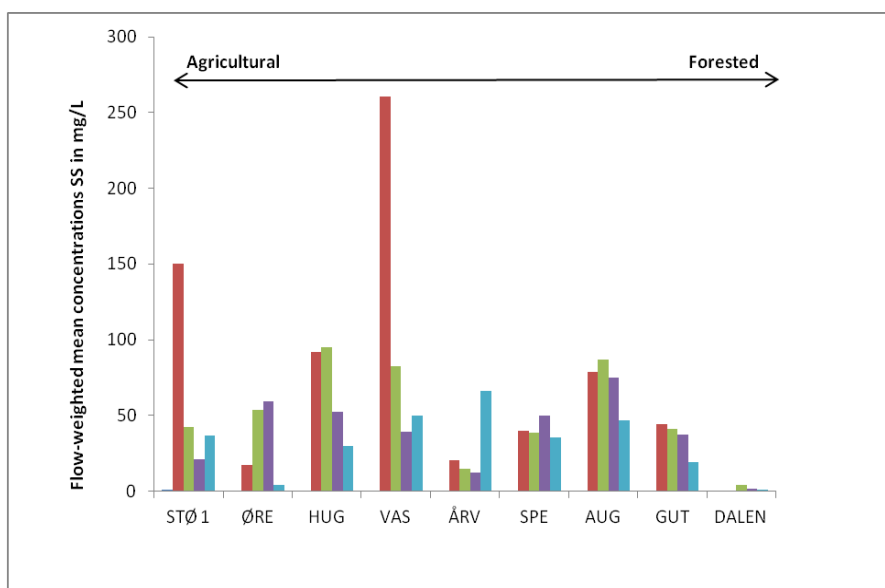


**Figure 39: Flow weighted mean concentration of SS in the nine investigated streams during the four hydrological years (Bioforsk data).**

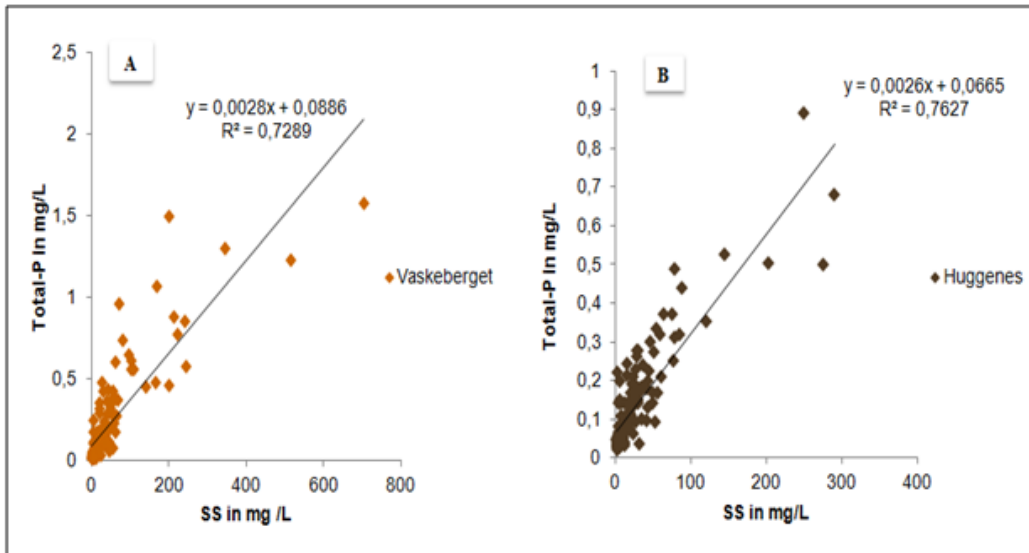


Figure 40: Relation between the SS and total-P in the (A) Vaskeberget and (B) Huggenes streams (Bioforsk data).

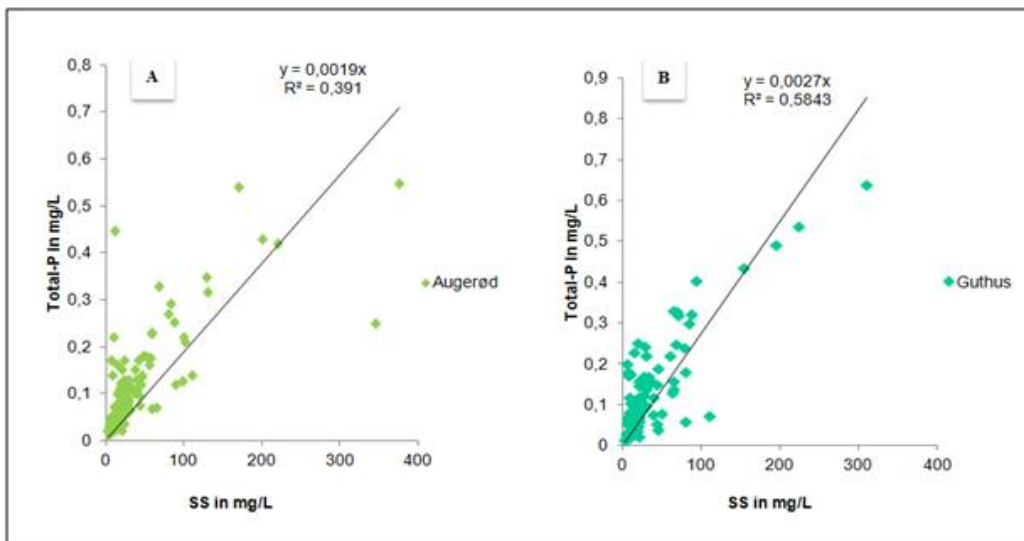
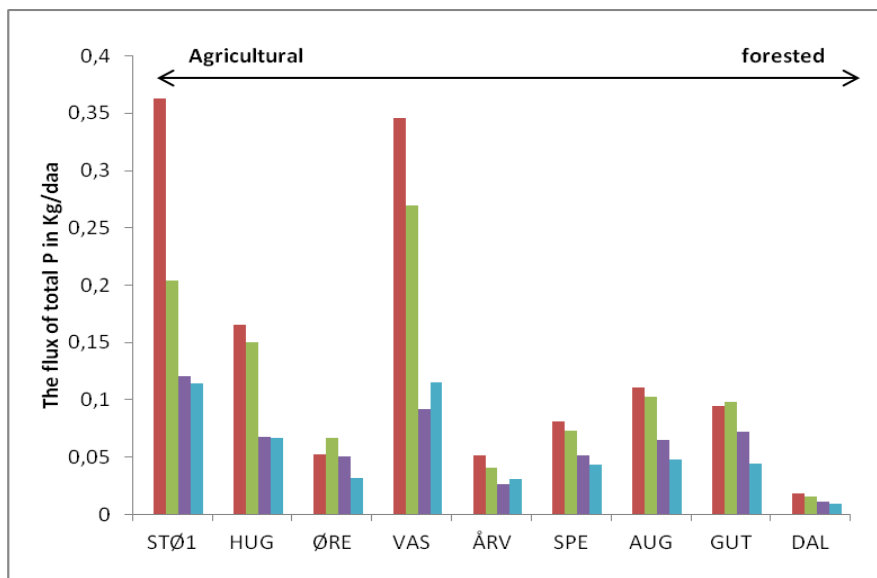


Figure 41: Relation between the SS and total-P in the (A) Augerød and (B) Guthus streams (Bioforsk data).

#### 4.1.8 Flux of total-P to the lake

The flux of total-P to the lake from nine investigated streams during the hydrological years 2006-2010 is shown in Figure 42. The calculation was done by using linear interpolation (see section 3.6).





**Figure 42: Inter-annual fluctuations in flux of total-P to the lake from the nine investigated streams (Bioforsk data).**

The streams that are located on Raet (Støa1, Huggenes and Vaskeberget) contribute a major flux of total P to the lake. Results show a decreasing trend in the P fluxes. This may be partly due to the abatement actions that are implemented.

The Støa1, Augerød and Dalen streams were selected to assess estimated total-P release during the four hydrological years. This is because each stream represents different land use. The correlation between total-P flux and runoff will inherently be strong mainly due to that the total-P release is estimated from the runoff. Opland (2011) also reported similar total P release pattern for the Huggenes stream. Even though the pattern will be the same, this pattern is useful to illustrate the effect of climate change and hydrological cycle on the total P release.

Figure 18(A) shows the runoff and temperature for the hydrological year 2006/2007. Figure 43 and Figure 44 shows the estimated total-P release in Støa1 and Augerød stream, respectively, for the same hydrological year. The data from the Dalen stream is not presented for hydrological year 2006/2007 due to no available data for the year 2006.

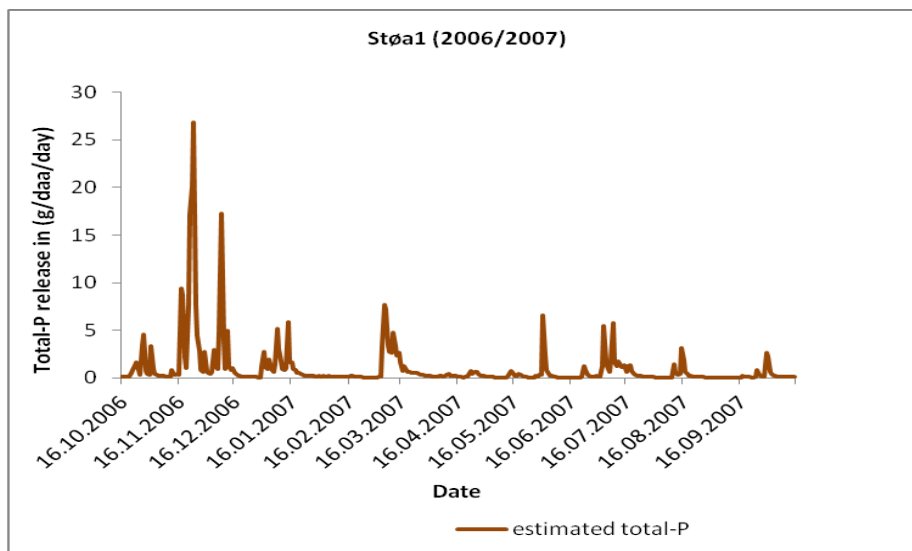


**Figure 43: Estimated daily total-P release (g/daa/day) in the Støa1 stream for 06/07.**

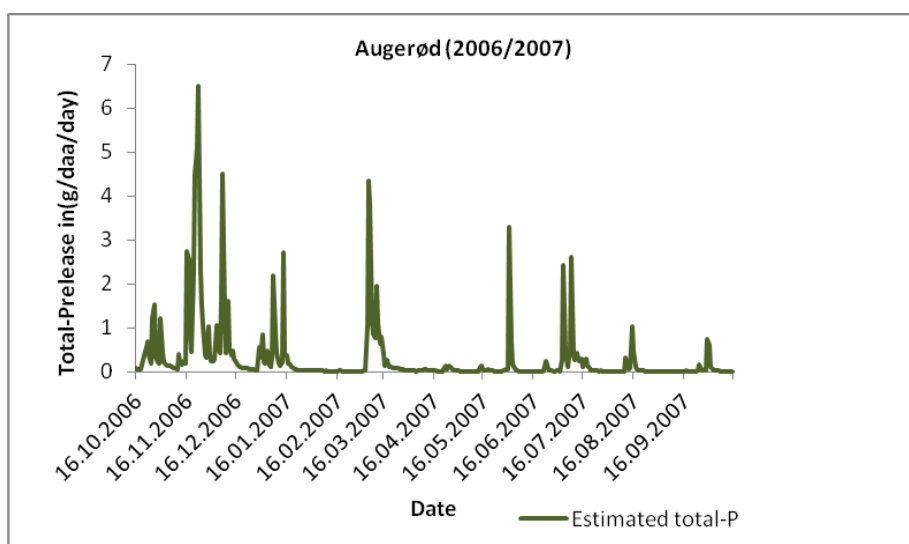


**Figure 44: Estimated daily total-P release (g/daa/day) in the Augerød stream for 06/07.**

During the hydrological year 2006/2007 the main peak of the total-P release is found to be during the second half of the November and partly in December month. The most severe erosion usually occurs on soils with vegetable production due to that these soils are then ploughed in the fall. Soil loss during the late autumn and winter period depends to a large extent on whether or not farmer had tilled the soil after the harvest in the fall (Øyegarden, 2008). An increased in autumn ploughing in the agricultural catchments around the Western Vansjø was reported due to the favourable condition for planting winter wheat in autumn

2006 (Øgaard et al., 2010). Therefore, the main peak of total-P release is found to be during November and December months.

The Augerød stream also shows high total-P release during March which is the snowmelt season. Several researches have recognized that snowmelt can be of great importance for soil erosion (Van Vliet et al., 1976; Ketcheson, 1977). Such a release of total-P is related to freeze - thaw cycling which is further discussed below.

Figure 18(B) shows the runoff and temperature for the hydrological year 2007/2008. Figure 45, Figure 46 and Figure 47 shows the estimated total-P release in the Støa1, Augerød and Dalen streams, respectively, for the same hydrological year.

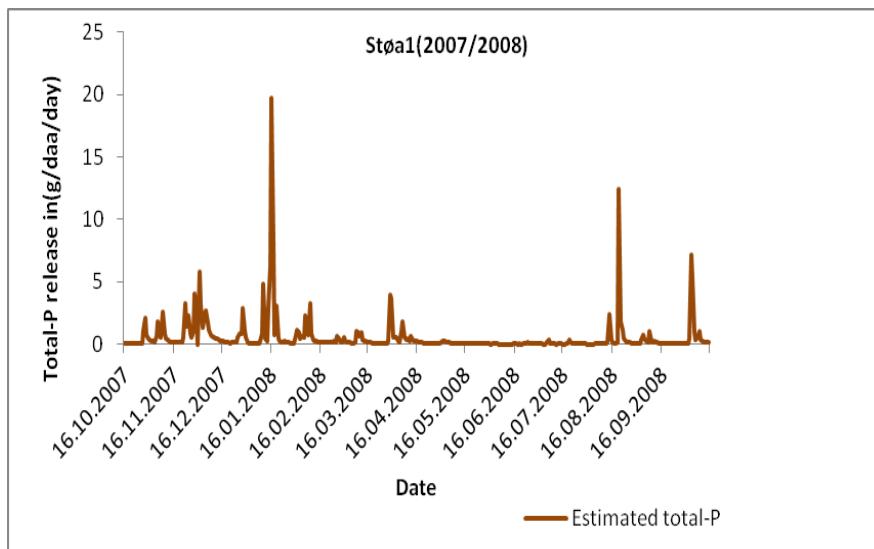


**Figure 45: Estimated daily total-P release (g/daa/day) in the Støa1 stream for 07/08.**

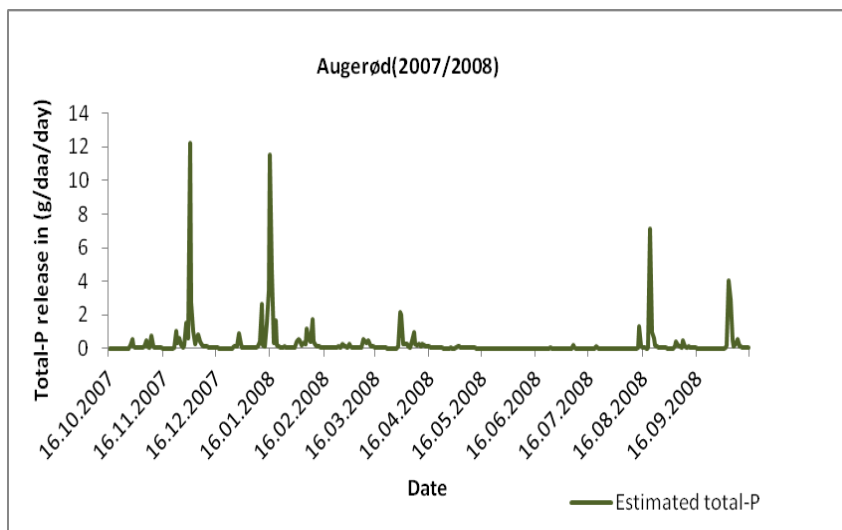


**Figure 46: Estimated daily total-P release (g/daa/day) in the Augerød stream for 07/08.**

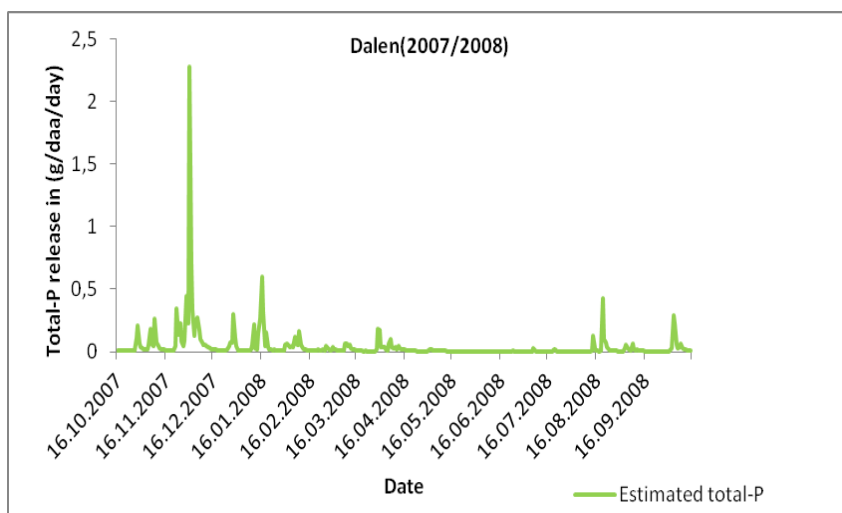


**Figure 47: Estimated daily total-P release (g/daa/day) in the Dalen stream for 07/08.**

Figure 18(B) show that the winter of 2007/08 was relatively warm with temperature remaining almost constantly above the freezing point. The hydrograph shows several winter episodes during December and January, due to the higher temperature and precipitation. The main peak of total-P released in Støa1 occurred during the first half of the January, whereas in the Dalen stream, the main peak of the total-P released occurred in the beginning of December. In the Augerød streams, the main peak of total-P release is found to be during the beginning of the December and also in the first half of the January. The high total-P release during winter in Støa1 stream, which mainly drains agricultural land, is due to freeze/thawing

of the exposed frozen and barren agricultural soils and greater overland flow due to low ability for the water to percolate into the frozen soil, accompanied with factors like partial ploughing, low evaporation, no transpiration and also no assimilation of P due to the dormant period. Frame et al. (1992), studying rill erosion, found a 24 times greater soil loss on frozen soils than in soils with no freezing.

The higher release of total-P during December in the Dalen stream is partly due to the freezing of plants. Freezing causes lysis of plant cell releasing P that is not assimilated due to the dormant vegetation. This allows for organic P and orthophosphate to become mobilized and increase the flux of total-P to runoff (Bechmann et al., 2005). The total-P release pattern in the Augerød stream represents the combined effect of forest and agricultural land use, as it has two main peak of total-P release. One peak is similar to that found in the Støa1 whereas other peak is similar to that found in the Dalen stream. Mohr (2011) found high organic P content in top soils in the organic forest floor (O horizon) in the Dalen catchments. This is mainly due to that this soil horizon is situated within the large internal nutrients cycle of the forest. Mohr (2011) found also higher amount of Ca-P in the valley bottom of the Dalen catchment due to marine deposit relatively rich in phosphorous. About 90% of the Morsa catchment is below the marine limit rendering more P rich soils. The concentration of organic bound P is thus likely also more significant in the runoff from the forested land located below marine limit.

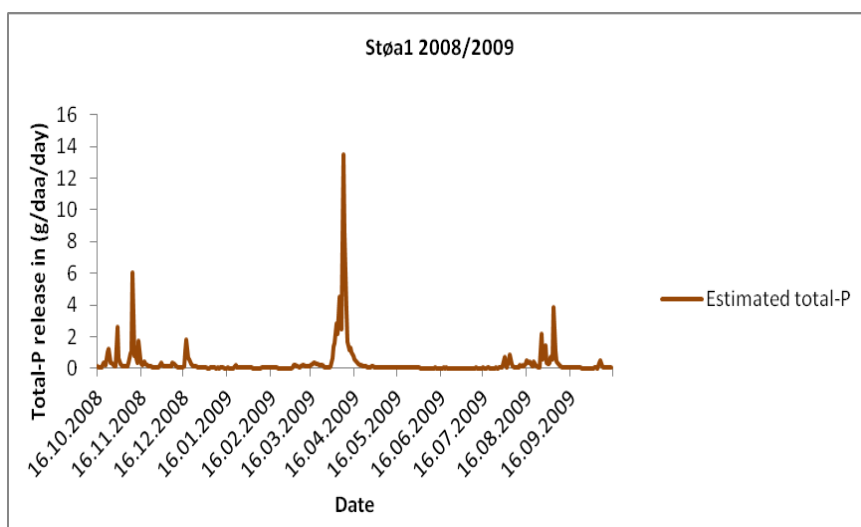


**Figure 48: Estimated daily total-P release (g/daa/day) in the Støa1 stream for 08/09.**

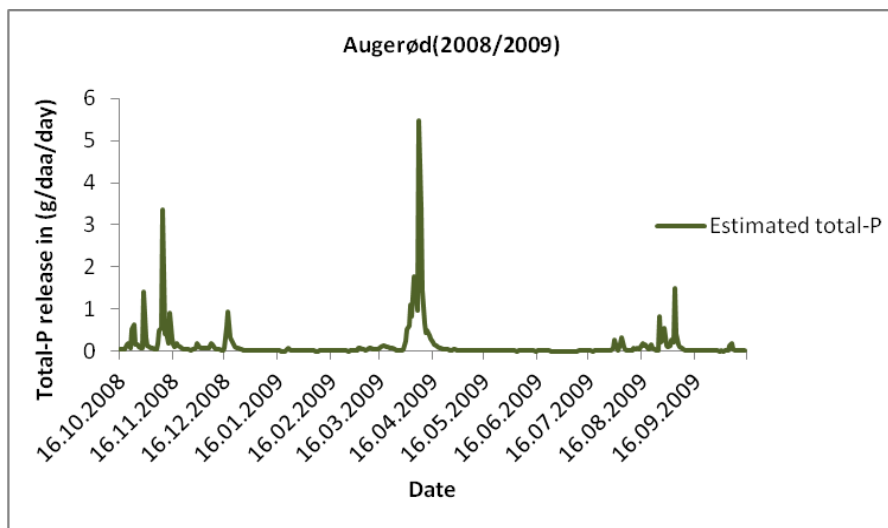


**Figure 49: Estimated daily total-P release (g/daa/day) in the Augerød stream for 08/09.**

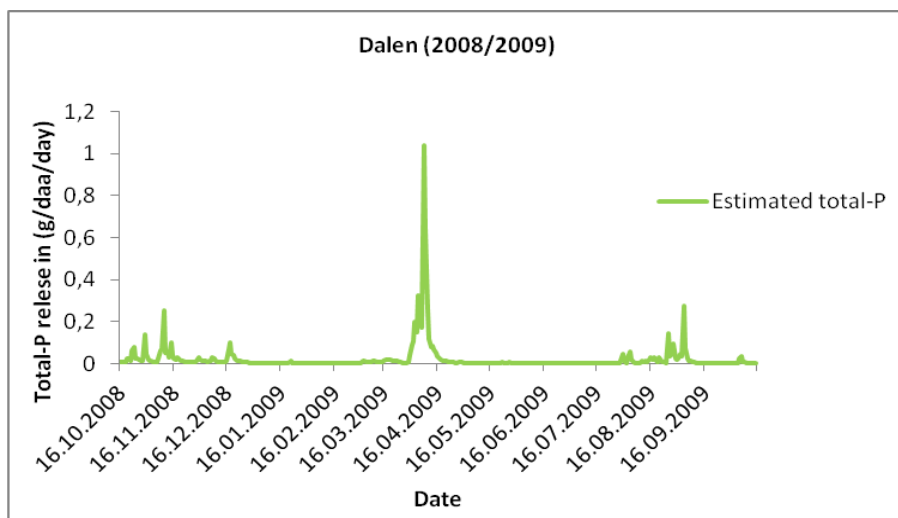


**Figure 50: Estimated daily total-P release (g/daa/day) in the Dalen stream for 08/09.**

Figure 19(A) shows the runoff and temperature for the hydrological year 2008/2009. Figure 48, Figure 49 and Figure 50. The hydrograph (Figure 19(A)) show that the winter temperature remained below 0<sup>0</sup>C for long periods of time and there is no runoff discharge that occurred during the winter. The main peak of the total P released in all three streams is found during the beginning of the April due to the spring snowmelt accompanied with precipitation. Such condition causes a strong hydrological response due to that the soil becomes water saturated allowing for overland flow (Coote et al., 1988). The release of total-P during the snowmelt

season in the Dalen stream is, as mention above, partly due to build-up of a labile pool of P through lysis of plant cell releasing P.

In 2009/2010 the winter was cold and the temperature remained below freezing point allowing for stable hydrological condition (Figure 19(B)). There were therefore no winter discharge episodes generating a low estimated release of total-P during the winter season. The main peak of total-P release in all three streams occurred during the snowmelt in the beginning of April (Figure 51, Figure 52 and Figure 53). Opland (2011) showed through flux estimations that as much as 23 % of the total-P load for this hydrological year may have been released during only four days (31.03.10 – 03.04.10).

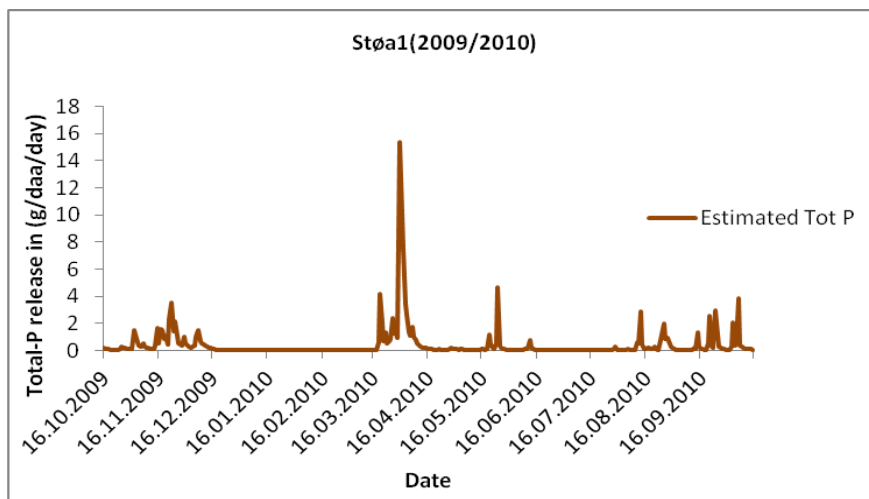


Figure 51: Estimated daily total-P release (g/daa/day) in the Støa1 stream for 09/10.

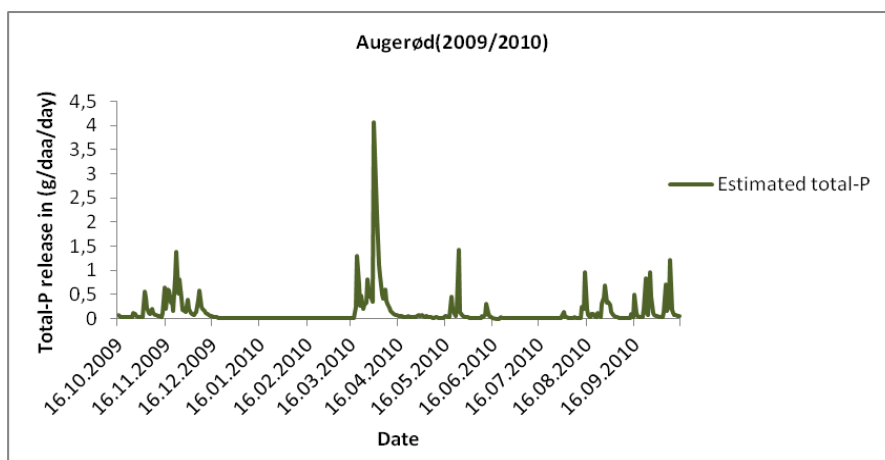


Figure 52: Estimated daily total-P release (g/daa/day) in the Augerød stream for 09/10.

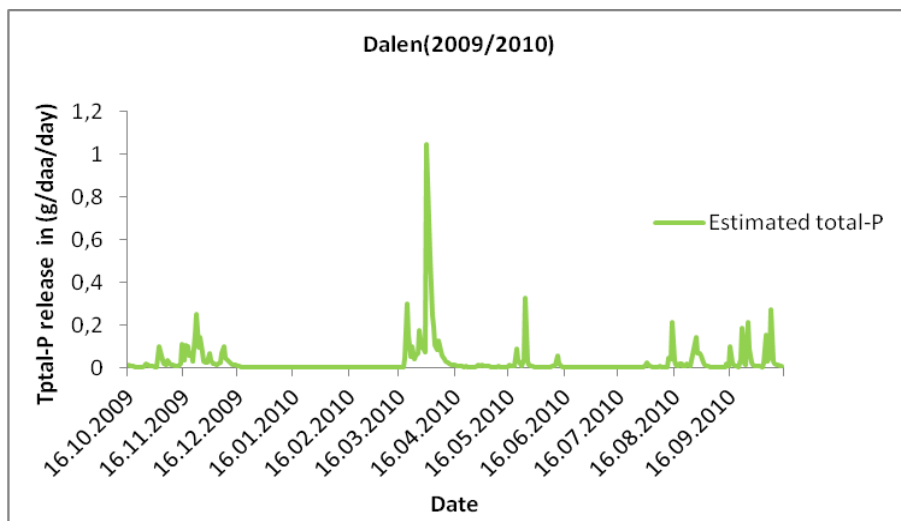


Figure 53: Estimated daily total-P release (g/daa/day) in the Dalen stream for 09/10.

There were no available data on all total-P fractions in the Støal and Augerød streams from Bioforsk and EUTROPIA data sets that are collected on 31.03.10 from the snowmelt episode that can be compared with the main peak of total-P release. There was one EUTROPIA- sample from the Dalen stream collected during 31.03.10. Runoff on this day was the highest runoff (~30 L/s) of the year 2010. DOM-P was found to be dominating fraction in this sample constituting 70% of the total-P while Free-PO<sub>4</sub> and PP made up only 18% and 11%, respectively.

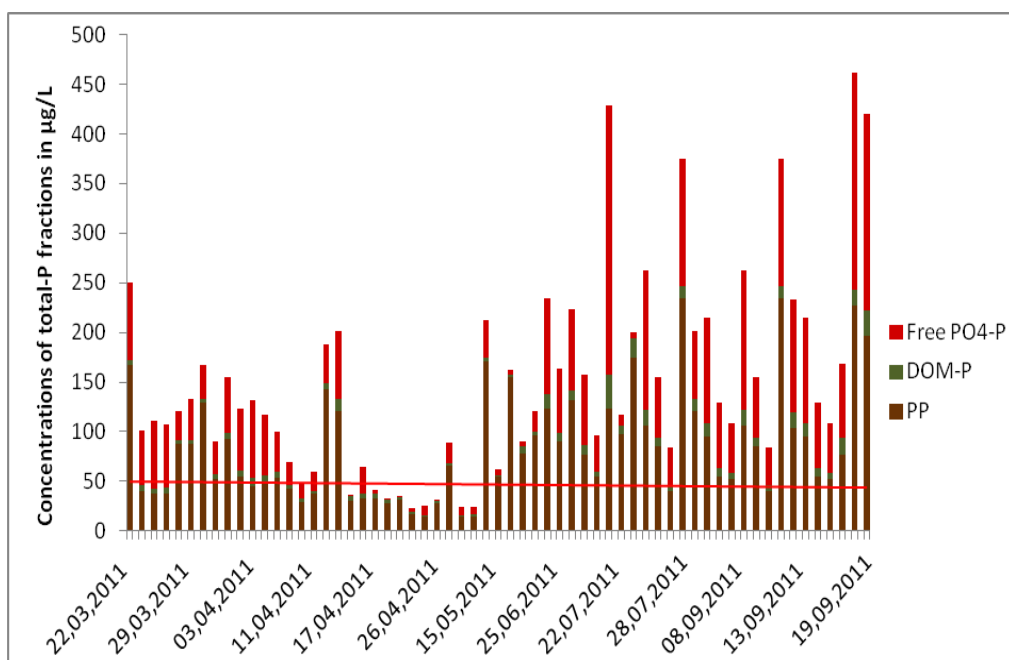
#### 4.1.9 Total-P fractions (EUTROPIA data set) during the snow free period in the Støal and Dalen streams

Figure 54 shows the temporal seasonal fluctuations in concentrations of total-P fractions (EUTROPIA data set) during the snow free period 22.3.2011 to 19.9.2011 in the Støal stream. Significant elevated concentrations of free-PO<sub>4</sub> are found during this period. There is a relatively low amount of free-PO<sub>4</sub> during April and May, but it constitutes a significant part of the total-P fractions in July-September, especially in September when a new flood was reported. Low concentration of free-PO<sub>4</sub> from end of April to end of June can be explained by the assimilation of free-PO<sub>4</sub> during the growth season. The amount of precipitation in the summer of 2011 was almost twice the norm. This may have led to the higher concentration free-PO<sub>4</sub> in July-September due to water saturation in the soil that reduces soil ability to hold



PO<sub>4</sub> (see section 2.1.6 & 4.1.5.4). This is an important factor that may explain much of the increased leaching of bioavailable P during and after flooding. Opland (2011) also showed higher concentration of free-PO<sub>4</sub> from the Huggenes stream during August - September.

Figure 55 shows the data from snow free period 22.03.2011 to 19.09.2011 from the Dalen stream. There is a significant amount of organic bound P from 9.09.2011 to 20.09.2011. Samples collected on 2.04.2011 and 12.09.2011 shows higher amount of free-PO<sub>4</sub>. This is mainly due to that the precipitation was much higher during these periods. This has led to higher runoff in the Dalen stream causing a flushing of the high concentrations of P in the forest floor from the large internal P cycling in the forest into the stream. The runoff in the Dalen stream (when the highest P concentrations were found on 12.09.2011) was high (8 L/s), indicating that higher runoff may lead to higher amount of free-PO<sub>4</sub> in the forested catchments.



**Figure 54: Concentrations of P fractions during the snow free period 22.3.2011 to 19.9.2011 in the Støa1 stream. The red line shows the environmental goal for Western Vansjø (50µg/L).**

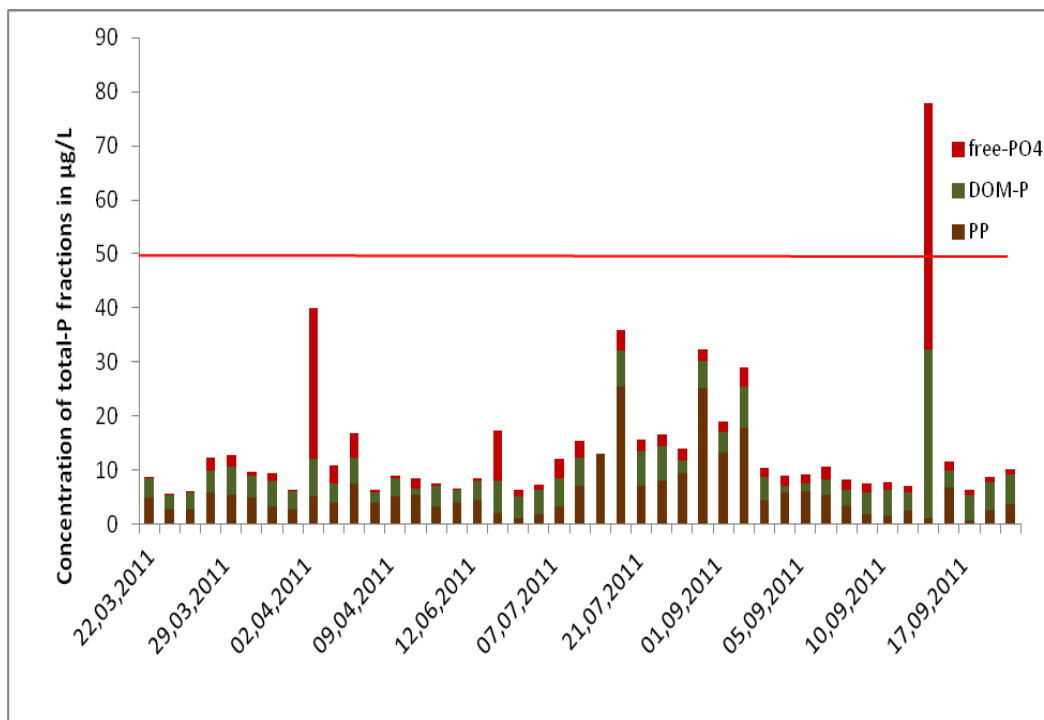


Figure 55: Concentrations of P fractions during the snow free period 22.3.2011 to 19.9.2011 in the Dalen stream. The red line shows the environmental goal for Western Vansjø (50µg/L).

#### 4.1.10 Statistical analysis on water samples (EUTOPIA data set)

##### 4.1.10.1 Cluster analysis

A cluster analysis of all the water chemistry data (Figure 56) reveal two main clusters explained by the effect of differences in the amount of agriculture or forest land-use within the catchment drained by the different streams. A large set of parameters, with high compactness (>99%), are clustered along with the contribution of agricultural land found within the watershed. These are mainly explanatory variables that have high values in the runoff from agricultural land due to the higher nutrient status ( $\text{NO}_3^-$ ,  $\text{K}^+$ ) and base saturation (Alkalinity,  $\text{HCO}_3^-$ ,  $\text{Ca}^{2+}$ ,  $\text{Mg}^{2+}$  and pH) of these soil. On the other side of the dendrogram, distinctly different from the agricultural cluster, there is a cluster of parameters that show high values in runoff from forests, i.e. the parameters governed by the amount of DNOM, such as DOC, DON and  $\text{H}^+$ . In between, closer related to agriculture than to forest, there is a third cluster of parameters with low compactness associated to the land coverage of other land use within the watershed. These typical parameters are found to be evenly or apparently randomly distributed in the different streams (such as the sea-salts  $\text{Na}^+$  and  $\text{Cl}^-$ ). All of the P fractions,

with the exception of DOM-P, are clustered together (Total-P, PP and Free-PO<sub>4</sub>) in a leaf of the agriculture cluster. The DOM-P is clustered with poor distinctness with the parameters associated with DNOM and the relative amount of forest cover in the watershed. A similar picture was found by Gebreslasse (2012) for P-pools, sediment characteristics and land-use in samples of the studied stream sediments.

This analysis illustrates the influence on land-use on the spatial variation in all the explanatory variables. The land use are thus a proxy for a number of co-varying explanatory variables. The extent of forest relative to agricultural land in the watershed can be used to deduce the importance of DOM-P relative to other P fractions, but unfortunately, the dendrogram also shows that land-use cannot be used as a proxy to assess the difference between the P fractions PP and free-PO<sub>4</sub>.

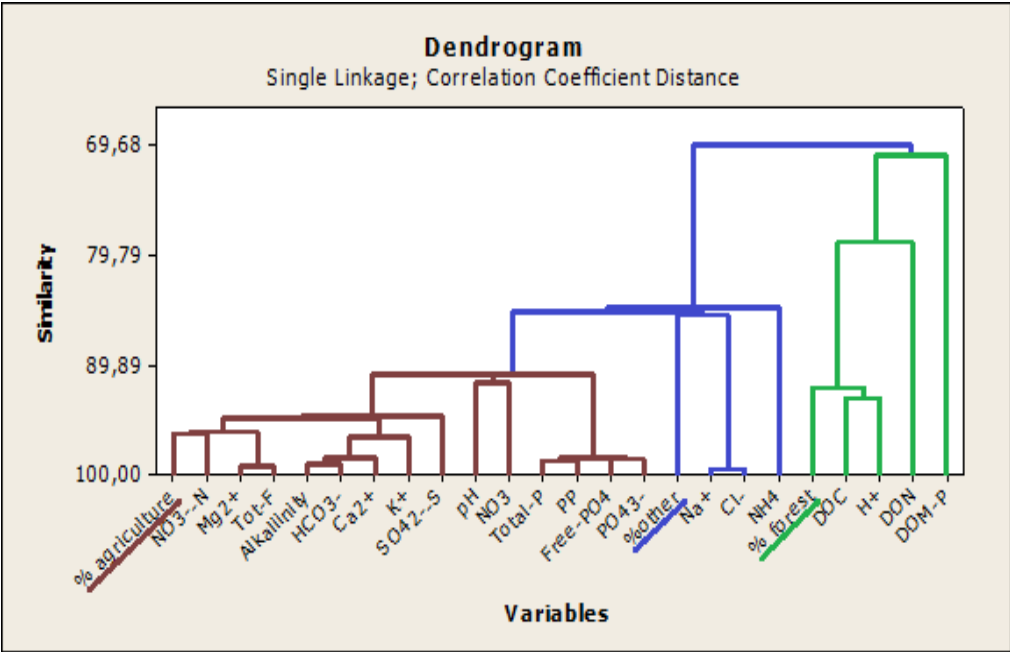


Figure 56: Dendrogram for P-pools with all explanatory variables.

**4.1.10.2 PCA loading of P-pools with explanatory variables**

A PCA was performed on the different P fractions with explanatory variables and inter parameters (e.g. major ion distribution, DOC, pH, alkalinity). This was done in order to map how the explanatory parameters are related to each and to the P fractions and expressing this

pattern in such a way as to draw attention to governing mechanisms explaining the temporal and spatial variation in P fractions. Component loading and correlation matrix on the same parameters is attached in Appendix H.

Principal Component 1 (PC1) and Principal Component 2 (PC2) explained 52.8 and 23.5 % of the variance, respectively. The distribution of the parameters loadings in a PC1 vs PC2 plane expresses generally the same findings as seen in the cluster analysis. The PC1 is mainly governed by the variation between the agriculture and forested land (Figure 57). The amount of forested land, DOC, DOM-P and  $H^+$  has negative loading on PC1. Though the explanatory variables alkalinity, and the inherently associated bicarbonate and pH, are found to have stronger positive loading than the relative amount of agriculture along the PC1. The percentage agriculture has also a significant loading along the PC2 and is negatively loaded relative to the percentage other land-use along this principal component. Similar to the cluster analysis the P fractions, with the exception of DOM-P, are clustered together with the amount of agricultural land. This represents that the variation of total-P fractions among the nine investigated streams is mainly governed by different land-use in the sub-catchments of the investigated streams.

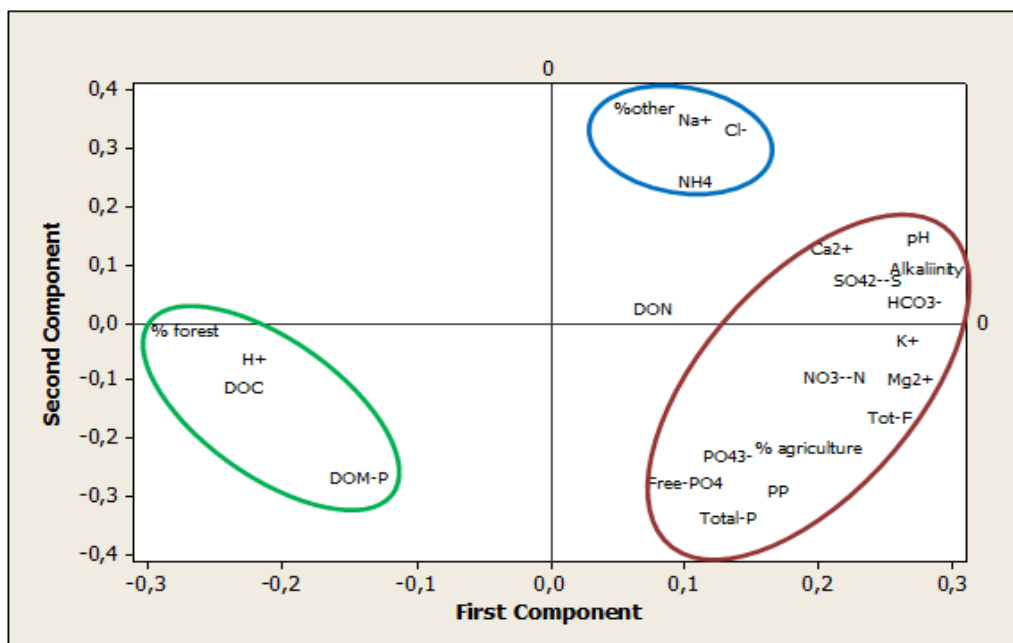


Figure 57: PCA loading plot

## 4.2 Results from DGT samplers -laboratory and field evaluation

### 4.2.1 Uptake of the organic P compounds AMP and IP<sub>6</sub> in a laboratory test

The amount of P adsorbed over time by DGT samplers immersed in a solution containing AMP is shown in Figure 58 and Figure 59. According to DGT theory, the mass of analyte accumulated by DGT samplers should increase linearly with time, providing the capacity of the adsorbent has not been exceeded and the uptake kinetics are rapid enough to ensure the concentration of analyte at the interface between the binding gel and diffusive gel is zero (Zhang & Davison,1995). Figure 58 and Figure 59 demonstrates a linear uptake of AMP as a function of time by DGT samplers containing Metsorb and ferrihydrite adsorbents, respectively. Results are practically identical and show good agreement between the mass of AMP accumulated by DGT samplers containing metsorb and ferrihydrite adsorbents.

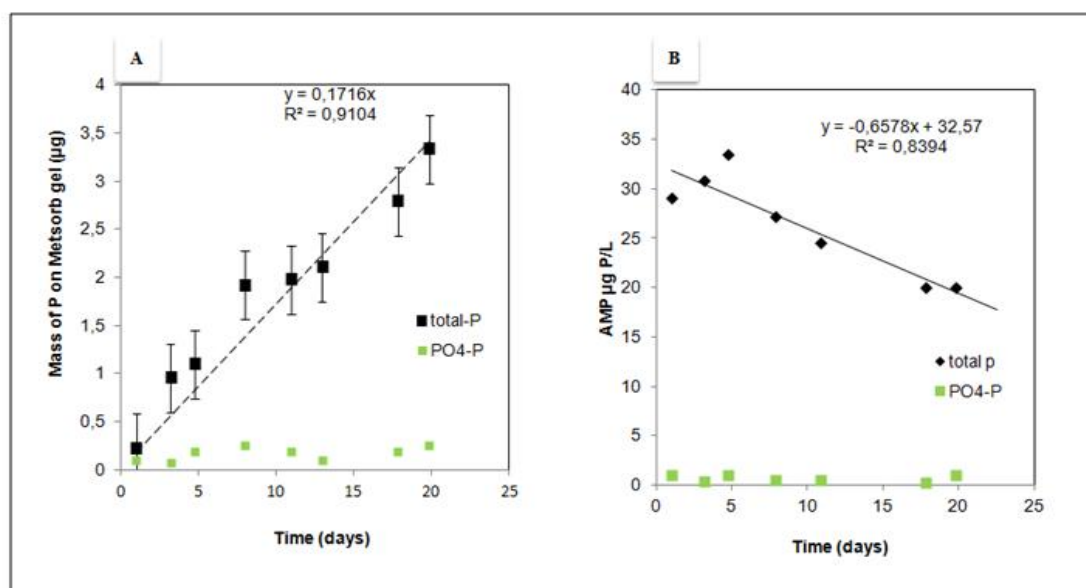
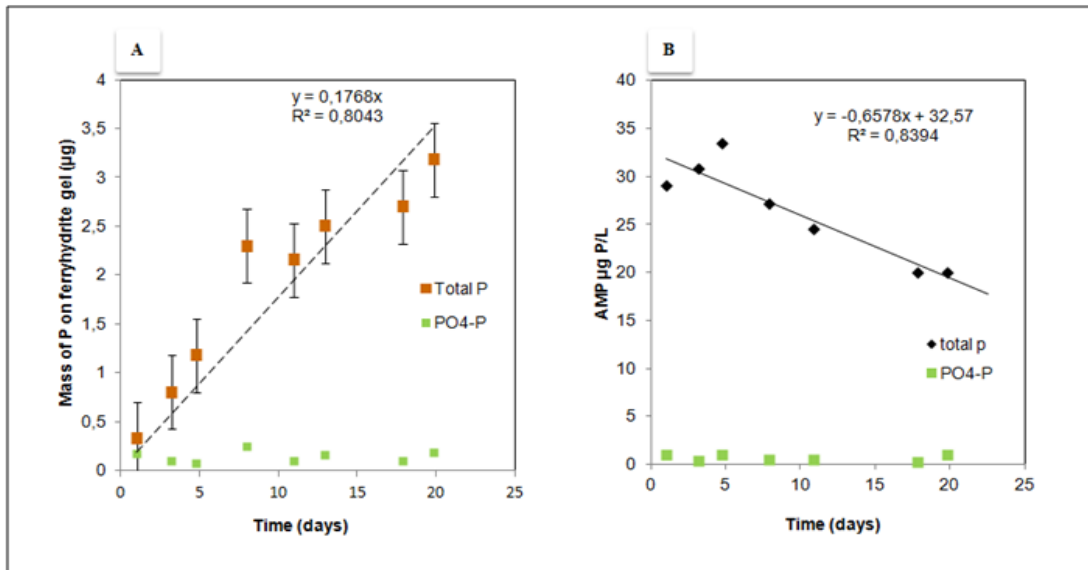


Figure 58: (A) Mass of AMP accumulated by Metsorb gel as a function of time and (B) The concentration of AMP in the test solutions throughout the experiment.



**Figure 59: (A) Mass of AMP accumulated by ferrihydrite gel as a function of time and (B) The concentration of AMP in the test solutions throughout the experiment.**

There is also an apparent minor uptake of free orthophosphate from the AMP solution by both DGT samplers. This indicates a decomposition of AMP during the experiment or during the elution process. Samples of the test solution throughout the experiment are also analysed in order to have a measure of change in AMP concentration. As can be seen from Figure 58 (B) and Figure 59 (B) a decrease in AMP concentration in the test solution is found throughout the experiment due to uptake in the DGT samplers. Figure 58 (B) and Figure 59 (B) also show that the concentration of free orthophosphate is found below the detection limit in the AMP test solutions. This indicates that decomposition of AMP probably occurred during the elution of P from the DGT adsorbent. Another explanation may be the storage of samples. Samples were stored for two months before being analysis (due to capacity problems in NIVAs laboratory performing the analysis) which may also cause decomposition of AMP. Amount of free orthophosphate that is accumulated is very small and results simply indicate that new Metsorb that has not been used in such studies before gives results in good agreement with the well-established ferrihydrite-DGT method.

Figure 60 shows the results from laboratory experiment that was performed by using Phytic acid (known as inositol hexaphosphate,  $IP_6$ ) test solution. Graph shows near to liner uptake of  $IP_6$  by ferrihydrite gel. Concentration of free orthophosphate below the detection limit indicates no decomposition of  $IP_6$  compound during the experiment or during the elution

process. Comparable data for DGT sampler containing Metsorb are not available. This is due to that sulphuric acid (4M as for ferrihydrite) was used for the elution of Metsorb adsorbent. The experiment demonstrated that sulphuric acid gave a poor elution efficiency of around 30 to 50% of the adsorbed IP<sub>6</sub> compound. After re-examining, the elution efficiency of Metsorb by using of 1 M NaOH showed much higher and reproducible elution efficiency. More detailed regarding elution efficiency is further presented in chapter 4.2.3.

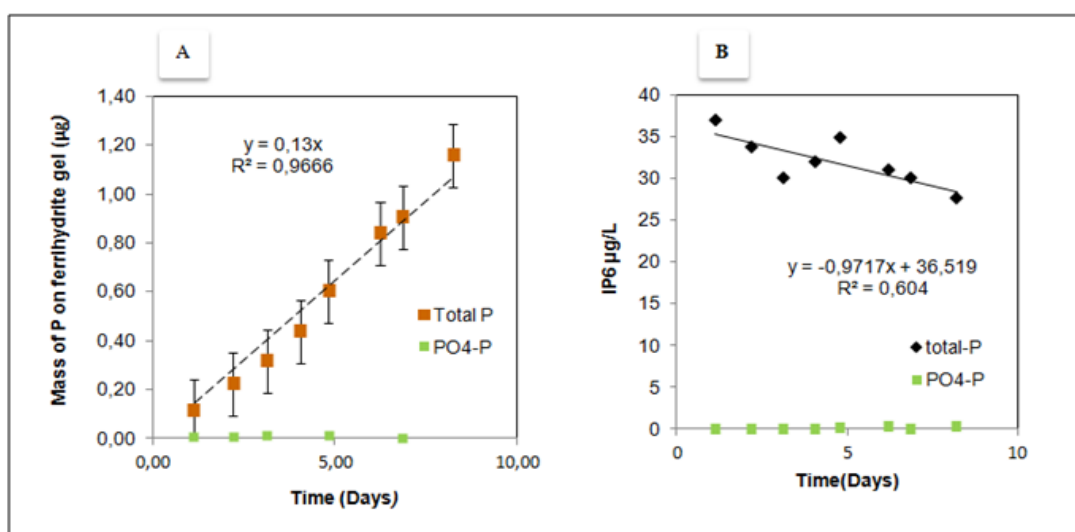


**Figure 60:** (A) Mass of IP<sub>6</sub> accumulated by ferrihydrite gel as a function of time and (B) The concentration of IP<sub>6</sub> in the test solutions throughout the experiment.

#### 4.2.2 Diffusion coefficients calculated from the laboratory test

Diffusion coefficients that are derived from the laboratory experiments discussed in section 4.2.1 are shown in Table 11 and Table 12. Diffusion coefficients obtained using AMP test solution is found to vary throughout the experiment whereas diffusion coefficients from the lab experiment by using IP<sub>6</sub> increased slightly over time. For AMP experiment, the diffusion coefficient for Metsorb ( $D_{DC \text{ Metsorb}}$ ) is not significantly different (checked by using paired t-test, see Table A17, Appendix E.3) from the diffusion coefficient for ferrihydrite ( $D_{DC \text{ ferrihydrite}}$ ). From Table 11 the average  $D_{DC \text{ Metsorb}}$  and  $D_{DC \text{ ferrihydrite}}$  for AMP (at average temperature 23<sup>0</sup> C) are found to be  $3.11 \cdot 10^{-6} \text{ cm}^2 \text{ s}^{-1}$  and  $3.26 \cdot 10^{-6} \text{ cm}^2 \text{ s}^{-1}$ , respectively. This

means that that both absorbents have almost same diffusion rate of ions through gel membrane, thus both adsorbents have similar binding ability.

**Table 11: Diffusion coefficients obtained from the lab experiment with AMP test solution.**

Sampling Time (days)	$D_{DC}^{Metsorb \text{ AMP}}$ ( $10^{-6} \text{ cm}^2/\text{s}$ )	$D_{DC}^{ferrihydrate \text{ AMP}}$ ( $10^{-6} \text{ cm}^2/\text{s}$ )
1	3,28	4,15
3	3,75	3,03
5	2,68	2,78
8	3,41	4,00
11	2,83	3,03
13	2,77	3,24
18	2,98	2,85
20	3,20	3,03
Average	3,11	3,26
St. dev	3,65	5,19
RSD %	11,76 %	15,93 %

The average  $D_{DC}^{ferrihydrate}$  for  $IP_6$  was found to be  $1.48 \cdot 10^{-6} \text{ cm}^2 \text{ s}^{-1}$  (Table 12). This is lower than the diffusion coefficients mention above for AMP. This is partly due to that the  $IP_6$  is a larger molecule than AMP, thus diffusion is slower than AMP.

**Table 12: Diffusion coefficients obtained from the lab experiment with  $IP_6$  test solution**

Sampling Time	$D_{DC}^{ferrihydrate \text{ IP}_6}$ ( $10^{-6} \text{ cm}^2/\text{s}$ )
1	1,27
2	1,26
3	1,27
4	1,35
5	1,58
6	1,69
7	1,66
8	1,77
Average	1,48
St. dev	2,14
RSD %	14,52 %



Table 13 shows the diffusion coefficients calculated from laboratory test compared with results for diffusion coefficients calculated by using Buffle's Equation (see section 2.2.5). This is based on empirical data for low molecular compounds. It provides a guide to expected value based on molecular weight. Table 13 also shows the expected diffusion coefficient for compound with different molecular weight. By using Buffle's Equation gives an idea of binding ability of adsorbents.

**Table 13: Comparison of diffusion coefficients obtained by DGT theory and from Buffle's equation.**

Compounds	Molecular weight g/mol	Diffusion coefficient from Buffle's equation	DGT based diffusion coefficients	
		In water	Metsorb	Ferrihydrite
		$10^{-6} \text{ cm}^2/\text{s}$	$10^{-6} \text{ cm}^2/\text{s}$	$10^{-6} \text{ cm}^2/\text{s}$
AMP	393,2	3,95	3,26(AMP)	3.11(AMP)
IP <sub>6</sub>	736,2	3,21	N/A	1,27 (IP <sub>6</sub> )
Small size ion	50	7,81		
Medium size ion	100	6,21		
large size ion	200	4,94		
Fulvic acid	1000	2,90		
	5000	1,70		
Humic acid	10000	1,36		
	20000	1,08		
Large molecule	50000	7,99( $10^{-7}$ )		

$D_{DC \text{ Metsorb}}$  and  $D_{DC \text{ ferrihydrite}}$  for AMP assessed by laboratory test are in reasonably agreement with the diffusion coefficient calculated by using Buffle's Equation. This indicates that the adsorption efficiency of the organic P compound AMP is nearly quantitative for both Metsorb and ferrihydrite DGT samplers. The  $D_{DC \text{ ferrihydrite}}$  for IP<sub>6</sub> is lower than the diffusion coefficients calculated by using Buffle's Equation. This is partly due to that the IP<sub>6</sub> is a larger molecule than AMP, thus diffusion is slower than AMP. Specific reason for this is not quite clear, but this was the first test performed, so that unknown errors may cause this. Nevertheless, the time linear uptake curve indicates that the organic compound IP<sub>6</sub> can be collected by both DGT sampler in the same way as for AMP. There is obviously need for more research on this topic, but the results so far indicate DGT based diffusion coefficient between 3 to  $3.5 \cdot 10^{-6} \text{ cm}^2 \text{ s}^{-1}$  for these low molecular organic P compounds.

### 4.2.3 Elution efficiency

Dilute sulphuric acid (4M) has been recommended for elution of P from the ferrihydrite adsorbent, when subsequently applying the molybdate blue colorimetric method for determination of phosphates (Røyset et al., 2004). A study by Zhang et al. (1998) reported elution efficiency up to 100% by using sulphuric acid to elute P from the ferrihydrite based DGT. Sulphuric acid was therefore selected as an extractant of P from ferrihydrite in this study. Elution efficiency for ferrihydrite gel by using sulphuric acid was 100 % since the ferrihydrite was completely dissolved into the solution, inherently releasing all P compounds.

Very low elution efficiency (~30-35%) was obtained by using sulphuric acid as an eluent for the Metsorb adsorbent. Panther (2011) (Pers.comm) suggested the use of 1M NaOH for extracting P from the Metsorb adsorbent. Sodium hydroxide has also previously been employed as an eluent to remove arsenic and selenium species bound to Metsorb adsorbent (Bennett et al., 2010). The use of NaOH as an extractant of P from Metsorb was therefore tested in this thesis. The elution curve obtained through field measurements is shown in Figure 61. Following Table 14 shows the average elution efficiency obtained through lab and field study. Elution of phosphate from the Metsorb adsorbent is a result of hydroxide either changing the surface charge of the adsorbent or affecting the surface complexation equilibrium, hence releasing phosphate into solution (Connor et al., 1999; Panther et al., 2010). The results indicate that an elution efficiency of about 85% is obtained by using 1M NaOH and therefore two extractions are recommended. Elution efficiency for organic compounds has not been reported before. The high elution efficiency can be considered as satisfactory.

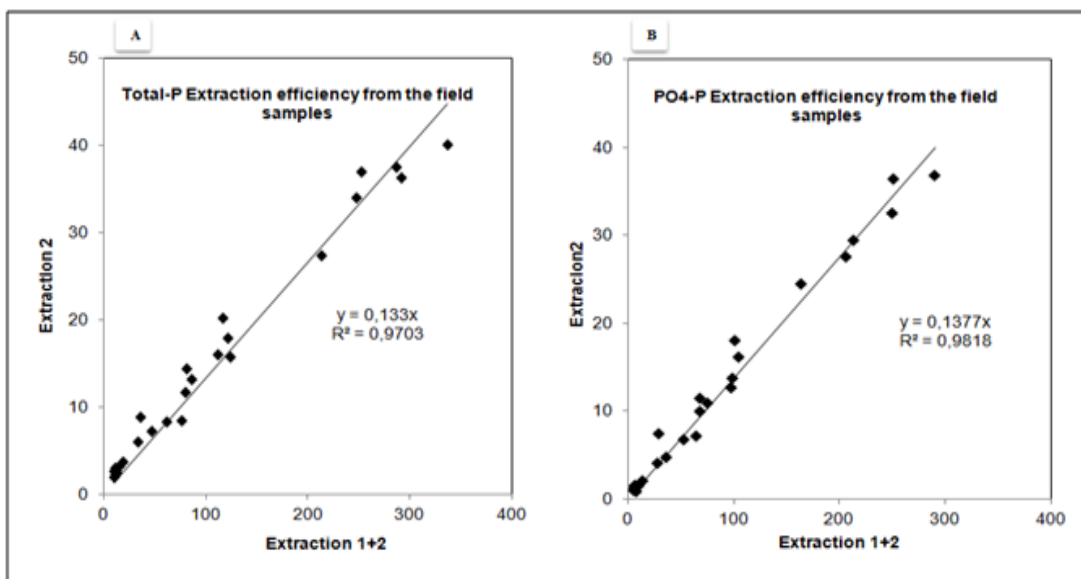


Figure 61: (A) Total-P and (B) PO4-P extraction efficiency from the field samples.

Table14: Elution efficiency accessed.

Test	Elution efficiency %	Standard deviation	%RSD
Field test (Støal, Huggenes Dalen)	87	17	4 %
Laboratory test	87	1	1 %

#### 4.2.4 Sampling precision of P by DGT samplers at the sampling location Støal

Four parallels of DGT samplers containing both Metsorb and Ferrihydrite adsorbents were immersed in the Støal stream in order to determine standard deviation of the sampling method. The results are shown in Table15. DGT samplers using ferrihydrite and Metsorb adsorbents show RSD values varies from ~ 8 to 25 % for the different P fractions. The RSD values for the Metsorb samplers are somewhat higher than the RSD values obtained for ferrihydrite samplers. Metsorb sampler contains one result being considerably higher than the others are (Parallel nr.4). When omitting value for this result RSD is becomes below 20 % for all the three fractions for Metsorb DGT sampler and the sampling precision becomes very similar for all three fractions both for Ferrihydrite and Metsorb DGT samplers. These results are considered as an acceptable sampling precision, especially taking into account that this is

the first field study, where neither field sampling and laboratory procedures has been fine-tuned for organic compound by using Metsorb DGT samplers. Probably there are considerable room for improvements, to reduce sampling precision down towards 10 %.

Fractions of total-P measured by Metsorb and ferrihydrite DGT methods were compared by paired t-test to check for significance difference. The concentrations of total-P (free-PO<sub>4</sub>+ organic P) and free-PO<sub>4</sub> fractions did not show significantly different results while organic P fractions showed significant higher concentrations by using Metsorb DGT method.(probability level 95%). The results and statistics are presented in Appendix E.4.

**Table15: Sampling precision of total P by DGT samplers containing Metsorb and ferrihydrite at Støa1 stream.**

Nr. of Parallels	Ferrihydrite			Metsorb		
	PO <sub>4</sub> -P µg P/L	Organic P µg P/L	PO <sub>4</sub> -P + Organic P µg P/L	PO <sub>4</sub> -P µg P/L	Organic P µg P/L	PO <sub>4</sub> -P + Organic P µg P/L
1	24,3	7,1	31,4	32,5	10,5	43,0
2	32,6	5,8	38,5	31,4	14,0	45,4
3	27,7	9,1	36,7	24,9	15,1	40,0
4	25,9	8,7	34,5	44,3	14,2	58,4
Average	27,6	7,7	35,3	33,3	13,4	46,7
St. dev	3,6	1,5	3,0	8,1	2,0	8,1
RSD %	13,0	19,4	8,6	24,2	15,0	17,4
After omitting parallel 4 (Metsorb DGT)			Average	29,6	13,2	42,8
			St. dev	4,1	2,4	2,7
			RSD %	13,9	18,1	6,4

#### 4.2.5 Fraction of total-P determined from DGT samplers and in the stream water

The concentrations of total-P fractions (organic-P + free-PO<sub>4</sub>) measured in the field using Metsorb and ferrihydrite DGT and determined directly from the stream water are shown in Figure 62. Figure 63 shows the correlation between the stream water concentrations and concentrations measured by using DGT samplers. Fractions of total-P measured in the field using Metsorb and ferrihydrite DGT in the monitoring streams differ by less than 25 % in all cases.

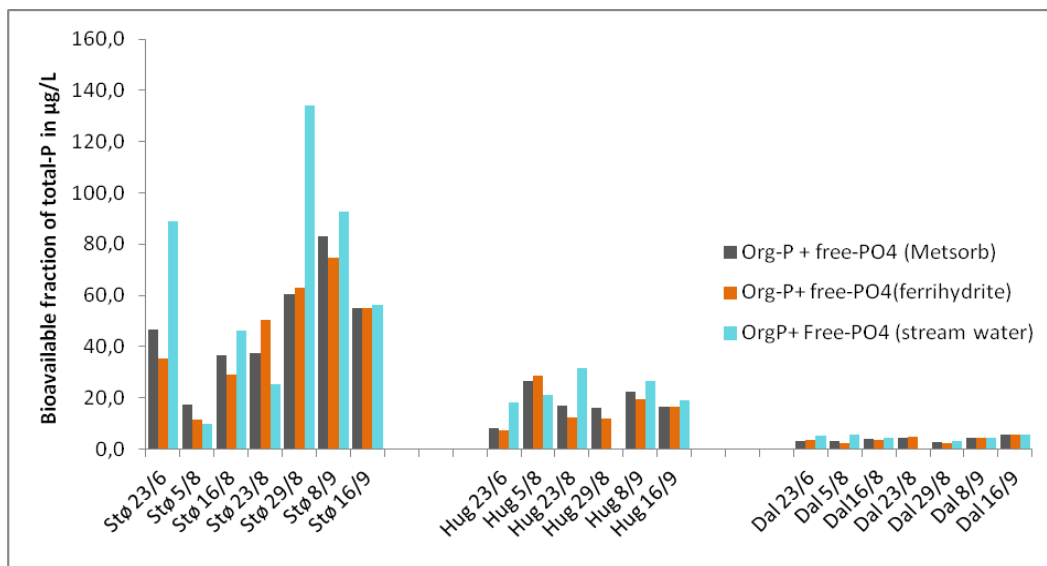


**Figure 62: The concentration of bio available fraction of total-P (organic-P + free-PO<sub>4</sub>) measured in the field using Metsorb and ferrihydrite DGT and determined directly from the stream water.**

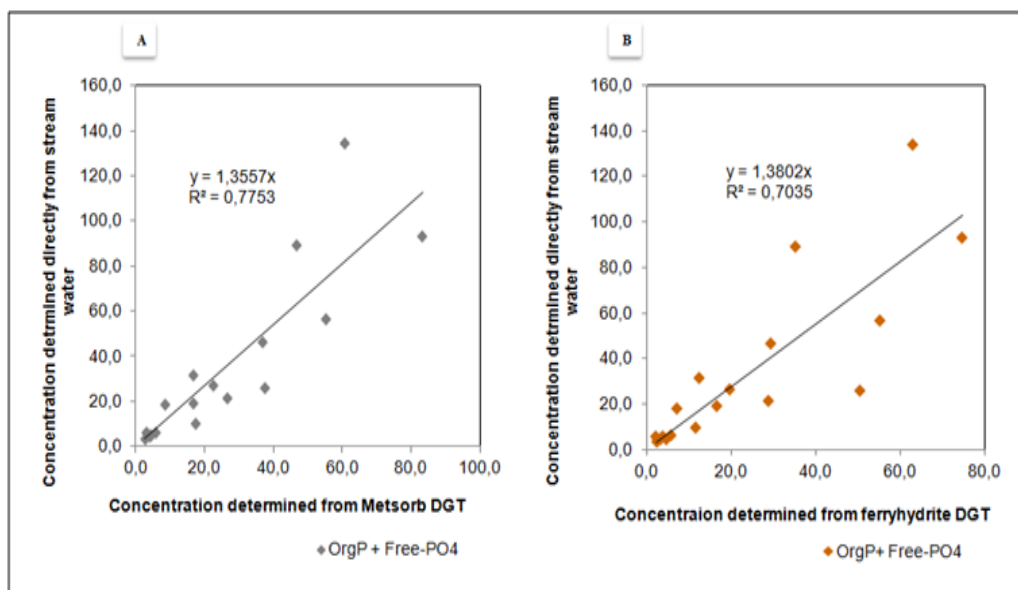


**Figure 63: Correlations between concentrations of total-P fractions measured directly and by using DGT samplers.**

Fractions of total-P measured by using Metsorb and ferrihydrite are found to be fairly well correlated ( $r = 0.88$  and  $r = 0.84$ ) with the concentration determined directly from the stream

water (Figure 63). Concentration determined directly from the stream water is found to be higher compared to the concentration measured by using DGT samplers, especially in the Støal stream. In the Dalen stream, concentrations in the stream water are found to be almost identical at 8.9.2011 and 16.9.2011 while they differ ~ 25 % at other sampling times.

There are several factors that may lead to deviation between stream water concentrations and concentrations measured by using DGT samplers. DGT samplers measure time averaged concentration while the concentration in the water samples reflects a momentary concentration. The daily concentration in the grab water sample is affected by hydrological condition, especially in the Støal and Huggenes stream that mainly drains agriculture catchments. The variation in these streams water concentration can be large during the hydrological discharge episodes. This variation can be corrected by using discharge data.

Another explanation can be high content of iron in the Støal and Huggenes streams. After exposure the DGT samplers were covered by a layer of red brown Fe (III) hydroxide as the water from, especially the Støal stream contain formed Fe (III). This may have been precipitated on the DGT samplers and clogged the filter of the DGT samplers causing underestimation of the concentrations.

#### **4.2.6 Organic P fraction determined from DGT samplers**

Figure 64 (A) shows concentration of organic P measured in the field by using Metsorb and ferrihydrite DGT samplers. The correlation between organic P collected by Metsorb and ferrihydrite DGT samplers are high ( $r=0.87$ ), but the mass of organic P accumulated by Metsorb DGT is found to be ~ 25% higher compared to mass accumulated by ferrihydrite DGT (Figure 64(B)). Figure 65 shows the correlation between the stream water concentrations of organic P and concentrations of organic P measured by using DGT samplers.

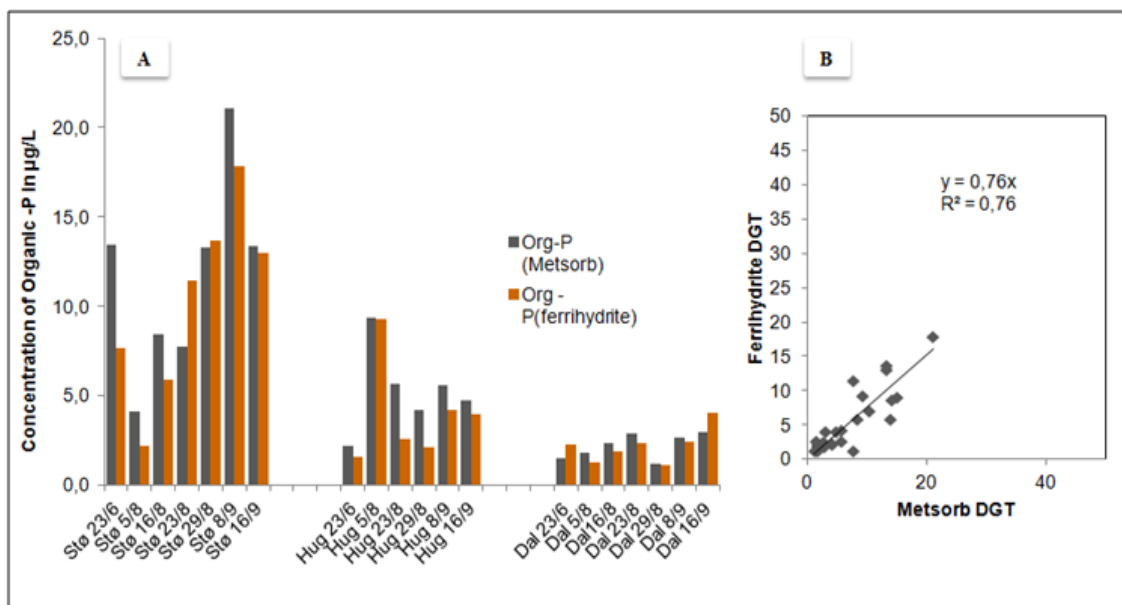


Figure 64: (A) Concentration of organic P measured by using Metsorb and ferrihydrite DGT samplers and (B) correlation between the two samplers.

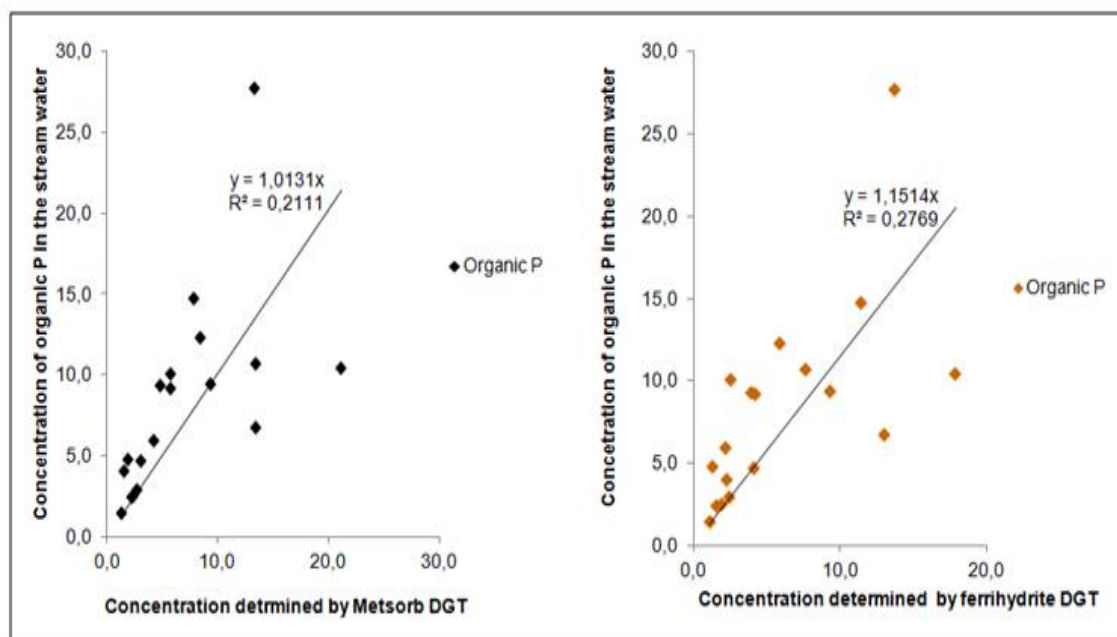
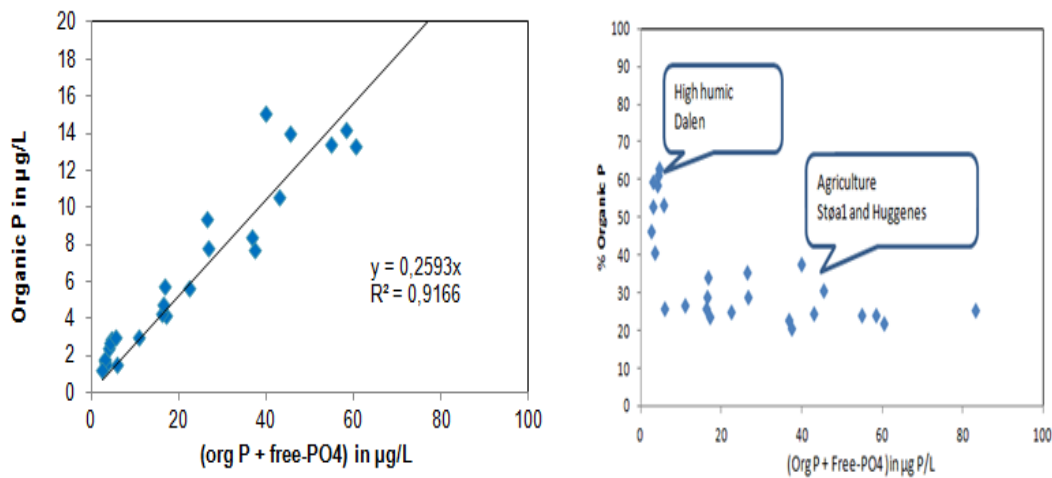


Figure 65: Correlations between concentrations of organic P fraction measured directly and by using DGT samplers.

Organic P is about 25 % of the total fraction collected by DGT at the studied streams and it depends on sources (Figure 66). Støa1 and Huggenes, that are predominantly draining

agriculture land, have organic P fraction that constitutes about quarter of the total DGT fractions. At the Dalen stream, draining forest land, the organic P accounts for almost half of the total DGT fractions. This difference is likely due to that the soils in Dalen catchment have higher content of organic matter (Mohr, 2010) than the agricultural soils (Opland, 2011). Results are more than satisfactory as expected DOM-P lies between 20-30% in the stream draining the agriculture catchments whereas forested stream represents 40- 50 % DOM-P.



**Figure 66: Percent Organic P in the fractions of total-P (org P +free-PO<sub>4</sub>).**

Earlier experiment done by Mohr (2010) and the results from the present laboratory and field evaluation demonstrate that DGT using both Metsorb and ferrihydrite adsorbents can passively accumulate organic P compounds and are able to sample Low Molecular Weight (LMW) organic P-compounds in a non-destructive manner, separately from free-PO<sub>4</sub>. Both adsorbents behave well, but Metsorb seems to be the best adsorbent for organic P. If this assumption is true than weekly or twice a week DGT-averages may therefore be a simple and cost-efficient alternative to daily grab-samples to get evaluations of the bioavailability of these P fractions.



#### 4.2.7 Fraction of free-PO<sub>4</sub> determined from DGT samplers and in the stream water

The concentrations of free-PO<sub>4</sub> measured in the field by using DGT samplers and determined directly from the stream water samples are shown in Figure 67. Figure 68 shows that concentration of free-PO<sub>4</sub> measured by using Metsorb and ferrihydrite is found to be well correlated ( $r = 0.88$  and  $r = 0.84$ ) with the concentration of free-PO<sub>4</sub> determined directly from the stream water. Concentrations of free-PO<sub>4</sub> determined in the stream water samples by conventional method are found to be ~ 50 % higher than by DGT samplers. The method agrees well for Dalen stream whereas deviations are large in the Støa1 and Huggenes streams, especially in the Støa1 stream. The large deviation in the Støa1 stream may, as described in section 4.3.1.2, be due to large variations in free-PO<sub>4</sub> concentrations with hydrological conditions. It may also partly be due to higher iron content in the Støa1 and Huggenes streams causing filter clogging, although it is probably a minor error (Røyset, 2011 (Pers.comm.)).

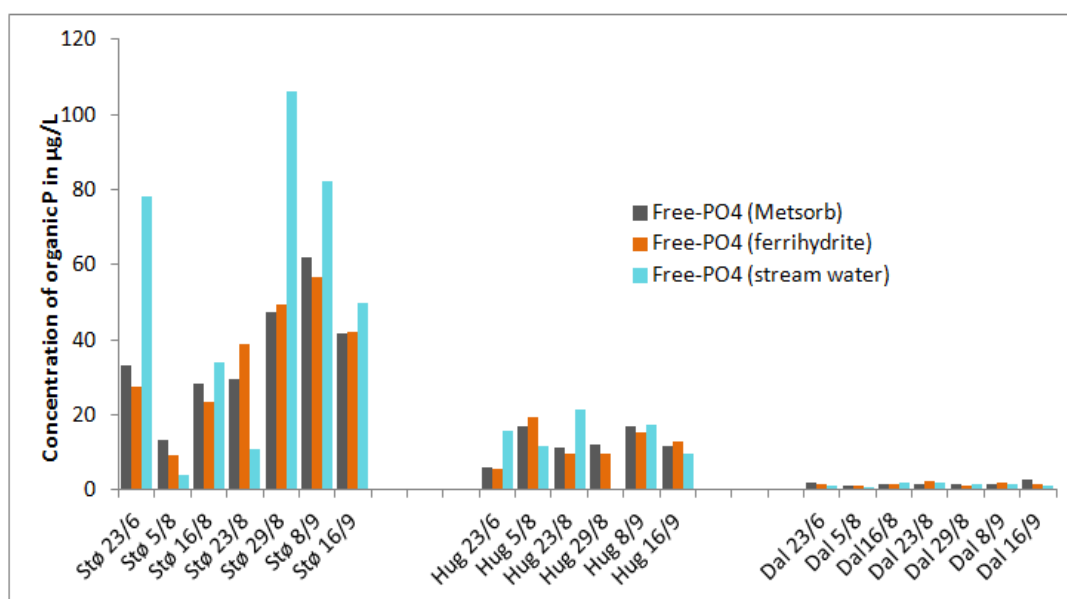
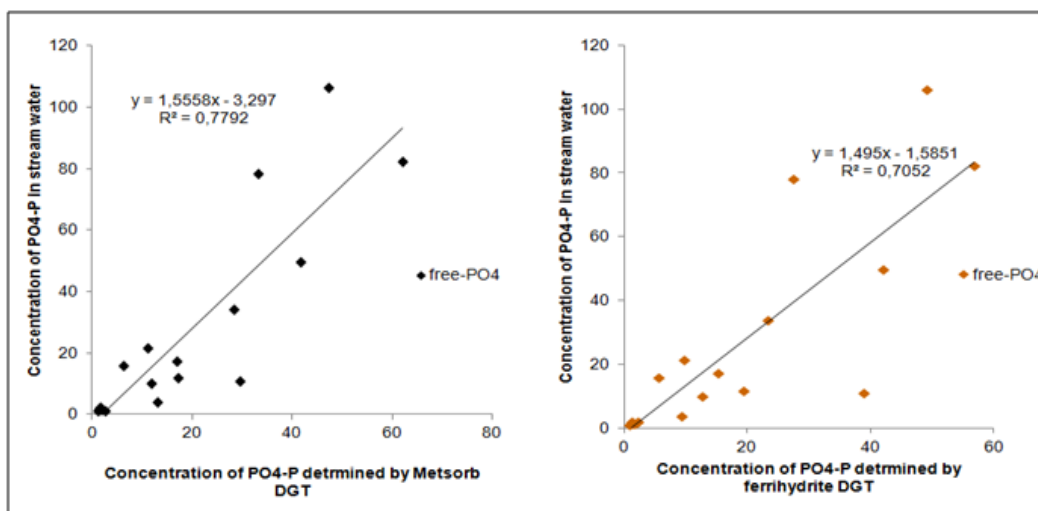


Figure 67: The concentration of free-PO<sub>4</sub> measured in the field using Metsorb and ferrihydrite DGT and determined directly from the stream water.



**Figure 68: Correlation between the stream water free-PO<sub>4</sub> concentrations and concentrations of free-PO<sub>4</sub> measured by using DGT samplers.**

It is much more likely that conventional method to determine total dissolved P (PO<sub>4</sub>-P and Org P) may overestimate total dissolved P, especially free-PO<sub>4</sub>. DGT samplers collect dissolved compounds that pass through the 10 nm (0,010 μm) pore size membrane and it excludes particles and colloids. Water samples were filtered by using Whatman GF/F 0,7μm, 47 mm. It may still include P in small colloids and surface adsorbed P while DGT samplers exclude P in small colloids and PO<sub>4</sub>-P surface adsorbed on colloids/particles. Therefore, it is assumed that DGT is a more suitable sampling device to collect the truly dissolved fraction of PO<sub>4</sub>-P in water.

It is not possible to draw a definite conclusion based on these data alone and therefore further research is required.

## Conclusion

Nine streams draining sub-catchments of Western Vansjø catchment comprising a gradient in land use from agriculture to increasing proportion of forested area were studied. Acid forested streams were efficiently neutralized within short stretch upon mixing with agriculture runoff. Higher content of dissolved organic carbon were also found to be lost by sorption to particles due to increased ionic strength upon passing through agriculture land. Dilute organic weak

acid and seasalt influenced (NaCl) water chemistry of the forested streams shifted toward neutral and hard ( $\text{CaCO}_3$ ) type of water chemistry with increasing amount of agriculture land due to soil-soil water interactions. These indicate that agriculture land has great influenced on the stream water chemistry, especially streams that represents combine land use (agriculture and forest).

Land distributions in the sub-catchment of the investigated were found to be the main factor explaining the spatial variation in P amount and P fractions. Principal Component Analysis (PCA) on the different P fractions with explanatory variables showed that forested land, DOC, DOM-P and  $\text{H}^+$  were clustered to gather with DOM-P, while the rest of the P fractions were clustered together with the amount of agricultural land.

Runoff was found to be main important factor governing temporal variation in P fractionation and concentration with higher concentration of total-P during episodes of increased discharge. Particulate bound P was found to be dominating fraction of total-P in the runoff from agriculture land mainly due to the erosion of over-fertilizing agriculture soils. In contrast, high amount of dissolved organic P (DOM-P) was found in runoff from forested streams due a high content of DNOM that inherently carry elevated concentration of DOM-P. In natural forest system, such as Dalen catchment, phosphorus is mainly transported by DNOM and concentrations of DOP are significant in the runoff from the forested catchments under marine limit, which contain soils that are naturally enriched in P.

Flow-weighted mean concentrations of total-P in the studied streams showed decreasing trend over the years from 2006/07, 2007/08, 2008/09 to 2009/10. This is partly due to the abatement actions and the recovery of the system after the flood in the year 2000. During the same period the concentration of suspended solids also showed decreasing trend. This likely mainly due to the abatement actions. A clear correlation was found between the amount of suspended solids and total-P. This is to be expected as particle bound P constitute the main fraction of total-P. It implies that the transport of suspended solid explains much of the spatial and temporal variation in the total-P concentrations since erosion and transport of particles from agricultural field plays important role in the inputs of total-P. Flow-weighted mean concentration of total-P greatly exceeded the environmental goal for Western Vansjø of  $50\mu\text{g/L}$ . According to daily estimated flux of total-P based on a linear regression, there is no apparent improvement in the eutrophic condition, despite an apparent decrease based on flow

weighted mean concentrations. This is postulated to be mainly due to the climate change. Increased runoff and inter-annual variations in winter temperature due to climate change are found to be two important climatic factors that govern the higher flux of total-P to the lake Vansjø during the years 2006/07 and 2007/08 compared to the years 2008/9 and 2009/2010, thus disguising the effect of mitigation measures.

Significant elevated concentration of bioavailable free-PO<sub>4</sub> was found in the stream water samples collected from the Støa1 when a new flood occurred in September 2011. This is believed to be mainly due to the reduction of Fe (III) to Fe (II), which subsequently captured as insoluble FeS, reducing soils ability to hold phosphate. This is may be an important factor governs the higher concentration of bioavailable P in streams during prolonged discharge episodes. During the September 2011, higher amount of both free-PO<sub>4</sub> and DOM-P were also found in the stream water draining the forested Dalen catchment.

Increased runoff and milder winter temperatures have led to increased leaching of bioavailable phosphorus by increased surface runoff, water clogged soils and through drainage pipes. In relation to massive amount of Particulate bound P that is fed into the lake from the tributary streams, there is little of this inorganic particulate P that is actually found in the lakes. It may indicate that particle bound P does not contribute much to the total amount of P to the lake as it is largely sedimented. If this is true then free-PO<sub>4</sub> and the increased background P loading of DOM-P from the forested catchments may plays a more important role in sustaining a high total-P loading to the lake. One-sided focus to reduce particles may on the contrary lead to more bioavailable P through internal loading of P in the lake. If this is the case then the effect of mitigation measures aimed at reducing erosion may actually be counterproductive in alleviating the eutrophication problem in lake Vansjø.

The Metsorb DGT method, studied in this master thesis, performed similarly compared to the more well-established ferrihydrite DGT method. The lab evaluation results showed that both ferrihydrite and metsorb DGT method efficiently collect the low molecular weight compounds (e.g. adenosine monophosphate and inositol phosphate, IP<sub>6</sub>). Elution efficiency for organic compound by using ferrihydrite and Metsorb DGTs method were found to be 100% and 85%, respectively. DGTs based diffusion-coefficients for AMP compounds was found  $\sim 3.5 \cdot 10^{-6} \text{cm}^2 \text{s}^{-1}$ . Diffusion coefficient for IP<sub>6</sub> was found to be  $1.4 \cdot 10^{-6} \text{cm}^2 \text{s}^{-1}$  due to that the IP<sub>6</sub> is a larger molecule than AMP, thus diffusion is slower than AMP.

The field evaluation results showed that both methods reflect the high spatial and temporal variation in the organic P fraction depending on the level of these compounds in the applied sources. Støal and Huggenes, predominantly draining agriculture land, have organic P fraction constitutes a quarter of the total DGT fractions, while the organic P accounts for almost half of the total DGT fractions in the Dalen stream. This suggests that DGT samplers can be used to determine potentially bioavailable organic phosphorus compounds in the water. This is a new result as the determination of organic P compounds by using DGT samplers has not been reported previously. Somewhat more puzzling was that the concentration of free-PO<sub>4</sub> measured in the stream water sample were found to be about 50% higher than measured by DGT samplers. It may possible that conventional method to determine free-PO<sub>4</sub> may overestimate the concentrations of bioavailable P due to that it may include P in small colloids and surface adsorbed P. In contrast, DGT samplers exclude these fractions. If this assumption is true, than the DGT samplers are better sampling device to collect the bioavailable free-PO<sub>4</sub> fractions.

## References

- Alfaro-De la Torre, M. C., Beaulieu, P-Y., Tessier, A.(2000).In situ measurement of trace metals in lakewater using the dialysis and DGT techniques. *Analytica Chimica Acta*, 418 (1), 53-68.
- Andersen, T. & Færøvik, P. J.(2007).Utredninger Vansjø 2006 - Undersøkelse av mulig interngjødsling i vestre Vansjø. *NIVA Rapport 5353 - 2007*. Oslo: NIVA.
- Appelo, C.A.J. & Postma, D.(2007).*Geochemistry, Groundwater and Pollution*. Amsterdam, The Netherlands: Balkema Publication.
- Aquarius (2010).“Farmers as Water managers in a Changing Climate” Østfold Baseline Report.
- Aylward, G.H. & Findlay, T.J.V.(2008).*Si Chemical Data*. 5th ed. Milton: Wiley.
- Barnes, R. B.(1975).The determination of specific forms of aluminium in natural water. *Chem. Geol.*, 15:177-191.
- Bartlett, R. J.(1986).Soil Redox Behaviour PP.179-207. IN D.L. SPARKS(ed), *Soil Physical chemistry*. CRC Press, Boca Raton; Florida.
- Bechmann, M.(2005).The phosphorus index tool for assessing phosphorus transfer from agricultural areas in Norway. Doctor Scientarum, Universitetet for miljø- og biovitenskap.
- Bechmann, M & Stålnacke, P.(2005).Effect of policy induced measures on suspended sediments and total phosphorus concentrations from three Norwegian agricultural catchments. *The Science of the Total Environment* 344: 129-142.
- Bechmann, M. E., Berge, D., Eggestad, H. O., Vandsemb, S. M.(2005).Phosphorus transfer from agricultural areas and its impact on the eutrophication of lakes - two long-term integrated studies from Norway. *J. Hydrol. (Amsterdam, Neth.)* 304, 238-250.
- Bechmann, M. E., Kleinman, P. J. A., Sharpley, A. N., Saporito, L. S.(2005).Freeze–thaw effects on phosphorus loss in runoff from manured and catch-cropped soils. *Journal of Environmental Quality*, 34 (6): 2301-2309.
- Bechmann, M., Eggestad, H. O., Kvernø, S.(2006).Lokale fosfortilførsler til vestre Vansjø og Mosseelva. *Bioforsk Rapport*, Vol. 1, Nr. 3. Ås: Bioforsk Jord og Miljø.
- Bechmann, M. & Eggestad, H.O.(2007).Lokale fosfortilførsler til vestre Vansjø og Mosseelva. *Bioforsk Rapport*, Vol. 2, Nr. 36. Ås: Bioforsk Jord og Miljø.
- Bennett, W. W., Teasdale, P. R., Panther, J. G., Welsh, D. T., Jolley, D. F.(2010).New diffusive gradients in a thin film technique for measuring inorganic arsenic and selenium(IV) using a titanium dioxide based adsorbent. *Anal. Chem.* 82 (17),7401–7407.
- Bioforsk.(2011).*Surveillance data from Bioforsk [Raw data]*. Available through the Morsaproject.
- Bjørndalen, K., Andersen, T., Færøvig, P.J.(2007).*Utredninger Vansjø - Kartlegging av vannkvalitet i 2006*. Oslo: NIVA.
- Blankenberg, A. G. B., Turtumøygard, S., Pengerud, A., Borch, H., Skarbøvik, E., Øygarden, L., Bechmann, M., Syversen, N., Vagstad, N.H.(2008).Tiltaksanalyse for Morsa: ”Effekter av fosforreduserende tiltak i Morsa 2000-2006”.
- Brady, N. C. & Weil, R. R. (2004). *Elements of the Nature and Properties of Soils*. 2<sup>nd</sup> ed.Upper Saddle River, NJ: Prentice Hall.

- Braskerud, B. & Hauge, A.(2008).Veileder –Fangdammer for partikkel- og fosforrensing. Bioforsk FOKUS, Vol.3 nr. 12. 38 s.
- Broberg, O.(1984).Phosphate removal in acidified and limed lake water. *Water Research*. 18 (10), 1273-1278.
- Buffle, J., Zhang, Z., Startchev, K.(2007).Metal Flux and Dynamic Speciation at (Bio)interfaces. Part I: Critical Evaluation and Compilation of Physicochemical Parameters for Complexes with Simple Ligands and Fulvic/Humic Substances. *Environmental Science & Technology* .41 (22), 7609-7620.
- Carpenter, S. R.(2005).Eutrophication of aquatic ecosystems: Bi-stability and soil phosphorus. Proc. Natl. Acad. Sci. U. S. A. 102.10002-10005.
- Connor, P. A. & McQuillan, A. J.(1999).Phosphate adsorption onto TiO<sub>2</sub> from aqueous solutions: An in situ internal reflection infrared spectroscopic study *Langmuir*. 15 (8) 2916– 2921.
- Cooke, G. D., Welch, E. B.,Martin, A. B., Fulmer, D. G., Hyde, J. B.,Schriever, G. D.(1993).Effectiveness of Al, Ca, and Fe salts for control of internal phosphorus loading in shallow and deep lakes. *Hydrobiologia*. 253 (1), 323-335.
- Coote, D. R., Malcolm-Mc Govern, C. A., Wall, G. J., Dickinson, W. T., Rudra, R. P.(1988).Seasonal variation of erodibility indices based on shear strength and aggregate stability in some Ontario soils. *Canadian Journal of Soil and Science* 68, 405-416.
- Crank, J.(1975).The mathematics of diffusion. Second Edition. Oxford University Press, London, 1.
- Currie, W. S., Aber, J. D., McDowell, W. H., Boone, R. D., Magill, A. H.(1996).Vertical transport of dissolved organic C and N under long term N amendments in pine and hardwood forests.*Biogeochemistry*.35, 471±505.
- Cussler, E. L.(1997).Diffusion Mass transfer in fluid systems. Cambridge University Press, Cambridge.
- Davison, W. & Zhang, H.(1994).In situ speciation measurements of trace components in natural waters using thin-film gels. *Nature*, 367, 546-548.
- Direktoratgruppen Vanndirektivet.(2009).*Veileder 01:2009 Klassifisering av miljøtilstand i vann*: Direktoratgruppen for gjennomføringen av vanndirektivet.
- Djordjic, F.(2001).Displacement of phosphorus in structured soils. Dissertation. Uppsala, Sweden.
- Dodson, S. I.(2005).*Introduction to Limnology*. Boston: McGraw-Hill.
- Driscoll, C. T.(1984).A procedure for the fractionation of aqueous aluminium in dilute acidic waters. *International Journal of Environmental Analytical Chemistry*, 16:267-283
- Esbensen, K., Schönkopf, S., Midtgaard, T.(1994).Multivariate Analysis - in practice. A Training Package.
- European Commission.(2006).Main Sources of Eutrophication in Europe. In Bio intelligence service, European Commission, ed.
- European Commission.(2010).European Commission, Water is for life:How the Water Framework Directive helps safeguard Europe's resources (Belgium, Luxembourg: Publications Office of the European Union).
- European Commission.(2011).*Introduction to the new EU Water Framework Directive*. Available at: [http://ec.europa.eu/environment/water/waterframework/info/intro\\_en.htm](http://ec.europa.eu/environment/water/waterframework/info/intro_en.htm) (accessed: 06.03.12).
- FAO.(2004).Use of phosphate rocks for sustainable agriculture. FAO fertilizer and plant nutrition Bulletin 13. Food and Agriculture Organization of the United Nations. Rome.

- Fettig, J., Ødegaard, H., Eikebrokk B.(1988).Humic substances removal by alumcoagulation - direct filtration at low pH. In proceedings: *Pre-treatment Chem. Water Wastewater Treat., Gothenburg Symposium*, edited by H. H. Hahn, and R. Klute, 3rd (pp 55-66).Springer.Berlin. Fed. Rep. Germany.
- Frame, P. A., Burney, J. R., Edward, L. M.(1992).Laboratory measurements of freeze/thaw, compaction, residue and slope effects on rill erosion. *Canadian Agricultural Engineering* 34(2), 143-149.
- Førland, E.J, Alfenes, E., Amundsen, H., Asvall, R.P. et al.(2007).*Climate change and natural disasters in Norway*. Meteorologisk institutt, Oslo. Available at:  
[http://met.no/english/r\\_and\\_d\\_activities/publications/2007/06\\_2007/report\\_06\\_2007.pdf](http://met.no/english/r_and_d_activities/publications/2007/06_2007/report_06_2007.pdf)(accessed: 05.03.12).
- Garmo, Ø, A., Røyset, O., Steinnes, E., Flaten, T, P.(2003).Performance study of diffusive gradients in thin films for 55 elements. *Analytical Chemistry*, 75, 3573-3580.
- Garmo, Ø. A.(2006).Diffusive gradients in thin films as a tool for metal fractionation and assessment of metal bioavailability to fish. Thesis for the degree doctor philosophiae. Department of Chemistry. Norwegian University of Science and Technology. Faculty of Natural Sciences and Technology. University of Trondheim.
- Gebreslasse, Y. K.(2012).*Particle transport of phosphorus in streams draining catchments with different land uses*. Master's Thesis. Department of Chemistry. University of Oslo.
- Gerke, J.(1993).Phosphate adsorption by humic/Fe-oxide mixtures aged at pH 4 and 7 and by poorly ordered Fe-oxide. *Geoderma*, 59 (1-4), 279-288.
- Goldman, J. C.(1979).Physiological processes, nutrient availability, and the concept of relative growth rates in marine phytoplankton ecology. In Falkowski, P.G.(ed.), *Primary Productivity in the Sea*.Plenum, New York.pp. 179-194.
- Haaland, S., Hongve, D., Laudon, H., Riise, G.,Vogt, R. D.(2010).Quantifying the Drivers of the Increasing Colored Organic Matter in Boreal Surface Waters. *Environmental Science & Technology*, 44 (8), 2975-2980.
- Haygarth, P.M. & A.N. Sharpley.(2000).Terminology for Phosphorus transport. *J. Environ. Qual.* 29:10-15.
- Heathwaite, A. L., Haygarth, P.M, Dils, R.M.(2000).*Pathways of phosphorus transport*. In: Agriculture and Phosphorus Management. Lewis, CRC Press LLC, Boca Raton, USA, pp. 107-130.
- Henderson, B. & Markland, H. R.(1987).Decaying lakes-The origins and control of cultural eutrophication. Chichester, New York, Brisbane, Toronto, Singapore. John Wiley & Sons.
- Holtan, H., Kamp-Nielsen, L., Stuanes, A. O.(1988).Phosphorus in soil, water and sediment: an overview. *Hydrobiologia*, 170 (1): 19-34.
- Hongve, D., Riise, G., Kristiansen, J.(2004).Increased colour and organic acid concentrations in Norwegian forest lakes and drinking water – a result of increased precipitation? *Aquatic Sciences - Research Across Boundaries*, 66 (2), 231-238.
- Hovedstyret for Morsa-prosjektet.(2003).*Handlingsplan for Morsa 2002-2005. En sammenstilling av kommunenes og landbrukets planer*. Morsaprojektet.
- ISO 7888.(1985).Water quality-Determination of electrical conductivity.
- ISO 10204-1.(1992).Water quality-Determination of dissolved fluoride, chloride, nitrate, orthophosphate, bromide, nitrate and sulphide ions, using liquid chromatography of ions.
- ISO 10523.(1994).Water quality-Determination of pH.
- ISO 6878.(2004).Water quality-Determination of phosphorus. Ammonium molybdate spectrometric method.



- ISO 22036.(2008).Soil quality-Determination of trace elements in extract of soil by inductively coupled plasma-atomic emission spectrometry (ICP-AES).
- Jolliffe, I. (2005).Principal Component Analysis, In:Encyclopedia of Statistics in Behavioral Science. John Wiley & Sons, Ltd.
- Ketcheson ,J. W.(1977).Conservation tillage in eastern Canada. *Journal of Soil and Water Conservation* 32. 57-60.
- Kirby, P.C and Mehuys, G.R.(1987).Seasonal variation of soils readabilities in south-western Quebec. *Journal of Soils and Water conservations* 42, 211-215.
- Klaff.(2002).Limnology: Inland Water Ecosystems. Prentice-Hall Inc., New Jersey.
- Kopáček, J., Ulrich, K.-U., Hejzlar, J., Borovec, J., Stuchlík, E.(2001).Natural inactivation of phosphorus by aluminum in atmospherically acidified water bodies. *Water Research*. 35 (16), 3783-3790.
- Krogstad, T. & Løvstad, Ø.(1987).Fosfor i jord og vann. *Jord og Myr*, 6: 189-208.
- Krogstad, T.(1992).Metoder for jordanalyser. *Rapport nr. 6/92*. Ås: Institutt for jordfag, Norges landbrukshøgskole.
- Lander, C. H. K, Moffitt, D., Alt, K.(1998).Nutrients Available from Livestock Manure Relative to Crop Growth Requirements.Resource Assessment and Strategic Planning Working Paper 98–1. US Department of Agriculture, NaturalResources Conservation Service, Washington, DC. Available at: <http://www.nhq.nrcs.usda.gov/land/pubs/nlweb.html>.(accessed 06.09.2011).
- Leinweber, P., Turner, B. L., Meissner, R.(2002).Phosphorus. In: Agriculture, Hydrologieand Water Quality (eds) Haygarth P.M. and Jarvis S. C. CABI Publishing, pp. 528
- Li, Y-H. & Gregory, S.(1974).Diffusion of ions in sea water and deep-sea sediments. *Geochimica et Cosmochimica Acta*, 38, 703-714.
- Lindsay, W. L.(1979).Chemical equilibria in soils. Joh Wiley and sons. NY.
- Lundekvam, H.(1998).P-losses from three soils types at different cultivation systems.*Kunliga Skog-og Lantbruksvitneskapliga Akademias tidskrift* 137:177-185.
- Lundekvam, H. & Skøien, S.(1998).Soil erosion in Norway. An overview of measurements from soil loss plots. *Soil Use and Management* 14: 84-89.
- Lundekvam, H. E., Romstad, E., Øygarden, L.(2003).Agricultural policies in Norway and effects on soil erosion. *Environmental Science & Policy*, 6 (1), 57-67.
- Mack, J.(2010).Eutrophication. In What is eutrophication? (Lake scientist), 1.
- Maher, W & Woo, L.(1998).Procedures for the storage and digestion of natural waters for the determination of filterable reactive phosphorus, total filterable phosphorus and total phosphorus. *Anal. Chim. Acta*, 375 (1-2), 5–47.
- Martinsen, Ø.(2007).Vansjø – en unik naturperle. Orion Forlag AS. PP 183.
- met.no.(2011).Meterologisk institutt. Available at: <http://met.no/> (accessed 11.01.2012).
- Meybeck, M.(1982).Carbon, nitrogen and phosphorus transport by world Rivers. *American Journal of Science* 287: 401-428.
- Minitab 16 Statistical Software.(2010).[Computer software]. State College, PA: Minitab, Inc. Available at: <http://www.minitab.com/> (accessed 10.12.2011).

- Mohr, C.W.(2010).*Monitoring of phosphorus fractions – Understanding the geochemical and hydrological processes governing the mobilization of phosphorus from terrestrial to aquatic environment*. Master's Thesis. Department of Chemistry. University of Oslo.
- Monbet, P & McKelvie, I. D.(2007).Phosphates. In *Handbook of Water Analysis*, 2nd ed.; Nollet, L. M. L., Ed.; CRC Press: Boca Raton.FL,.
- Moore, A. & Reddy, K. R.(1993).Role of Eh and pH on Phosphorus Geochemistry in Sediments of Lake Okeechobee, Florida. *J. Environ. Qual.* 23 (5), 955-964.
- Morgan, S.(1996).Aquatic chemistry.Chemical equilibria and rates in natural waters.
- Nasholm, T., Ekblad, A., Nordin, A., Giesler, R., Hogberg, M., Hogberg, P.(1998).Boreal forest plants take up organic nitrogen. *Nature* 392, 914-916.
- Newesely, H.(1989).Fossil bone apatite. *Applied Geochemistry* 4, 233-245.
- Norwegian Forest and Landscape Institute.(2011).Available at: <http://www.skogoglandskap.no/>(accessed: 22.03.12).
- Nriagu, J. O. & Moore, P. B.(1984).Phosphate minerals, Editors, Springer Verlag, Berlin.
- NS4733.(1983).Water analysis-Determination of suspended solids in waste water and their residue on ignition.
- NS4725.(1984).Bestemmelse av total fosfor.Oppslutting med peroksodisulfat.
- NS-EN ISO 9963-1.(1985).Water quality-Determination of alkalinity- Part 1: Determination of total and composite alkalinity.
- NS EN ISO 15691-1.(2004).Water quality-Determination of orthophosphate and total phosphorus contents by flow analysis(FIA and CFA). Method by flow injection analysis (FIA).
- NS EN ISO 15691-2.(2004).Water quality-Determination of orthophosphate and total phosphorus contents by flow analysis(FIA and CFA).Method by continuous flow analysis (CFA).
- NS-EN 872.(2005).Water quality-Determination of suspended solids-Method by filtration through glass fibre filters.
- Nygaard, P. H. & Wit, H. A. De.(2000).Effects of enhanced Al concentrations on fine root growth in a mature Norway spruce stand in southern Norway. *In: Nordic workshop on plant roots and mycorrhizas*, p. 21. Joensuu, Finland 14-18-June 2000.
- Opland, K. A. J.(2011).Processes governing mobility and transport of phosphorus from agricultural soil. Master's Thesis. Department of Chemistry. University of Oslo.
- Panther, J. G.,Teasdale, P. R., Bennett, W. W., Welsh, D. T., Zhao, H.(2010).Titanium Dioxide-Based DGT Technique for In Situ Measurement of Dissolved Reactive Phosphorus in Fresh and Marine Waters. *Environ. Sci. Technol.* 44, 9419-9424.
- Panther, J.G.(2011).Personal communication.
- Patrick, W.H. Jr & Jugsujinda, A.(1992).Sequential reduction and oxidation of inorganic nitrogen, manganese, and iron in flooded soil. *Soil Science Society of America Journal*, 56, 1071 - 1073.
- Paytan, A. & McLaughlin, K.(2007).The Oceanic Phosphorus Cycle. *Chemical Reviews* 107, 563-576.
- Pierzynski, G.M., Sims, J.T., Vance, G.F.(2005).Soils and Environmental Quality, Third Edition, Third edition Edition. CRC Press.

- Ponnamperuma, F. N.(1965).Dynamic aspects of flooded soils and the nutrients of the rice plants. In: The Mineral Nutrients of the Rice Plants. Research Paper Series, International Rice Research Institute, Manila.
- Ponnamperuma, F. N.(1972).The chemistry of submerged soils. *Advance in Agronomy* 24: 29-96.
- Rast, W. & Thornton, J. A.(1996).Trends in eutrophication research and control. *Hydrological Processes*, 10 (2), 295-313.
- Redfield, A.C.(1934).On the proportions of organic derivations in sea water and their relation to the composition of plankton. In James Johnstone Memorial, 177-192.
- Roden, E. E. & Edmonds, J. W.(1997).Phosphate mobilization in iron-rich anaerobic sediments: microbial Fe(III) oxides reduction versus iron-sulphide formation. *Arch. Hydrobiol.*, 139 .pp. 347–378.
- Roncal,T.(2009).Process controlling the concentration of phosphates in natural water. PhD thesis. University of Toulouse.
- Ruttenberg, K. C.(2003).The Global Phosphorus Cycle. In *Treatise on Geochemistry*, Editors-in Chief: Heinrich, D. H.; Karl, K. T., Eds. Pergamon: Oxford, 2003; pp 585-643.
- Ryding, S. & Rast, W.(1989).Man and the Biosphere serie.
- Røyset, O., Bjerke, E., Eich-Gretorex, S., Sogn,T. S., Ålmos, Å. R.(2004).Simultaneous sampling of phosphate, arsenate and selenate in water by Diffusive Gradients in Thin Films (DGT).NIVA.Norwegian Institute for Water Research.
- Røyset, O.(2011).Personal communication.
- Sangi, M. R., Halstead, M. J., Hunter, K. A.(2002).Use of the diffusion gradient thin film method to measure trace metals in fresh waters at low ionic strength. *Analytica Chimica Acta*, 456 (2), 241-251.
- Scalenghe, R., Edwards, A. C., Ajmone Marsan, F., Barberis, E.(2002).The effect of reducing conditions on the solubility of phosphorus in a diverse range of European agricultural soils. *European Journal of Soil Science*, 53 (3), 439-447.
- Schindler, D.W. (1977).Evolution of phosphorus limitation in lakes.*Science* (Washington, DC) 195:260-262.
- Schlesinger, W.H. (1997).*Biogeochemistry: An Analysis of Global Change* 2<sup>nd</sup> ed. Academic Press, San Diego.
- Senorge.no.(2011).*Vær, vann, snø og klima i Norge*. NVE, Meteorologisk institutt og Statens Kartverk. Available at: <http://www.senorge.no/> (accessed: 14.12.11).
- Sharpley, A. N.(1985).The selective erosion of plant nutrients in runoff. *Soil Science Society of America Journal*, 49 (6): 1527-1534.
- Sharpley, A. N & Rekolainen, S.(1997).Phosphorus in agriculture and its environmental implications. *Phosphorus loss from soil to water*. Wallingford (United Kingdom). CAB International. ISBN 08-519-91564.
- Sharpley, A. N.(2000).Editor Agriculture and Phosphorus Management.The Chesapeake Bay. CRC Press, Boca Raton, FL.
- Sharpley, A. N., McDowell, R. W., Kleinman, P. J. A.(2001).Phosphorus loss from land to water: integrating agricultural and environmental management. *Plant and Soil*, 237 (2), 287-307.
- Shenker, M., Seitelbach, S., Brand, S., Haim, A., Litaor, M. I.(2005).Redox reactions and phosphorus release in re-flooded soils of an altered wetland. *European Journal of Soil Science*.56 (4), 515-525.

- Sibbesen, E. & Sharpley A.N.(1997).Setting and justifying upper critical limits for phosphorus in soils, p. 151-176 in Tunney H., Carton O.T., Brookes P.C. and Johnston A.E. (eds). Phosphorus loss from soil to water. Center for Agriculture and Biosciences (CAB) International, Wallingford, U.K.
- Simard, R. R., Cluis, D., Gangbazo, G., Beauchemin, S. (1989).Phosphorus status of forest and agricultural soils from a watershed of high animal density. *J. Environ. Qual.*, 24: 1010-1017.
- Sims,J. T & Sharply,A. N.(2005).Phosphorous Agricultural and the Environment. American Society of Agronomy nr 46,Inc.
- Skarbøvik, E., Barkved, L.J. og Stålnacke, P.G.(2007).Tilførsler av partikler og fosfor til Storefjorden - Utredninger Vansjø 2006. (*Inputs of sediments and phosphorus to Storefjorden– Vansjø; in Norwegian*). NIVA-Rapp 5389. 38 pp.
- Skarbøvik, E. & Bechmann, M.(2010).Some characteristics of the Vansjø-Hobøl (Morsa) catchment. *Bioforsk Report*, Vol. 5, No.128. Ås: Bioforsk Jord og Miljø.
- Skarbøvik, E., Bechmann, M., Rohrloack, T., Haande, S.(2011).Overvåking Vansjø/Morsa 2009-2010. Resultater fra overvåking av innsjøer, elver og bekker i perioden oktober2009 – oktober 2010. *Bioforsk Rapport*, Vol. 6, Nr. 31. Ås: Bioforsk Jord og Miljø.
- Skjelkvåle, B. L. R & Wollan .A. K.(2009).Overvåking av langtrasporterte forurensninger 2008.Sammenderag rapport.Oslo.NIVA.OR-5810:89.
- Solheim, A. L., Vagstad, N., Kraft, P., Løvstad, Ø., Skoglund, S., Turtumøygard, S., Selvik,J.-R.(2001). Tiltaksanalyse for Morsa (Vansjø-Hobøl-vassdraget) - Sluttrapport.*NIVA Rapport*. Available at: <http://www.morsa.org/pdf/tiltaksanalyse.pdf> (accessed:14.12.11).
- Sonzogni,W. C., Chapra.S. C, Armstrong .D. E., Logan.T. J.(1982).Bioavailability of phosphorous input to lake. *Journal of Environmevnt Quality* 11: 555-563.
- Steen, P.(1998).Phosphorus Availability in the 21st Century: Management of a Non Renewable Resource. *Phosphorus and Potassium* 217, 25-31.
- Stewart, W.(2005).Phosphorus as natural resource. In: Phosphorus: Agriculture and the Environment. Agronomy Monograph n°46. (eds. Sims T. and Sharpley A.), Madison, USA.
- Stumm, W. & Morgan J. J.(1981).Aquatic Chemistry. An Introduction Emphasizing Chemical Equilibria in Natural Waters. John Wiley and Sons, NY. 780 pp.
- Sullivan, T. J., Seip, H. M., Muniz, I. P.(1986).A comparison of frequently used methods for the determination of aqueous aluminium. *International Journal of Environmental Analytical Chemistry*, 26:61-75.
- Turner B. L. & Haygarth P. M.(2000).Phosphorus forms and concentrations in leachate under four grassland soil types. *Soil Sci. Soc. Am. J.*, 64: 1090-1097.
- UNESCO.(2005).Water Resources Systems Planning and Management. ISBN 92-3-103998-9.
- vanLoon, G. W. & Duffy, S. J.(2007).Environmental Chemistry. A Global Perspective. 2nd edition. Oxford University Press.
- Vannområdeutvalget .(2011).*Vestre Vansjø*. Vannområdeutvalget for Vansjø/Hobøl og Hølenvassdragene med kystområder. Available at: <http://morsa.org/vestrevansjo.php> (accessed: 10.01.12).
- Vannportalen.no.(2011).*The Water Framework Directive in Norway*. Available at: <http://www.vannportalen.no/enkel.aspx?m=40354> (accessed: 25.03.11).

Van Vaiet, L. J. P, Wall, G. J, Dickinson, W.T.(1976).Effect of agricultural land use on potential sheet erosion losses in southern Ontario. *Canadian Journal of Soil Science* 56, 443-451.

Vogt, R. D.(2011).Personal communication.

WFDN.(2011).The Water Framework Directive in Norway (WFDN). In Transposition of the WFD in Norway: The Water Regulation (Norway, vannportalen).

Wikipedia.(2011).Molecular structures of (IP)6 and AMP. Available at:  
<http://en.wikipedia.org/wiki/File:Phytate.png> and  
[http://en.wikipedia.org/wiki/File:AMP\\_chemical\\_structure.png](http://en.wikipedia.org/wiki/File:AMP_chemical_structure.png) (accessed: 14.2.12).

Zhang, H. & Davison, W.(1995).Performance characteristics of diffusion gradients in thin films for the in situ measurement of trace metals in aqueous solution. *Analytical Chemistry*, 67, 3391-3400.

Zhang, H., Davison, W., Gadi, R., Kobayashi, T.(1998).In situ measurement of dissolved phosphorus in natural waters using DGT, *Anal. Chim. Acta.* 370, 29-38.

Zhang, H. & Davison, W.(1999).Diffusional characteristics of hydrogel used in DGT and DET techniques. *Anal. Chem. Acta.* 398: 329-340.

Zhang, H.(2005).DGT-for measurements in water sols and sediments.DGT Research Ltd, Lancaster.

Øygarden, L., Kværner, J., Jenssen, P.D.(1997).Soil erosion via preferential flow to drainage systems in clay soils. *Geoderma* 76: 65-86.

Øygarden, L.(2000).Soil erosion in small agricultural catchments, south-eastern Norway. *PhD Thesis*. Department of soil and water sciences. Agricultural university of Norway.

Øgaard, A. F. & Bechmann, M.(2010).Fosfor i vestre Vansjø – effekt av tiltak. *Bioforsk FOKUS*, 5 (1): 38-43. Available at:<http://www.bioforsk.no/ikbViewer/Content/69960/Jord%20og%20Plantekulturartikkel%202010.pdf> (accessed:14.12.11).

## List of Appendix

Appendix A: Filtration of water samples .....	120
A.1 Calculations for determining PMT, PMI and PMO.....	120
A.2 Standard Operating Procedure for filtration of water samples .....	120
Appendix B: Raw data for pH, major ions, aluminium, DOC, total-P and total-P fractions. ....	121
B.1 Correlations between the sum of anions and cations .....	122
Appendix C: Results of total-P concentrations under different hydrological regimes .....	125
C.1 Total-P fractions under high flow and low flow regime .....	125
C.2 Results showing P fractions during different flow regimes in the Støa1 stream .....	126
C.3 Results showing P fractions during different flow regimes in the Støa1 stream .....	126
Appendix D: Compilation of P results from EUTROPIA-data and Morsa monitoring programme-data .....	127
Appendix E: DGT Lab experiments and field evaluation .....	130
E.1 Preparation of AMP stock solution.....	130
E.2 Preparation of IP6 stock solution.....	130
E.3 Results from student test performed on the results from lab experiments .....	130
E.4 Raw data from the ferrihydrite DGT method field evaluation.....	131
E.5 Raw data from the metsorb DGT Method field evaluation.....	132
E.6. Statistics for the student test performed on the results from the Sampling precision of P by DGT samplers at the sampling location Støa1 .....	133
Table A21: Statistics for the paired t-test.....	133
Appendix F: Flow-weighted mean concentration and linear interpolations.....	133
F.1 Equation for flow weighted mean concentration .....	133
F.2 Linear interpolation curves .....	134
Appendix G: Correlation between SS and total-P in Støa1 stream (Eutropia samples).....	134
Appendix H: Statistical Analysis .....	135
H.1 PCA on water samples.....	135
H.2 Pearson Correlation analysis data.....	136
Appendix I: Maps of quaternary deposits of the investigated streams.....	137
Appendix J: Map of erosion risk in the investigated streams.....	140

## Appendix A: Filtration of water samples

### A.1 Calculations for determining PM<sub>T</sub>, PM<sub>I</sub> and PM<sub>O</sub>

The total particulate matter concentrations (PM<sub>T</sub>) were calculated according to Equation A.

$$PM_T = \frac{(b-a)}{V} \quad (A)$$

Inorganic Particulate Matter (Equation B) is found by weighing the filter before and after combustion at 450°C.

$$PM_I = \frac{(c-a)}{V} \quad (B)$$

Organic Particulate Matter is calculated by difference between Total and Inorganic Particulate Matter according to Equation C.

$$PM_O = PM_T - PM_I \quad (C)$$

PM<sub>T</sub> = Total Particulate Matter (mg/L)

PM<sub>O</sub> = Organic Particulate Matter (mg/L)

PM<sub>I</sub> = Total Inorganic Matter (mg/L)

a = mass of clean filter (mg)

b = mass of filter with mass dried at 105°C (mg)

c = mass of filter with mass burned at 550°C (mg)

V = volume of sample (L)

### A.2 Standard Operating Procedure for filtration of water samples

This SOP is based on the Norwegian Standard NS-EN 872 and Sample Filtration Forms can be found in the folder named BLANKE LOGG ARK in the Environmental lab (V111).

Glass micro fibre filters of the type *Whatman 1825-047, 47 mm* should be used. Always include 3 blanks throughout the whole procedure. Always use the same balance to weigh the samples (in room V115, weighs to the nearest 0.1 mg).

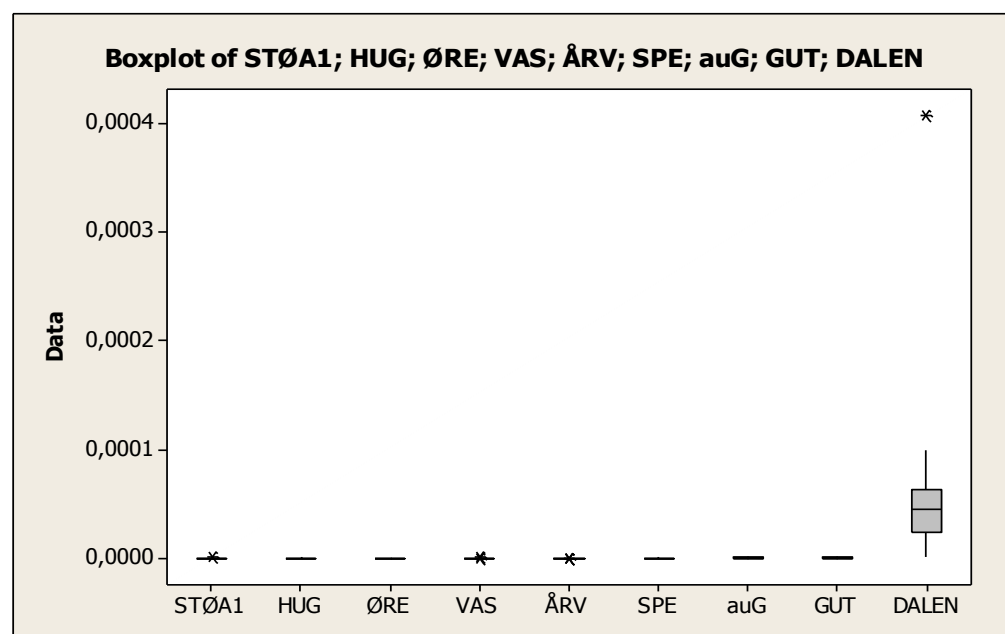
The balance should be switched on and allowed to warm up for 30 minutes. Press one of the tare keys to zero the weight display. You must adjust or calibrate your balance at the place of installation after each warm up period and before the first measurement. When the display shows zero readout, press the CAL key to activate the calibration function. During each weighing, the *Reference Filter* should also be weighed. Remember to write down the weight of the reference filter on the Sample filtration form.

## Appendix B: Raw data for pH, major ions, aluminium, DOC, total-P and total-P fractions.

Only the median and quartiles values are presented in the table form due to the large number of data set. These values are obtained by using Minitab 16 statistical package (2011) as shown in Figure A1.

**Table A1: Raw data for pH (Figure 27) of the studied streams.**

Sites	Median pH	Q1=75th quartile	Q3=25th quartile	Number of samples
STØ1	7,22	7,52	6,75	22
HUG	7,15	7,25	6,5	21
ØRE	6,97	7,4	6,96	19
VAS	7,06	7,38	6,69	20
ÅRV	7,11	7,38	7,01	15
SPE	6,60	6,91	6,37	16
AUG	6,61	6,86	6,43	16
GUT	6,45	6,79	6,5	22
DALEN	4,35	4,61	4,2	43

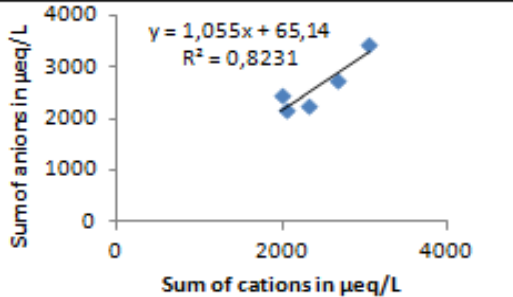
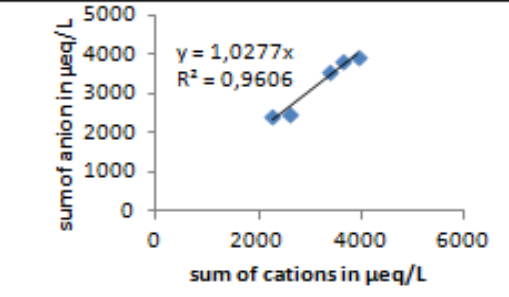
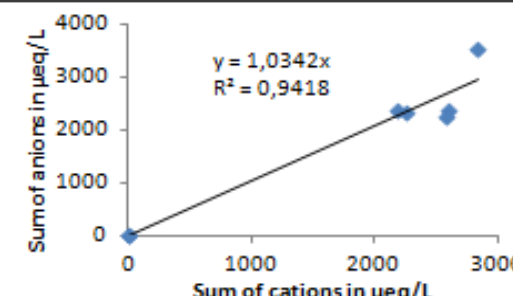
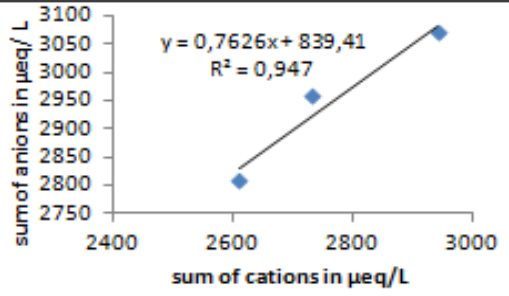
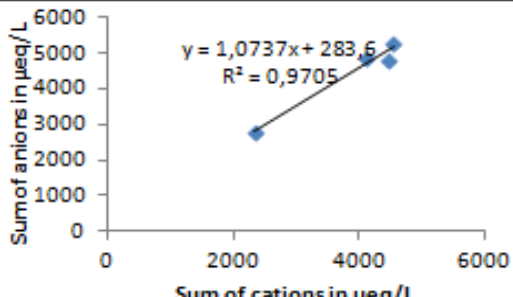
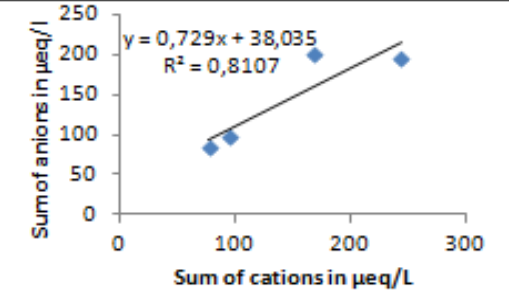
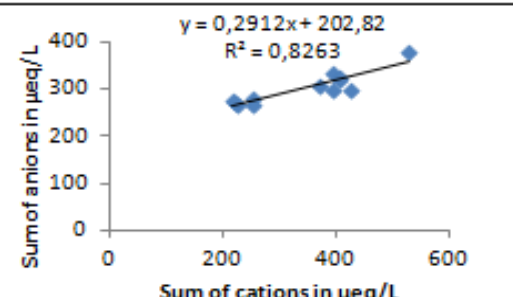
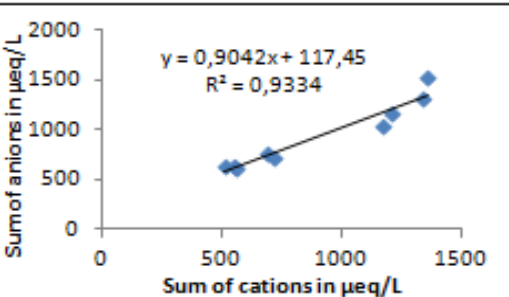


**Figure A1: Box plot of pH**



**B.1 Correlations between the sum of anions and cations**

**Table A2: Figures showing correlations between the sum of anions and cations in the studies streams.**

<p><b>Huggenes stream</b></p>  <p>Sum of anions in µeq/L</p> <p>Sum of cations in µeq/L</p> <p><math>y = 1,055x + 65,14</math> <math>R^2 = 0,8231</math></p>	<p><b>Støal stream</b></p>  <p>sum of anion in µeq/L</p> <p>sum of cations in µeq/L</p> <p><math>y = 1,0277x</math> <math>R^2 = 0,9606</math></p>
<p><b>Vaskeberget stream</b></p>  <p>Sum of anions in µeq/L</p> <p>Sum of cations in µeq/L</p> <p><math>y = 1,0342x</math> <math>R^2 = 0,9418</math></p>	<p><b>Ørejordet stream</b></p>  <p>sum of anions in µeq/L</p> <p>sum of cations in µeq/L</p> <p><math>y = 0,7626x + 839,41</math> <math>R^2 = 0,947</math></p>
<p><b>Arvold stream</b></p>  <p>Sum of anions in µeq/L</p> <p>Sum of cations in µeq/L</p> <p><math>y = 1,0737x + 283,6</math> <math>R^2 = 0,9705</math></p>	<p><b>Augerød stream</b></p>  <p>Sum of anions in µeq/L</p> <p>Sum of cations in µeq/L</p> <p><math>y = 0,729x + 38,035</math> <math>R^2 = 0,8107</math></p>
<p><b>Dalen Stream</b></p>  <p>Sum of anions in µeq/L</p> <p>Sum of cations in µeq/L</p> <p><math>y = 0,2912x + 202,82</math> <math>R^2 = 0,8263</math></p>	<p><b>Guthus stream</b></p>  <p>Sum of anions in µeq/L</p> <p>Sum of cations in µeq/L</p> <p><math>y = 0,9042x + 117,45</math> <math>R^2 = 0,9334</math></p>

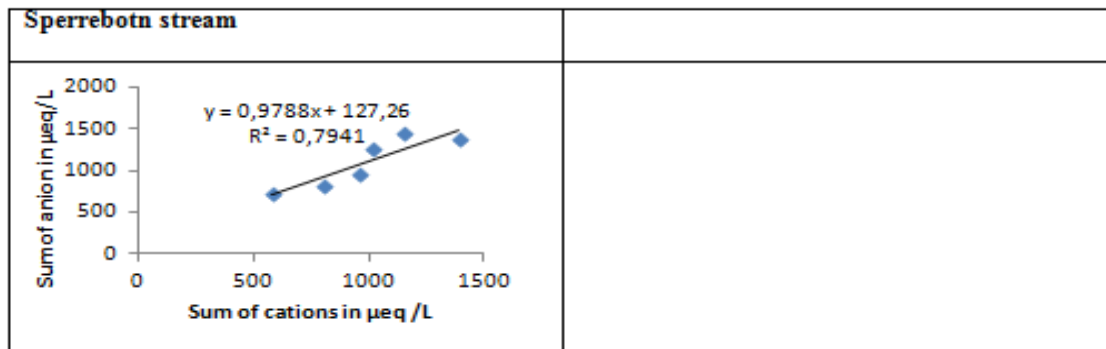


**Table A3: Raw data for major ions (Figure 28) in the studied streams.**

Sites	Number of samples	Major anions and cations in µmol /L										
		H+	Ca <sup>2+</sup>	Mg <sup>2+</sup>	Na <sup>+</sup>	K <sup>+</sup>	HCO <sub>3</sub> <sup>-</sup>	NO <sub>3</sub> <sup>-</sup>	Tot-F	Cl <sup>-</sup>	PO <sub>4</sub> <sup>3-</sup>	SO <sub>4</sub> <sup>2-</sup>
STØ1	5	0,05	1979	640	390	151	1689	189	14	643	19	708
ØRE	5	0,01	1676	302	767	90	1037	86	7	1164	0,50	717
HUG	5	0,09	1358	540	398	117	914	254	11	510	1	921
VAS	5	0,11	1346	747	309	86	1233	285	14	498	1	534
ÅRV	4	0,11	1821	511	1184	113	1499	100	12	1849	2	682
SPE	6	0,49	350	217	377	40	386	28	6	422	1	247
AUG	4	0,13	259	184	337	33	295	29	6	435	3	192
GUT	9	0,37	313	231	315	40	286	17	5	324	1,96	297
DAL	12	10,8	61	35	188	45	143	1	3	146	1	23

**Table A4: Raw data for concentration of total-P (Figure 31) in µg/L the studied streams.**

Sites	Median con. Of total -P µg/l	Q1=25th quartile µg/L	Q3=75th quartiles µg/L	Number of samples
STØ1	110,5	64,8	152,13	122
HUG	45,6	30,5	80,94	114
ØRE	12,15	7,06	20,02	14
VAS	35,22	19,75	51,65	12
ÅRV	10,5	7,49	15	11
SPE	25,24	11,47	36,12	18
AUG	14,14	10,3	29,37	18
GUT	31,1	15,95	44,07	21
DALEN	9,79	7,17	18,2	210

**Table A5: Raw data for concentrations of different P fractions (Figure 32) in µg/L in the studied streams.**

	DOM-P µg/L	Free-PO4 µg/L	PP µg/L
STØ1 (n=122)	5,91	40	50
ØRE (n=114)	2,55	1,16	5,5
HUG (n=14)	5,4	7,56	29
VAS (n=12)	3,28	2,41	20,26
ÅRV (n=11)	2,7	1,69	7,2
SPE (n=18)	6,49	5,89	6,56
AUG (n=18)	3,99	2,98	7,06
GUT (n=21)	8,1	4,5	12,92
DALEN (n=210)	4,98	1,34	3,8

**Table A6: Raw data for concentration of DOC (Figure 29) in mg/L in the studied streams.**

Sites	Median DOC mg C/L	Q1=25th quartile	Q3=75th quartile	Number of samples
STØ1	6,2	5,07	9,39	12
HUG	4,7	6,39	7,21	6
ØRE	7,2	3,6	13,33	10
VAS	3,8	2,51	9,11	9
ÅRV	5,1	4,83	6,02	7
SPE	9,11	7,85	13,34	9
AUG	9,12	5,99	11,56	10
GUT	14,35	13,14	16,26	13
DALEN	22,5	19,13	27,46	47

**Table A7: Concentration of aluminium in (section 4.1.2.1) the Dalen stream.**

Concentration of aluminium at Dalen stream				
	Median mg Al/L	Q1=25th quartile	Q3=75th quartile	Number of samples
Alo µg/L	0,379	0,341	0,431	110
Ali µg/L	0,123	101,5	156,25	110

**Table A8: Concentration of total-N fractions (Figure 30) in the studied stream.**

Streams	Concentrations of total-N fractions in mg/L			Number of samples	
	NO3	DON	NH4		
STØ1	0,98408	0,31913	0,035362	10	
ØRE	1,27566	0,21094	0,081604	5	
HUG	1,3014	0,294767	0,0109	5	
VAS	1,416533	0,2825	0,01375	5	
ÅRV	1,569984	0,444084	0,020273	4	
SPE	0,57725	0,223925	0,007475	9	
AUG	0,923225	0,248977	0,008578	7	
GUT	0,545064	0,359593	0,01434	10	
DAL	0,065532	0,450004	0,055885	15	

## Appendix C: Results of total-P concentrations under different hydrological regimes

### C.1 Total-P fractions under high flow and low flow regime

**Table A9: Total-P fractions under high flow and low flow regimes (Figure 33 & Figure 34) in the studied stream.**

Streams	Total-P fractions under high- flow regimes in (µg/L)				Total- P fractions under low -flow regime (µg/L)		
	Number of samples	DOM-P	Free-PO4	PP	DOM-P	Free-PO4	PP
STØ1	7	14,79	104,6	154,8	2,39	3,81	16,50
ØRE	1	3,1	1,12	10,3	2,55	1,16	5,50
HUG	17	8,6	11,4	91,6	6,56	2,90	20,52
VAS	4	6,1	26,17	41,7	13,70	13,20	18,83
ÅRV	1	2,0	7,58	14,8	5,20	1,20	7,90
SPE	1	13,6	21,7	46,0	6,49	5,89	6,56
AUG	4	4,2	2,7	13,8	3,99	2,98	7,06
GUT	1	14,4	5,9	32,9	4,80	2,40	7,30
DALEN	25	5,2	1,0	2,9	4,5	1,34	3,8

### C.2 Results showing P fractions during different flow regimes in the Støa1 stream

**Table A10: Total- P fractions under high flow and low flow regimes from Støa1 stream (Figure 35 and Figure 36).**

Total P fractions under high flow regime in µg/L				Total P fractions under high flow regime in µg/L			
PP	DNOM-P	Free-PO4	Runoff L/S	PP	DNOM-P	Free-Po4	Runoff L/S
40,4	5,3	55,5	1,25	30,01074	4,665552	2,048301	0,59
38,2	4,8	68,0	1,49	32,90751	4,66788	3,640967	0,27
51,6	6,7	61,6	0,95	28,07802	2,847166	0,738567	0,23
59,6	9,6	69,5	2,04	31,94393	2,585879	0,646884	0,18
142,3	6,2	39,0	1,74	16,50727	2,399995	3,817219	0,14
93,9	12,3	67,1	1,78	13,82994	2,355871	9,332119	0,11
362,0	7,6	59,1	3,63	27,43161	2,298962	0,177442	0,09
114,5	14,8	127,5	2,02	14,78323	1,031623	8,670172	0,03
81,3	16,7	132,7	1,44	14,1164	2,391508	7,932482	0,02
105,6	18,7	195,6	3,63	22,75793	4,401557	17,95158	0,22
184,2	27,2	111,5	3,17	46,3	7,8	3,9	0,18

Mean difference	$\sqrt{n}$	STDEV	$t = (\text{mean difference} \times \sqrt{n}) / Sd$	t10 from table
183,25	3,31	104,11	5,82	2,26

The critical value is t (11) (degrees of freedom) = 2.26 (P=0.05) (Miller & Miller, 2005). The calculated value of t is higher than this, which indicates that the null hypothesis is rejected. The conclusion is that the methods give significantly different results for high flow and low flow samples.

### C.3 Results showing P fractions during different flow regimes in the Støa1 stream

**Table A11: Total- P fractions under high flow and low flow regimes from Huggenes stream (Figure 37).**

Total-P fractions during high flow in µg/L			Total-P fractions during low flow in µg/L		
PP	DNOM-P	Free-PO4	PP	DNOM-P	Free-PO4
155	15	105	50	6	40
91,6	8,66	11.46	28	5	8
42	7	27	20	2	3
11	4	2	5,5	2	3

## Appendix D: Compilation of P results from EUTROPIA-data and Morsa monitoring programme-data

**Table A12: Results for total-P generated by EUTROPIA project and by Morsa project.**

Streams site	Sampling time	Total-P analysed at UiO in $\mu\text{g P/L}$	Total-P analysed at Eurofins AS in $\mu\text{g P/L}$	Ratio
ØRE	12.01.2010	4,4	20	4,55
VANU	12.01.2010	18	28	1,56
SVIU	12.01.2010	23,64	41	1,73
MJÆR	12.01.2010	11,47	18	1,57
HOBK	12.01.2010	16,6	32	1,93
SVIU	27.01.2010	24,87	40	1,61
HOBK	27.01.2010	14,43	35	2,43
STØA1	07.04.2010	41,2	87	2,11
KRÅB	07.04.2010	37,4	100	2,67
HOBK	07.04.2010	31,7	63	1,99
ØRE	07.04.2010	7,9	18	2,28
SVIN	07.04.2010	15,1	35	2,32
VAS	07.04.2010	13,4	41	3,06
MJÆR	07.04.2010	7,8	22	2,82
ÅRV	07.04.2010	10,3	25	2,43

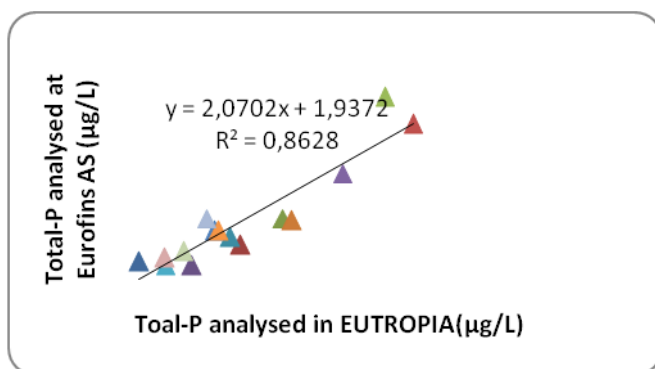


*Figure A2: Correlation between the data from EUTROPIA and Morsa. Based on table above.*

**Table A13: Results for free-PO<sub>4</sub> on samples generated by EUTROPIA and Morsa projects.**

Streams site	Sampling time	Free-PO <sub>4</sub> analysed by UiO in $\mu\text{g P/L}$	Free-PO <sub>4</sub> analysed by EUROFINS AS $\mu\text{g P/L}$	Ratio
ØRE	09.02.2010	1,1	14	12,73
MJÆR	09.02.2010	0,8	10	12,50
SVIU	09.02.2010	5,4	18	3,33
SVIU	09.02.2010	2,7	13	4,81
VANU	09.02.2010	2,6	9	3,46

MJÆR	09.02.2010	0,9	6	6,67
D	20.04.2010	1	2	2,00
SVIU	05.05.2010	3,5	16	4,57
VANU	05.05.2010	3,1	5	1,61
HUG	05.05.2010	5,4	31	5,74
SVIN	05.05.2010	5,6	12	2,14
ENGS	05.05.2010	2	17	8,50
ÅRV	05.05.2010	1	9	9,00
VAS	05.05.2010	1,2	14	11,67
VEID	05.05.2010	3,3	4	1,21
HOBK	05.05.2010	1,4	4	2,86
VANU	05.05.2010	0,4	6	15,00
GUT	05.05.2010	2,4	5	2,08
KRÅB	05.05.2010	2,7	8	2,96
MJÆR	05.05.2010	1	3	3,00
MØRK	05.05.2010	1,3	5	3,85
ØRE	05.05.2010	1,5	8	5,33
D	19.05.2010	1,3	2	1,54
ØRE	02.06.2010	1	3	3,00
GUT	02.06.2010	2,8	3	1,07
KRÅB	02.06.2010	3,6	7	1,94
MØRK	02.06.2010	1	2	2,00
SVIN	02.06.2010	2,2	4	1,82
HOBK	02.06.2010	1,8	2	1,11
HUG	02.06.2010	9,5	20	2,11
STØA1	02.06.2010	1,4	8	5,71
ÅRV	02.06.2010	2,2	4	1,82
MJÆR	02.06.2010	1,3	1	0,77
VANU	02.06.2010	0,7	1	1,43
SVIU	02.06.2010	2,8	4	1,43
VAS	02.06.2010	1,2	8	6,67
VEID	02.06.2010	3,3	4	1,21
VANU	02.06.2010	1,6	3	1,88
STØA1	05.05.2010	3,9	68	17,44

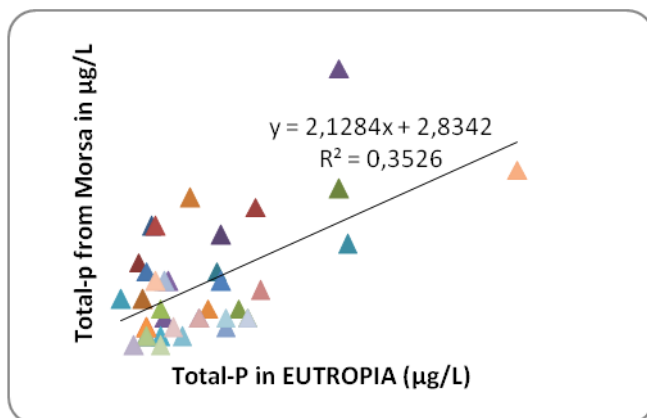


Figure A3: Correlation between the data from EUTROPIA and Morsa. Based on table above. One outlier omitted.

Table A14: Control samples analyzed by NIVA.

Samples	Results obtained by Environmental Analysis group, UiO		Results obtained at Eurofins AS in µg/L
	Parallel 1 in µg/L	Parallel 2 in µg/L	
Control total-P 4,85 µg/L	5	4,1	14
Control total-P 48,5 µg/L	49	48,7	33
Control PO4 4 µg/L	4,1	4,5	11
Control PO4 40 µg/L	40,5	41	46

Table A15: Stream water samples analyzed by UiO.

Samples	Results obtained by Environmental Analysis group ,UiO	
	Raw water total-P in µg/L	Raw water free-PO4 in µg/L
GUT stream water	24,7	3,5
STØA 1 stream water	24,4	11,7
ÅRV stream water	5,9	4,6

Table A16: Stream water sent to Eurofins AS.

Samples	Results obtained at Eurofins AS	
	Raw water total-P in µg/L	Raw water free-PO4 in µg/L
GUT stream water	180	13
STØA 1 stream water	64	44
ÅRV stream water	10	4,2

All the controls and stream water samples were handled in the same manner prior to arrival at the laboratory for analysis. Eurofins AS was informed that samples were not sewage samples.



## Appendix E: DGT Lab experiments and field evaluation

### E.1 Preparation of AMP stock solution

The preparation of test solution containing AMP was done by diluting 26, 5mL of AMP stock solution (0,558 µg/L AMP stock solution) with ~45L of Type II water. Thereafter the pH was adjusted to reach 5.5 by adding 1M acetic acid-sodium acetate buffer solution. The ionic strength was slightly increased by adding NaCl to 0,001 M. The solution was left to stabilize for 24 hour.

### E.2 Preparation of IP6 stock solution

The preparation of test solution containing AMP was done by diluting 45 mL of AMP stock solution (0,101 µg/L IP6 stock solution) with ~45L of Type II water. Thereafter the pH was adjusted to reach 5.5 by adding 1M acetic acid-sodium acetate buffer solution. The ionic strength was slightly increased by adding NaCl to 0,001 M. The solution was left to stabilize for 24 hour.

Start pH was 5.5 and temperature was 23<sup>0</sup> C during both experiments.

### E.3 Results from student test performed on the results from lab experiments

Table A17: Statistics for the paired t-test for lab experiment.

Paired t-test for lab- experiments.				
Mean difference	√n	STDEV	t=(mean difference × √n)/Sd	T3 from table
1,25 E-07	2,82	4,86 E-07	0,072	3,18

The critical value is t (3) (degrees of freedom) = 3.18 (P=0.05) (Miller&Miller,2005).The calculated value of t is lower than this, which indicates that the null hypothesis is retained. The conclusion is that the methods do not give significantly different results for ferrihydrite and Metsorb DGT methods.

Table A18: results from Experiment 2 (with IP6 stock solution)

Sampling Time (Days)	Tot-P adsorbed (P µg)	AMP tank µg /L	PO4 adsorbed (µg)	Diffusion coefficients calculated
1,14	0,12	37,04	0,0048	1,27E-06
2,21	0,22	33,80	0,0012	1,26E-06
3,15	0,32	30,02	0,0072	1,26E-06
4,06	0,44	32	-0,015	1,34E-06
4,82	0,60	34,89	0,006	1,57E-06
6,24	0,84	31	-0,0165	1,69E-06
6,86	0,90	30	0	1,65E-06
8,23	1,16	27,70	-0,021	1,76E-06

Calculation of diffusion coefficient was based on Equation  $D = \frac{X \cdot L}{C \cdot T \cdot A}$  Where, X=total-P adsorbed in ng, L= Length 0,102 in cm, C= concentration of AMP test solution in  $\mu\text{g/L}$ , T= time in seconds and A= exposure areal to solution 3.14 in  $\text{cm}^2$ .

#### E.4 Raw data from the ferrihydrite DGT method field evaluation

Table A19: Results from the ferrihydrite DGT method

Sampling site	Sampling time (S)	Total-P in $\mu\text{g/L}$	Free-PO4 in $\mu\text{g/L}$	Organic P in $\mu\text{g/L}$	volume ml	Adsorbed total-P from DGT sampler $\mu\text{g/L}$	Adsorbed free-PO4 from DGT sampler $\mu\text{g/L}$	Adsorbed organic-P from DGT sampler $\mu\text{g/L}$	Temperature corrected factor
STØ 1	1125300	182,9	159,7	23,2	30	24,35	7,07	31,42	0,71
STØ 1	1125300	233,2	214	19,2	30	32,63	5,85	38,48	0,71
STØ 1	1125300	211,2	181,5	29,7	30	27,67	9,05	36,73	0,71
STØ 1	1125300	198	169,6	28,4	30	25,85	8,67	34,53	0,71
STØ1	950400	60,1	53,7	6,4	30	9,43	2,24	11,66	0,73
STØ1	596700	94,2	83,6	10,5	30	23,39	5,89	29,28	0,73
STØ1	525300	148,3	129,3	19	30	38,93	11,44	50,37	0,77
STØ1	865200	298,9	262,5	36,5	30	49,28	13,69	62,96	0,75
STØ1	689400	264,1	228,3	35,8	30	56,81	17,83	74,63	0,71
STØ1	431400	122,5	106,2	16,3	30	42,22	12,97	55,2	0,71
DALEN	1128660	17,6	11	6,6	30	1,67	2,01	3,68	0,71
DALEN	1128660	16,8	8,4	8,4	30	1,28	2,56	3,84	0,71
DALEN	930900	9,1	5,5	3,6	30	0,99	1,29	2,28	0,73
DALEN	623400	9	5,4	3,6	30	1,45	1,93	3,38	0,73
DALEN	509400	11,2	7,4	3,8	30	2,3	2,36	4,66	0,77
DALEN	867600	9,9	6,9	3	30	1,29	1,11	2,41	0,75
DALEN	695700	13,5	8,5	5	30	2,11	2,47	4,57	0,71
DALEN	426600	9,3	4,2	5,1	30	1,7	4,09	5,79	0,71
HUG	1124160	38,7	34,2	4,5	30	5,22	1,37	6,59	0,71
HUG	1124160	46,6	40,8	5,9	30	6,22	1,79	8,02	0,71
HUG	952500	137,3	110,7	26,6	30	19,4	9,32	28,72	0,73
HUG	594600	17,9	15,7	2,2	30	4,4	1,24	5,64	0,73
HUG	524700	36,7	32,5	4,3	30	9,79	2,57	12,36	0,77
HUG	865200	57,6	51,9	5,7	30	9,74	2,15	11,89	0,75
HUG	691800	70,5	62,1	8,4	30	15,41	4,18	19,58	0,71
HUG	429900	36,8	31,8	5	30	12,71	3,99	16,7	0,71

### E.5 Raw data from the metsorb DGT Method field evaluation

**Table A20: Results from the Metsorb DGT method**

Sampling site	Sampling time (S)	Total-p in µg/L	Free-PO4 in µg/L	Organic P in µg/L	volume ml	Adsorbed total-P from DGT sampler µg/L	Adsorbed free-PO4 from DGT sampler µg/L	Adsorbed organic-P from DGT sampler µg/L	Temperature corrected factor
STØ 1	1125300	247,4	212,99	34,4041	30	32,474	10,49096	42,96476	0,71
STØ 1	1125300	252,0	206,25	45,7524	30	31,446	13,95145	45,39747	0,71
STØ 1	1125300	212,7	163,25	49,4054	30	24,89	15,06536	39,95556	0,71
STØ 1	1125300	336,8	290,29	46,4874	30	44,259	14,17556	58,43442	0,71
STØ1	950400	86,4	74,699	11,713	30	13,116	4,113112	17,22868	0,73
STØ1	596700	116,1	101,08	15,0547	30	28,269	8,420244	36,68886	0,73
STØ1	525300	111,4	98,515	12,8416	30	29,669	7,734872	37,40406	0,77
STØ1	865200	287,0	251,52	35,4584	30	47,216	13,31292	60,52905	0,75
STØ1	689400	292,0	249,56	42,407	30	62,108	21,10762	83,21564	0,71
STØ1	431400	121,6	104,77	16,7845	30	41,667	13,35066	55,01728	0,71
DALEN	1128660	15,1	9,6413	5,416	30	1,4656	1,646602	3,112204	0,71
DALEN	1128660	18,5	13,734	4,74863	30	2,0878	1,443705	3,531463	0,71
DALEN	930900	11,8	6,7692	4,9894	30	1,2134	1,788767	3,0022	0,73
DALEN	623400	10,7	6,2514	4,40287	30	1,6734	2,357102	4,030469	0,73
DALEN	509400	10,1	5,4373	4,66943	30	1,6886	2,900321	4,588969	0,77
DALEN	867600	10,8	7,5567	3,25166	30	1,4147	1,217465	2,632132	0,75
DALEN	695700	12,2	6,8069	5,36372	30	1,6787	2,645557	4,324251	0,71
DALEN	426600	10,2	6,4968	3,74385	30	2,6129	3,011417	5,624306	0,71
HUG	1124160	33,3	28,362	4,97453	30	4,3286	1,51844	5,84703	0,71
HUG	1124160	61,9	52,327	9,56893	30	7,9862	2,920847	10,90709	0,71
HUG	952500	124,4	97,71	26,6508	30	17,118	9,338023	26,45607	0,73
HUG	594600	81,4	67,579	13,812	30	18,965	7,752486	26,71791	0,73
HUG	524700	46,2	36,719	9,46764	30	11,071	5,709156	16,78036	0,77
HUG	865200	75,6	64,278	11,3165	30	12,067	4,248806	16,31547	0,75
HUG	691800	79,4	68,034	11,3501	30	16,873	5,629786	22,50263	0,71
HUG	429900	35,4	29,422	5,97576	30	11,742	4,769786	16,51199	0,71

**E.6. Statistics for the student test performed on the results from the Sampling precision of P by DGT samplers at the sampling location Støal**

**Table A21: Statistics for the paired t-test**

Paired t-test for Free-PO4				
Mean difference	$\sqrt{n}$	STDEV	$t=(\text{mean difference} \times \sqrt{n})/Sd$	t3 from table
5,65	2	9,78	1,15	3,18
Paired t-test for organic P				
Mean difference	$\sqrt{n}$	STDEV	$t=(\text{mean difference} \times \sqrt{n})/Sd$	t3 from table
-9,525	2	1,97	5,86	3,18
Paired t-test for total-P(Free-PO4+ organic P)				
Mean difference	$\sqrt{n}$	STDEV	$t=(\text{mean difference} \times \sqrt{n})/Sd$	t3 from table
11,42	2	8,98	2,54	3,18

Calculation of adsorbed total-P and free-PO4 was based on Equation  $C = X / T^*(DA/L)$  Where, X=total-P accumulated by DGT sampler in  $\mu\text{g} / L$ , L= Length 0,102 in cm, C= concentration measured in  $\mu\text{g} / L$ , T= time in seconds and A= exposure areal to solution 3, 14 in  $\text{cm}^2$  and D= diffusive coefficients in  $\text{cm}^2/\text{s}$ .

D values for organic P =  $4.00 \text{ E-}06 \text{ cm}^2/\text{s}$  and free-PO4=  $8.00 \text{ E-}06 \text{ cm}^2/\text{s}$  (Røyset, 2011 (Per.comm)) that were used in the calculations.

## **Appendix F: Flow-weighted mean concentration and linear interpolations**

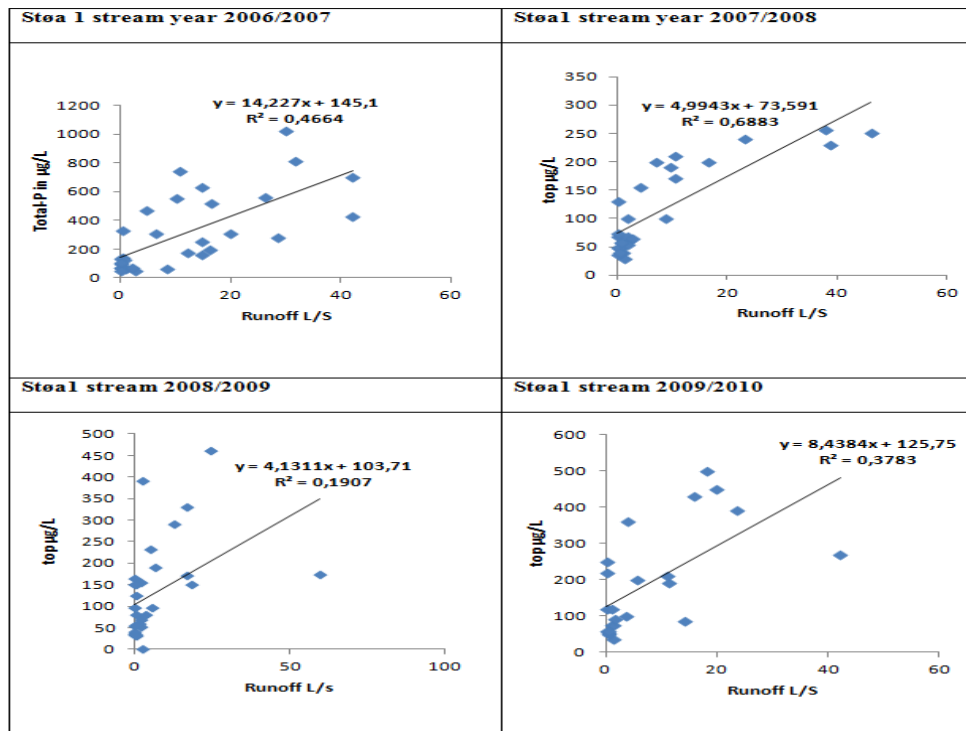
### **F.1 Equation for flow weighted mean concentration**

Concentration  $\times$  Runoff = Transport  
 Transport/runoff = flow-weighted mean concentration

## F.2 Linear interpolation curves

Only the curves from the Støa1 shown due to the large number of figures.

**Table A22:** Figures showing correlations between runoff and total-P in the Støa1 stream for hydrological years 2006-2010.



## Appendix G: Correlation between SS and total-P in Støa1 stream (Eutropia samples)

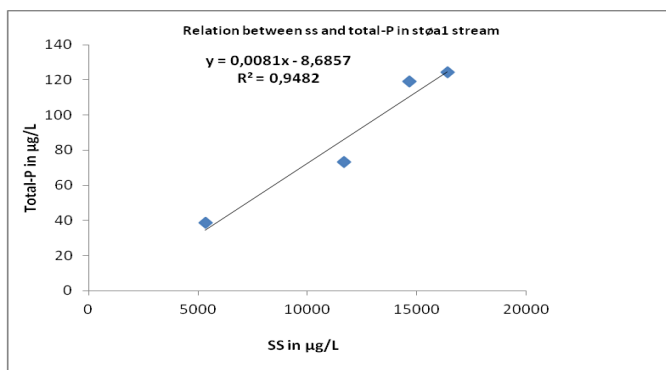


**Figure A4:** SS vs. tot-P in the Støa1 stream (Eutropia samples).

## Appendix H: Statistical Analysis

### H.1 PCA on water samples

**Table A23: Component loadings for water samples**

Variable	Component				
	PC1	PC2	PC3	PC4	PC5
% Agriculture	0,193	-0,246	0,277	0,115	-0,02
% Forest	-0,279	-0,042	-0,015	-0,125	0,176
% Other	0,072	0,338	-0,311	0,121	-0,171
pH	0,273	0,072	-0,05	0,087	0,061
Alkalinity	0,265	0,004	-0,151	-0,043	0,112
Total-P	0,143	-0,331	-0,22	-0,007	-0,004
DOM-P	-0,141	-0,299	-0,156	-0,147	-0,408
PP	0,17	-0,322	-0,11	0,03	-0,096
free-Po4	0,131	-0,294	-0,331	-0,03	0,168
DOC	-0,227	-0,144	-0,136	-0,2	-0,312
H+	-0,22	-0,095	0,013	-0,186	-0,078
Ca2+	0,272	0,067	-0,096	-0,038	-0,086
Mg2+	0,24	-0,119	0,243	-0,027	0,012
Na+	0,109	0,318	-0,09	-0,361	0,016
K+	0,267	-0,061	-0,096	-0,081	-0,184
HCO3-	0,272	0,006	-0,049	-0,122	0,128
NO3-N	0,212	-0,126	0,32	0,183	-0,2
Tot-F	0,245	-0,122	0,204	-0,084	0,175
Cl-	0,139	0,303	-0,085	-0,334	0,089
PO43-	0,133	-0,26	-0,343	-0,075	0,345
SO42-	0,237	0,043	0,002	0,036	-0,57
NO3-N	0,217	0,196	0,258	-0,114	0,005
DON	0,078	-0,005	0,064	-0,68	-0,126
NH4	0,108	0,211	-0,4	0,295	-0,138

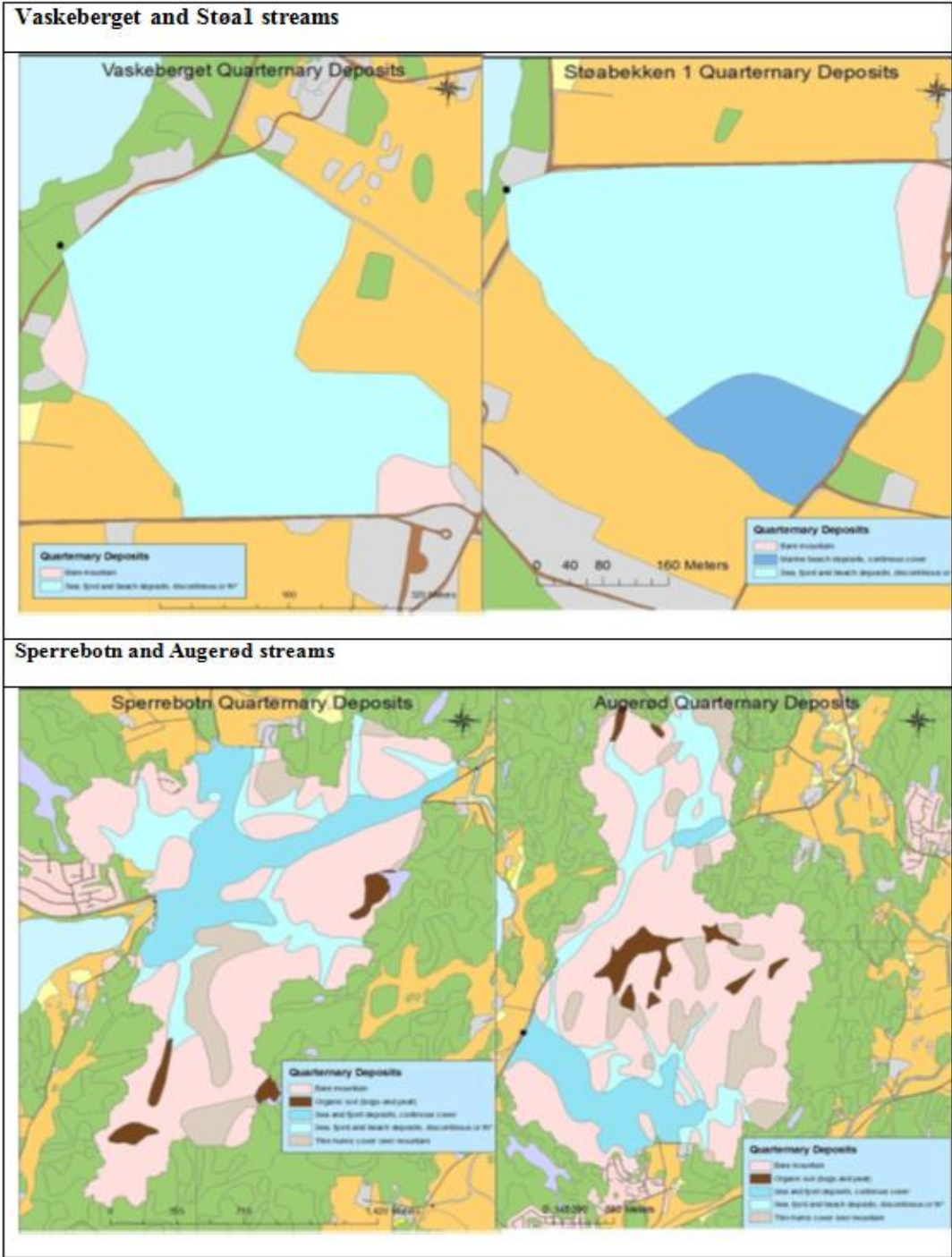
Extraction Method: Principal Component Analysis.5 components extracted.

Proportion	0,528	0,235	0,099	0,076	0,031	0,020	0,010	0,000
Cumulative	0,528	0,764	0,863	0,939	0,970	0,990	1,000	1,000

## H.2 Pearson Correlation analysis data

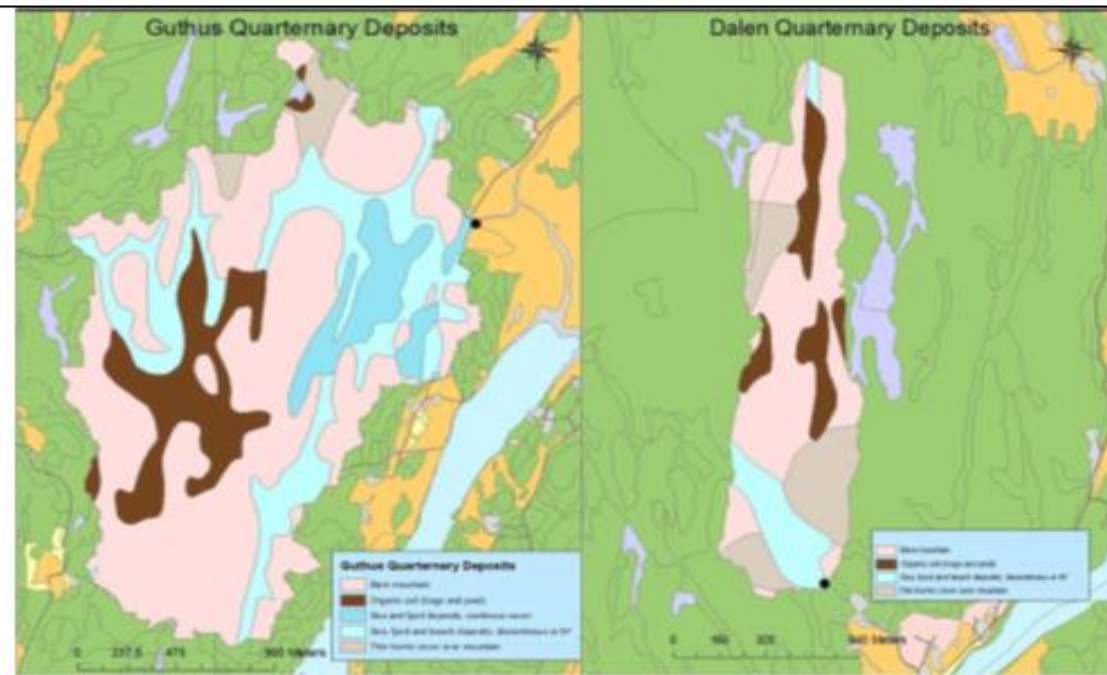
	% Agriculture	% forest	% Other	pH	Alkalinity	Total-P	DOM-P	PP	Free-PO4	DOC	H+	Ca+2	Mg+2	Na+	K+	HCO3-	NO3	Tot-F	CL-	PO4-3	SO4	NO3	DON	
% Forest	-0,691																							
	0,039																							
% Other	-0,335	-0,431																						
	0,349	0,246																						
pH	0,52	-0,778	0,357																					
	0,151	0,014	0,346																					
Alkalinity	0,355	-0,895	0,357	0,934																				
	0,172	0,003	0,385	0																				
Total-P	0,691	-0,462	-0,265	0,353	0,541																			
	0,039	0,211	0,49	0,351	0,166																			
DOM-P	-0,11	0,412	-0,52	-0,143	-0,422	0,382																		
	0,979	0,27	0,151	0,714	0,298	0,311																		
PP	0,815	-0,577	-0,272	0,419	0,58	0,974	0,289																	
	0,007	0,104	0,479	0,262	0,132	0	0,45																	
Free-PO4	0,536	-0,38	-0,177	0,292	0,556	0,967	0,342	0,893																
	0,137	0,313	0,648	0,446	0,153	0	0,368	0,001																
DOC	-0,549	0,841	-0,402	-0,95	-0,74	-0,247	0,398	-0,337	-0,195															
	0,125	0,004	0,283	0	0,036	0,522	0,289	0,375	0,616															
H+	-0,401	0,583	-0,253	-0,961	-0,664	-0,261	-0,023	-0,3	-0,196	0,86														
	0,284	0,1	0,512	0	0,072	0,498	0,952	0,417	0,614	0,003														
Ca+2	0,596	-0,963	0,501	0,714	0,958	0,474	-0,434	0,553	0,44	-0,767	-0,499													
	0,09	0	0,169	0,031	0	0,197	0,243	0,122	0,236	0,016	0,171													
Mg+2	0,911	-0,866	-0,017	0,709	0,762	0,556	-0,218	0,689	0,424	-0,756	-0,558	0,803												
	0,001	0,003	0,966	0,032	0,028	0,12	0,572	0,04	0,256	0,018	0,118	0,009												
Na+	-0,074	-0,746	0,708	0,464	0,426	-0,222	-0,548	-0,205	-0,159	-0,512	-0,359	0,612	0,237											
	0,85	0,195	0,033	0,208	0,293	0,566	0,127	0,596	0,683	0,159	0,342	0,08	0,538											
K+	0,716	-0,886	0,252	0,553	0,904	0,682	-0,24	0,75	0,631	-0,579	-0,334	0,931	0,789	0,416										
	0,03	0,001	0,514	0,122	0,002	0,043	0,534	0,02	0,069	0,102	0,38	0	0,012	0,265										
HCO3-	0,682	-0,917	0,335	0,688	0,978	0,547	-0,394	0,615	0,52	-0,748	-0,475	0,969	0,865	0,554	0,923									
	0,043	0	0,378	0,041	0	0,127	0,294	0,078	0,151	0,021	0,196	0	0,03	0,121	0									
NO3-N	0,925	-0,813	-0,102	0,554	0,576	0,494	-0,227	0,666	0,316	-0,636	-0,405	0,68	0,922	0,018	0,717	0,698								
	0	0,008	0,794	0,121	0,135	0,176	0,557	0,05	0,408	0,066	0,28	0,044	0	964	0,03	0,036								
Tot-F	0,906	-0,847	-0,035	0,695	0,796	0,59	-0,244	0,698	0,49	-0,756	-0,534	0,813	0,983	0,284	0,813	0,898	0,873							
	0,001	0,004	0,929	0,038	0,018	0,095	0,527	0,037	0,18	0,018	0,139	0,008	0	0,459	0,008	0,01	0,002							
CL-	0,014	-0,556	0,701	0,503	0,533	-0,147	-0,601	-0,121	-0,086	-0,567	-0,372	0,69	0,33	0,991	0,497	0,646	0,105	0,379						
	0,971	0,12	0,035	0,168	0,173	0,707	0,087	0,756	0,825	0,112	0,324	0,04	0,386	0	0,174	0,06	0,787	0,314						
PO43-	0,479	-0,351	-0,144	0,281	0,58	0,915	0,231	0,834	0,973	-0,194	-0,182	0,442	0,402	-0,09	0,601	0,541	0,249	0,48	-0,008					
	0,192	0,355	0,711	0,464	0,132	0,001	0,549	0,005	0	0,616	0,639	0,233	0,283	0,817	0,087	0,133	0,517	0,191	0,984					
SO42-	0,629	-0,934	0,423	0,75	0,717	0,43	-0,256	0,549	0,319	-0,749	-0,594	0,895	0,758	0,5	0,865	0,801	0,746	0,723	0,545	0,253				
	0,07	0	0,256	0,02	0,045	0,249	0,506	0,126	0,402	0,02	0,092	0,001	0,018	0,17	0,003	0,01	0,021	0,028	0,129	0,512				
NO3	0,553	-0,858	0,419	0,831	0,616	0,1	-0,571	0,243	0,01	-0,908	-0,711	0,809	0,773	0,648	0,636	0,771	0,686	0,755	0,701	0,037	0,817			
	0,122	0,003	0,262	0,006	0,104	0,799	0,109	0,529	0,98	0,001	0,032	0,008	0,015	0,059	0,065	0,015	0,041	0,019	0,035	0,925	0,007			
DON	-0,06	0,237	-0,232	-0,514	0,282	-0,048	0,008	-0,059	-0,036	0,522	0,574	-0,052	-0,086	0,184	0,096	0,03	-0,174	-0,049	0,179	0,033	-0,18	-0,226		
	0,878	0,539	0,548	0,157	0,499	0,903	0,983	0,881	0,927	0,15	0,106	0,893	0,825	0,636	0,807	0,939	0,654	0,901	0,645	0,933	0,644	0,559		
NH4	-0,405	-0,146	0,694	-0,24	0,509	-0,106	-0,312	-0,144	0,002	0,15	0,394	0,237	-0,238	0,191	0,162	0,109	-0,186	-0,255	0,215	0,03	0,075	-0,106	0,032	
	0,279	0,708	0,038	0,534	0,198	0,785	0,271	0,712	0,995	0,699	0,295	0,539	0,538	0,623	0,677	0,78	0,632	0,508	0,758	0,928	0,847	0,786	0,936	

**Appendix I: Maps of quaternary deposits of the investigated streams**

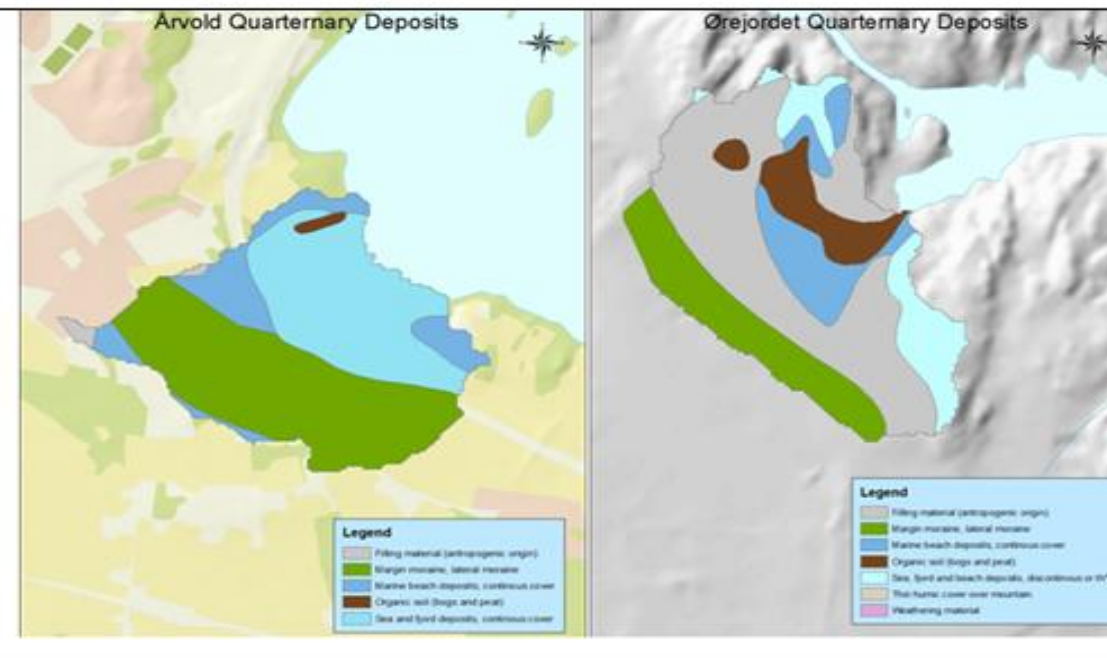




### Guthus and Dalen streams



### Årvold and Ørejordet streams



### Huggenes stream



## Appendix J: Map of erosion risk in the investigated streams

